Unravelling molecular and biochemical dysfunction by Shiga toxin: implication for thrombotic microangiopathy in Hemolytic Uremic Syndrome

Unravelling molecular and biochemical dysfunction by Shiga toxin: implication for thrombotic microangiopathy in Hemolytic Uremic Syndrome

Marina Morigi

Unravelling molecular and biochemical dysfunction by Shiga toxin: implication for thrombotic microangiopathy in Hemolytic Uremic Syndrome

PROEFSCHRIFT

ter verkrijging van de graad van doctor
aan de Universiteit Maastricht,
op gezag van de Rector Magnificus,
Prof. mr. G.P.M.F. Mols,
volgens het besluit van het College van Decanen,
in het openbaar te verdedigen
op donderdag 16 Maart 2006 om 14.00 uur

door

Marina Morigi

geboren op 30 Augustus 1961 te Ravenna, Italie

Supervisors

Prof.dr. G. Remuzzi, Bergamo

Prof.dr. K.M.L. Leunissen

Beoordelingscommissie

Prof.dr. J.Rosing, (voorzitter)

Prof.dr. R. Donckerwolcke

Dr. K. Hamulyak

Prof.dr. L. Monnens, UMC St. Radboud

Prof.dr. G. J. Navis, UCM Groningen

To: Arturo, Francesco, and Matteo

CONTENTS

CHAPTER 1

INTRODUCTION

In part published in :The role of the endothelium in Hemolytic Uremic Sindrome.
C. Zoja, M. Morigi, G. Remuzzi.

J Nephrol 2001: 14: S58-S62.

INTRODUCTION

Hemolytic uremic syndrome (HUS) is a disease of non-immune microangiopathic hemolytic anemia, thrombocytopenia and acute renal failure that mainly affects infants and small children. The characteristic lesion, thrombotic microangiopathy, is unique to this syndrome and consists of vessel wall thickening, with swelling and detachment of endothelial cells from the basement membrane, accumulation of fluffy material in the subendothelium and platelet thrombi in the microcirculation of the kidney and other organs [1-3]. In its typical presentation, HUS manifests as an acute disease, with gastrointestinal or respiratory tract prodromes, that recovers without sequelae in 80 to 90 % of cases, either spontaneously (as in most cases of childhood HUS) or following plasma infusion or exchange (as in adult or severe forms of HUS). Typical HUS is triggered by environmental factors, drugs or infective agents such as Shiga toxin-producing *E.coli*; systemic immune disorders or cancer may also cause the disease [1, 2]. These forms of HUS may subside when the underlying condition has been treated or removed. However, there are rare forms, often occurring in families, which frequently relapse even after complete recovery of the presenting episode, with death or permanent neurological or renal sequelae being the final outcome in the large majority of cases. These atypical forms are considered to be supported by a genetic background which predispose to microvascular thrombosis. Both autosomal recessive and autosomal dominant mode of inheritance have been recognized, with precipitating events such as pregnancy, virus-like disease or sepsis being identified in some but not in all series.

Shiga toxin as fosterer of HUS

In 90% of cases of typical diarrhea-associated (D+) HUS in children, infection with *E.coli* producing a verotoxin (VT) also termed Shiga toxin (Stx) has been strongly implicated as the most common causative agent of this disease [1, 4-6]. More than 100 *E. coli* serotypes have been found to produce Stx, but only few of them have been involved in human disease. The serotype 0157:H7 is the most common pathogen in the United States and

Europe, but other strains, particularly the 0111:H-serotype, are frequently reported in other areas of the world [7]. Infection by Stx-producing *Shighella dysenteria* serotype 1 has been commonly linked to Stx-HUS in developing countries of Asia [8] and Africa [9], but rarely in industrialized countries [10]. Of note, *E. coli* 0157:H7 strains that are isolated from patients with HUS, usually produced both Stx-1 and 2. It is estimated that following exposition to *E.coli* O157:H7, 38% to 61% of persons develop hemorrhagic colitis, and 2% to 7% of these patients progress to overt HUS. The reservoir of *E. coli* 0157:H7 is the gastrointestinal tract of the domestic animals. The microorganism is transmitted to person by ingestion of contaminated food or water/water-borne, directly from person to person [7, 11, 12] and also through occupational exposure. Undercooked ground beef, meat patties, roastbeef, ham, turkey, cheese, fruits and vegetables, radish sprouts and sausages, unpastorized milk and apple juice have all been implicated in the transmission of *E. coli* [7]. After ingestion of contaminated food or water, *E.coli* 0157:H7 reaches the gut and closely binds to the epithelial cells of the gastrointestinal mucosa. Adhesion by a 97 kD outer membrane protein intimin, encoded by the *eae* gene, produces characteristic "attaching and effacing" lesions aimed at preventing the expulsion of the microorganisms [13]. The intimin receptor named Tir (translocated intimin receptor), is produced in the bacteria and translocated via a secretory pathway into the eucariotic cell, where it is phosphorylated and interacts with the host cell cytoskeleton [14]. The consequent disruption of the brush border *per se* is sufficient to produce non-bloody diarrhea. *E.coli* 0157:H7 (as well as *E.coli* 0111, non motile 026:H11, or 0103:H2) may produce large amount of Stx, that traverses polarized gastrointestinal epithelial cells, probably via transcellular pathways [14] and gains access to the systemic circulation.

Recent studies have contributed to clarify how Stx/VT once has reached the circulation is transferred to the kidney [15]. It has been shown that VT-1 when incubated in whole blood *in vitro*, bound rapidly and completely to human polymorphonuclear leukocytes (PMN). Binding studies with ^{125}I-VT-1 showed a single class of binding sites on freshly isolated, non stimulated human PMN. Interestingly, the Kd of the high affinity receptor for VT on PMN was 100-fold less than that found for the functional receptor Gb3, on glomerular

microvascular endothelial cells (GMVEC). As a consequence, incubation of PMN that had bound fluorescent VT, with GMVEC resulted in passing of the toxin to GMVEC and subsequent inhibition of protein synthesis and cell death [15]. Stimulating the GMVEC with inflammatory mediators, such as TNFα or lipopolysaccharide (LPS), upregulated the VT receptor Gb3 on cell surface and favored transfer of Stx from PMN. These *in vitro* data were further supported by the detection of VT-2 in the circulation of 9 out of 10 patients with the epidemic form of HUS, bound exclusively to PMN [16]. The detection of VT-2 bound to PMN was associated with the presence of diarrhea at the time the blood samples were obtained. It has been demonstrated that *in vitro* purified human monocytes bound VT significantly after activation by LPS through a different receptor, globotetraosyl-ceramide (Gb4). After toxin challenge, monocyte release of cytokines like IL-1 and TNF, preceded by the nuclear translocation of the transcriptional activator NF-kB and Ap-1, remarkably potentiated the sensitivity of vascular endothelial cells to VT by upregulating endothelial Gb3 receptors [17, 18]. Endothelial cells are not the only targets for Stx in the kidney and other cells as mesangial, glomerular visceral epithelial cells, proximal and distal tubular cells express the receptor for Stx and are damaged by the toxin.

Shiga toxin and the specific receptors

Several members of Shiga toxin/Verotoxin family (69 kDa) produced by *E. coli* have been characterized, Stx-1, Stx-2, Stx-2c, and Stx2e. Stx-1 is almost identical to Stx from *Shighella dysenteriae* type 1 differing by a single aminoacid, and is 50% homologous with Stx-2 [19].

Stx consists of a biologically active A subunit (35kD) and five B subunits (7-8kD) that allow binding of the toxin to specific glycosphingolipid receptors located on the plasma membrane of target cells. The binding is followed by internalization via endocytosis [20] of the A subunit, an RNA N-glycosidase that inhibits protein translation by removing specific adenine residue from ribosomal RNA and causes cell death [17] or apoptosis [21].

The neutral glycolipid globotriaosylceramide Gb3 also known as Gal α1-4Gal β1-4Glc ceramide binds all Stx members, except Stx-e, which preferentially binds to Gal NAc β1-

3Gal α1-4 Gal β1-4Gcl ceramide (Gb4), the P antigen on human erytrocytes. The Gb3 receptor is the Pk antigen of the P blood group system [22] and it has been suggested that Stx might bind to blood red cells as a function of their P blood group phenotype. Evidence are available showing that individuals with high expression of P blood group glycolipids containing the disaccharide Gal α(1-4)Gal structure necessary for toxin binding, are at reduced risk of HUS after Stx-producing *E. coli* infection, because the red cells act as a sink to mop up systemic toxin and prevent access to the more critical renal endothelial cells. Gb3 (CD77) is also a marker for germinal center B lymphocytes [23] and is the Burkitt lymphoma antigen [24].

The Gb3 fatty acid chain length and the degree of unsaturation markedly affect the ability of the toxin to bind [25]. These latter effects can only be demonstrated within a lipid matrix and show that there is a lower limit (14 carbons) on the fatty acid chain length that allows effective toxin recognition. Increasing chain length increases receptor activity for Stx-1 to a maximum at 20-22 carbons; above a chain length of 22 carbons, binding declines. In contrast, Stx-2c which has 90% similarity with Stx-2, preferentially binds to Gb3 containing C18 fatty acids. For both Stx-1 and Stx-2c incorporation of unsaturated fatty acids increases Gb3 receptor activity [25], suggesting that lateral mobility within the phospholipid bilayer may be involved in glycolipid receptor activity. There is also evidence that Gb3 receptor containing shorter fatty acid species directs the toxin to the endoplasmic reticulum rather than to the Golgi apparatus, and increases Stx cytotoxicity [26]. Genetic differences in Gb3 fatty acid composition might therefore account for different individual susceptibility to the effect of Stx [26].

In human renal tissue Stx-1 binds primarily to collecting ducts and distal convoluted tubules, expecially those adjacent to glomeruli. The toxin also binds to the glomeruli of infants but not of adults [27], implying that Gb3 is expressed in the renal glomeruli of children and that it is a developmentally regulated expression and decreased during ontogenesis. This is in concordance with the finding of HUS being more prevalent in young children than adults. Of interest, a recent study in baboons [28] that share with humans a similar distribution of gastrointestinal and renal tubular Gb3 receptors, demonstrated that

Stx injection induced direct cell injury to the endothelial and epithelial cells of the gastrointestinal apparatus and of the renal microcirculation [28].

The degree of upregulation of Gb3 synthesis at the time of illness could be important in determining toxicity. Cytokines known to increase cell expression of the Gb3 receptor include IL-1 and TNF. TNF acts mainly via its 55kDa receptor, TNFR-p55, present on endothelial cells [17, 29]. It is possible that cytokines induce breakdown of sphingomyelin, by the activation of sphingomyelinase, to ceramide which favors Gb3 synthesis [30].

Shiga toxin and endothelial cell injury

Endothelial injury predominantly of glomerular capillaries, has been recognized as the inciting event in the development of microangiopathic process of HUS. It is generally assumed that Stx is cytopathic for endothelial cells. *In vitro* studies have indicated that priming of endothelial cells by cytokines as IL-1 and TNF is required for Stx cytotoxicity. These mediators remarkably potentiate the sensitivity of vascular endothelial cells to Stx by upregulating endothelial Gb3 receptor expression [20]. This finding is closely related to the observation that Stx induced apoptosis in human glomerular endothelial cells only when cells were pre-exposed to TNFα [21].

Increasing evidences suggests that Shiga toxins by favoring interaction of endothelial cells with leukocytes serve to amplify and extend the injury at renal level. First, the number of neutrophils is elevated in HUS, and it was suggested that it is a predictive factor for the outcome of the disease [31]. In addition, Fitzpatrick et al. [32] described that neutrophils of HUS patients were activated as indicated by the fact that plasma concentrations of α1-antitrypsin -complexed elastase and the chemokine interleukin-8 (IL-8) - a potent activator of neutrophils- were remarkably higher in the acute phase of the disease. Neutrophils from children with acute phase of HUS adhered to endothelial cells in vitro more than normal neutrophils and induced endothelial injury by degrading endothelial cell fibronectin, possibly depending on the release of neutrophil-specific proteases [33]. A preliminary report showed that glomerular endothelial cells exposed to Stx became more susceptible to neutrophil-mediated oxidant injury [34] .

Histological examination of kidney specimens from HUS children with evidence of Stx-producing *E.coli* infection, revealed a conspicuous infiltration of mononuclear and polymorphonuclear cells within the glomeruli, along with microvascular injury [35, 36]. In those patients urinary levels of IL-8 and monocyte chemoattractant protein-1 (MCP-1), potent attractants of neutrophils, and monocytes/macrophages and T-lymphocytes, respectively, were elevated during the acute phase of the disease, and gradually declined until recovery, indicating an involvement these chemokines in the attraction of inflammatory cells at renal level [36, 37]. A recent study in cultured endothelial cells showed that subtoxic concentrations of Stx-1 and 2, exerting minimal influence on protein synthesis, were able to strongly upregulate inflammatory cytokines, chemokines, and adhesive molecules -IL-6, IL-8, ICAM-1 gene expression and GRO-1 and MCP-1 protein-possibly implicated in the recruitment and adhesion of circulating leukocytes to the endothelium [38].

Among the inflammatory mediators that are released from adherent neutrophils, reactive oxygen species have been shown to exert a direct cytotoxic effect on vascular endothelium. Neutrophils from patients with HUS produced excessive superoxide anion (O_2^-), which argued in favor of oxygen radicals as candidates for neutrophil-induced endothelial damage in these patients [39]. Injured endothelium changes its normal thromboresistant phenotype and becomes thrombogenic initiating microvascular thrombus formation.

In HUS structural damage of microvessels associated with narrowing of the lumina determines major changes in fluid shear stress, which would favor persistent endothelial damage, platelet activation and progression of microvascular thrombosis [40]. Changes in shear stress, the tractive force produced by blood flowing over the endothelial surface, have a profound influence on von Willebrand factor (vWF) handling, by promoting its endothelial secretion and enhancing its susceptibility to proteolytic cleavage [41]. vWF under condition of high shear stress undergoes conformational changes and serves to bridge subendothelial matrix to glycoprotein (GP) Ib expressed on platelet membrane [42]. The engagement of this receptor promotes activation of platelet α_{IIb}-β_3 (GPIIb/IIIa)

complex that binds to the RGD sequence of vWF leading to thrombus formation [42]. vWF via the RGD sequence may also bind vitronectin receptor ($\alpha_v\beta_3$), the major integrin expressed on endothelial cells [43] that promotes endothelial cell adhesion to the vascular matrix [44]. GPIb is also expressed on endothelial cells; however, controversial results about its function have been reported so far [45]. Relevant to the role of vWF in the pathogenesis of D+ HUS is also the evidence that in Stx-mediated primate model of HUS, vWF expression increased in glomeruli and peritubular capillaries [46].

Several distinct endothelial cell molecules have been reported to be involved in the binding of platelets to endothelial cells. P-selectin, which is stored in intracellular granules of platelets and endothelial cells together with vWF, and rapidly mobilizes to the cell surface upon stimulation [47], is required for platelet rolling and adhesion on activated endothelium [48]. Increased plasma levels of P-selectin have been measured in patients with HUS, possibly reflecting activation/damage of platelets and endothelial cells [49].

Shiga toxin and renal cells

HUS is commonly viewed as a disease of the vascular endothelium. However evidence is emerging that renal injury in D+HUS is not limited to glomerular vessels but also affects other compartment as mesangial, glomerular epithelial cells (GEC), proximal and distal tubular cells (PTEC). Mesangial cell injury in HUS ranges from mild cellular edema to severe mesangiolysis and eventual glomerulosclerosis. *In vitro* experiments documented that mesangial cells are direct targets of Stx-1 that exerts diverse biological effects on these cells ranging from activation of a chemokine gene as MCP-1 to a lethal toxic injury [50]. Inflammatory cytokines potentiate the effects of the toxin in these cells.

Recent study have indicated that *in vivo* glomerular epithelial cells, also called podocytes, are susceptible to the toxic effects of Stx because they express high levels of Gb3 and bind the toxin as described either in cultured podocytes [51] or in human renal biopsies [52]. In baboon model of HUS, swelling of podocytes with osmophilic inclusions was found together with the typical glomerular endothelial lesions after intravenous infusion of Stx [28]. *In vitro*, Stx-1 besides its cytotoxic effect on cell viability and protein synthesis,

activated podocytes to release inflammatory cytokines like IL-1 and TNF, an effect potentiated by lipopolysaccaride co-incubation [53]. Stx-1 also increased arachidonate release from human podocytes in association with the production of both TxA2 and PGI2 [54]. Finding that Stx modulates mesangial and GEC function could clearly have a significant impact on glomerular function through alteration of glomerular capillary surface area and filtration rate, thus contributing to glomerular ischemic changes and hemodynamic derangement in HUS.

Renal tubular epithelial cells also express high levels of Gb3 and bind to the toxin [27]. Studies on renal biopsy samples from children with D+HUS in the early stages revealed histologically apparent proximal tubular damage [3]. Apoptotic cell death of renal tubules was also observed [55]. Moreover, increased urine concentrations of N-acetyl glucosaminidase and β2 microglobulin, specific markers of tubular function, were found in these patients providing the evidence of impaired renal tubular function during the acute phase of the disease [56]. Hughes et al have found that PTEC in culture are exquisitely sensitive to the ribotoxic effects of Stx, thus indicating that the toxin directly injured these cells [57]. Treatment of ACHN cells (derived from renal tubular epithelial carcinoma) with Stx-2 induced prompt growth inhibition and fragmentation of the genomic DNA, typical of apoptosis, an effect which was potentiated by TNF [58].

OBJECTIVES OF THE THESIS

In this thesis further investigations were performed to identify the mediators and intracellular signalling underlying renal toxicity of Shiga toxin (Stx)-1 and 2, also called Verotoxin- (VT)1 and 2, the offending agents for typical childhood D+HUS.

Evidence on the role of endothelium in HUS have been reported and discussed in a review. Endothelial damage has been recognized as the trigger event in the development of microangiopathic lesion. Recent findings suggest that leukocytes as well as platelet activation participate in the development of endothelial injury. Intrinsic abnormalities of the complement system may also play a role in HUS (**Chapter 2**).

Endothelial injury and leukocyte activation are instrumental to the development of microangiopathic lesions in HUS. First, we studied whether VT-1 directly modulated leukocyte adhesion to vascular endothelium exposed to flow conditions that mimic postcapillary venule circulation. Experiments were planned to address the molecular determinants expressed by endothelium in response to VT-1 involved in the adhesive phenomena. Given that TNFα, appears a crucial molecule in the sequence of events that lead to endothelial damage, we also investigated the possible role of TNFα in amplifying VT-1 induced leukocyte adhesion on endothelial cells (**Chapter 3**).

To obtain more insight into the mechanisms favouring endothelium-leukocyte interaction, we studied the effect of Stx-2 on leukocyte adhesion and transmigration through human umbilical vein endothelial cells (HUVEC) and glomerular endothelial cells under flow conditions. Since in patients with HUS, kidney speciments reveald conspicuous infiltration of neutrophils and mononuclear cells, and urinary levels of the chemoattractants IL-8 and MCP-1 were elevated during the acute phase of the disease, we assessed the effect of Stx-2 on endothelial gene expression of IL-8 and MCP-1 and their functional role in the adhesive phenomena.

Based on the evidence that these chemokines are transcriptionally regulated by NF-kB, we verified whether Stx-2 induced the activation of this transcription factor and whether transfection of endothelium with recombinant adenovirus coding for IkBα, the natural inhibitor of NF-kB, resulted in the suppression of chemokine upregulation, and leukocyte adhesion and transmigration induced by the toxin (**Chapter 4**).

Thrombocytopenia and deposition of platelet thrombi that occlude the microcirculation of the kidney and other organs, are characteristic of VT-associated HUS. Why thrombi form only on arterioles and capillaries is not known. The present study was designed to investigate whether VT-1 affected endothelial anti-thrombogenic properties promoting platelet deposition and thrombus formation on endothelial cells under high shear stress. We also evaluated whether microvascular endothelium had a higher susceptibility to VT-1-induced thrombus formation in respect to endothelial cells derived from large vessels. Moreover, we wanted to identify platelet and endothelial adhesive proteins involved in the thrombotic process promoted by VT-1 (**Chapter 5**).

The kidney is the privileged target of Stx, with glomerular ischemic changes preceding microvascular thrombosis. Retraction and collapse of the capillary tuft in the glomerulus are also prominent and tipically occur in association with fusion of foot processes and swelling of glomerular visceral epithelial cells, termed podocytes. Since podocytes possess Stx receptor, are highly sensitive to Stx-2 cytotoxicity and represent an important source of vasoactive molecules, we studied whether Stx-2 modulates the production of the vasoconstrictor peptide ET-1, taken as candidate mediator of podocyte dysfunction, and the intracellular signals involved (**Chapter 7**).

Propedeutic to this work was a previous paper focused on the study of mechanisms and mediators underlyng phenotypic changes in podocytes induced by protein overload, that reproduced the condition of exaggerated protein traffic through the glomerular capillary barrier during proteinuric condition. Given that effacement of podocyte foot processes

occurring in many proteinuric nephropathies is accompanied by rearrangement of actin cytoskeleton, we tested the hypothesis that protein overload alters the F-actin-based contractile podocyte apparatus resulting in modulation of ET-1 gene expression and production of the vasoactive peptide. We also identified the possible relevant intracellular signals evocated by cytoskeletal changes ultimately leading to ET-1 gene expression (**Chapter 6**).

REFERENCES

1. Remuzzi G, Ruggenenti P: The hemolytic uremic syndrome. *Kidney Int* 47:2-19, 1995
2. Ruggenenti P, Noris M, Remuzzi G: Thrombotic microangiopathy, hemolytic uremic syndrome, and thrombotic thrombocytopenic purpura. *Kidney Int* 60:831-846, 2001
3. Remuzzi G, Ruggenenti P, Bertani T: Thrombotic microangiopathy, in *Renal Pathology With Clinical and Functional Correlations*, edited by Tisher CC, Brenner BM, 2 ed, Philadelphia, J.B. Lippincott Company 1994, pp 1154-1184
4. Karmali MA, Petric M, Lim C, Fleming PC, Arbus GS, Lior M: The association between idiopathic hemolytic uremic syndrome and infection by verotoxin-producing Escherichia Coli. *J Infect Dis* 151:775-782, 1985
5. Arbus GS: Association of verotoxin-producing E. coli and verotoxin with hemolytic uremic syndrome. *Kidney Int Suppl* 58:S91-96, 1997
6. Andreoli SP: The pathophysiology of the hemolytic uremic syndrome. *Curr Opin Nephrol Hypertens* 8:459-464, 1999
7. Mead PS, Griffin PM: Escherichia coli O157:H7. *Lancet* 352:1207-1212, 1998
8. Srivastava RN, Moudgil A, Bagga A, Vasudev AS: Hemolytic uremic syndrome in children in northern India. *Pediatr Nephrol* 5:284-288, 1991
9. Guerin PJ, Brasher C, Baron E, Mic D, Grimont F, Ryan M, Aavitsland P, Legros D: Shigella dysenteriae serotype 1 in west Africa: intervention strategy for an outbreak in Sierra Leone. *Lancet* 362:705-706, 2003
10. Houdouin V, Doit C, Mariani P, Brahimi N, Loirat C, Bourrillon A, Bingen E: A pediatric cluster of Shigella dysenteriae serotype 1 diarrhea with hemolytic uremic syndrome in 2 families from France. *Clin Infect Dis* 38:e96-99, 2004
11. Carter AO, Borczyk AA, Carlson JA, Harvey B, Hockin JC, Karmali MA, Krishnan C, Korn DA, Lior H: A severe outbreak of Escherichia coli O157:H7--associated hemorrhagic colitis in a nursing home. *N Engl J Med* 317:1496-1500, 1987

12. Pavia AT, Nichols CR, Green DP, Tauxe RV, Mottice S, Greene KD, Wells JG, Siegler RL, Brewer ED, Hannon D, et al.: Hemolytic-uremic syndrome during an outbreak of Escherichia coli O157:H7 infections in institutions for mentally retarded persons: clinical and epidemiologic observations. *J Pediatr* 116:544-551, 1990

13. Donnenberg MS, Tzipori S, McKee ML, O'Brien AD, Alroy J, Kaper JB: The role of the eae gene of enterohemorrhagic Escherichia coli in intimate attachment in vitro and in a porcine model. *J Clin Invest* 92:1418-1424, 1993

14. Acheson DW, Moore R, De Breucker S, Lincicome L, Jacewicz M, Skutelsky E, Keusch GT: Translocation of Shiga toxin across polarized intestinal cells in tissue culture. *Infect Immun* 64:3294-3300, 1996

15. te Loo DM, Monnens LA, van Der Velden TJ, Vermeer MA, Preyers F, Demacker PN, van Den Heuvel LP, van Hinsbergh VW: Binding and transfer of verocytotoxin by polymorphonuclear leukocytes in hemolytic uremic syndrome. *Blood* 95:3396-3402, 2000

16. Te Loo DM, van Hinsbergh VW, van den Heuvel LP, Monnens LA: Detection of verocytotoxin bound to circulating polymorphonuclear leukocytes of patients with hemolytic uremic syndrome. *J Am Soc Nephrol* 12:800-806, 2001

17. van de Kar NCAJ, Monnens LAH, Karmali MA, van Hinsbergh VWM: Tumor necrosis factor and interleukin-1 induce expression of the verocytotoxin receptor globotriaosylceramide on human endothelial cells: implications for the pathogenesis of the hemolytic uremic syndrome. *Blood* 80:2755-2764, 1992

18. van Setten PA, Monnens LA, Verstraten RG, van den Heuvel LP, van Hinsbergh VW: Effects of verocytotoxin-1 on nonadherent human monocytes: binding characteristics, protein synthesis, and induction of cytokine release. *Blood* 88:174-183, 1996

19. Tesh VL, Burris JA, Owens JW, Gordon VM, Wadolkowski EA, O'Brien AD, Samuel JE: Comparison of the relative toxicities of Shiga-like toxins type I and type II for mice. *Infect Immun* 61:3392-3402, 1993

20. van Setten PA, van Hinsbergh VW, van der Velden TJ, van de Kar NC, Vermeer M, Mahan JD, Assmann KJ, van den Heuvel LP, Monnens LA: Effects of TNF alpha on verocytotoxin cytotoxicity in purified human glomerular microvascular endothelial cells. *Kidney Int* 51:1245-1256, 1997

21. Pijpers AH, van Setten PA, van den Heuvel LP, Assmann KJ, Dijkman HB, Pennings AH, Monnens LA, van Hinsbergh VW: Verocytotoxin-induced apoptosis of human microvascular endothelial cells. *J Am Soc Nephrol* 12:767-778, 2001

22. Lingwood CA: Role of verotoxin receptors in pathogenesis. *Trends Microbiol* 4:147-153, 1996

23. Maloney MD, Lingwood CA: CD19 has a potential CD77 (globotriaosyl ceramide)-binding site with sequence similarity to verotoxin B-subunits: implications of molecular mimicry for B cell adhesion and enterohemorrhagic Escherichia coli pathogenesis. *J Exp Med* 180:191-201, 1994

24. Nudelman E, Kannagi R, Hakomori S, Parsons M, Lipinski M, Wiels J, Fellous M, Tursz T: A glycolipid antigen associated with Burkitt lymphoma defined by a monoclonal antibody. *Science* 220:509-511, 1983

25. Kiarash A, Boyd B, Lingwood CA: Glycosphingolipid receptor function is modified by fatty acid content. Verotoxin 1 and verotoxin 2c preferentially recognize different globotriaosyl ceramide fatty acid homologues. *J Biol Chem* 269:11138-11146, 1994

26. Arab S, Lingwood CA: Intracellular targeting of the endoplasmic reticulum/nuclear envelope by retrograde transport may determine cell hypersensitivity to verotoxin via globotriaosyl ceramide fatty acid isoform traffic. *J Cell Physiol* 177:646-660, 1998

27. Lingwood CA: Verotoxin-binding in human renal sections. *Nephron* 66:21-28, 1994

28. Taylor FB, Jr., Tesh VL, DeBault L, Li A, Chang AC, Kosanke SD, Pysher TJ, Siegler RL: Characterization of the baboon responses to Shiga-like toxin: descriptive study of a new primate model of toxic responses to Stx-1. *Am J Pathol* 154:1285-1299, 1999

29. van de Kar NCAJ, Kooistra T, Vermeer M, Lesslauer W, Monnens LAH, van Hinsbergh VWM: Tumor necrosis factor α induces endothelial galactosyl transferase activity and verocytotoxin receptors. Role of specific tumor necrosis factor receptors and protein kinase C. *Blood* 85:734-743, 1995

30. Kaye SA, Louise CB, Boyd B, Lingwood CA, Obrig TG: Shiga toxin-associated hemolytic uremic syndrome: interleukin-1 beta enhancement of Shiga toxin cytotoxicity toward human vascular endothelial cells in vitro. *Infect Immun* 61:3886-3891, 1993

31. Milford DV, Staten J, MacGreggor I, Dawes J, Taylor CM, Hill FG: Prognostic markers in diarrhoea-associated haemolytic-uraemic syndrome: initial neutrophil count, human neutrophil elastase and von Willebrand factor antigen. *Nephrol Dial Transplant* 6:232-237, 1991

32. Fitzpatrick MM, Shah V, Trompeter RS, Dillon MJ, Barratt TM: Interleukin-8 and polymorphoneutrophil leucocyte activation in hemolytic uremic syndrome of childhood. *Kidney Int* 42:951-956, 1992

33. Forsyth KD, Simpson AC, Fitzpatrick MM, Barratt TM, Levinsky RJ: Neutrophil-mediated endothelial injury in haemolytic uraemic syndrome. *Lancet* II:411-414, 1989

34. Andreoli SP, Green DF: Verotoxin promotes nitric oxide generation in glomerular endothelial cells (GEC) and accelerates PMN mediated GEC injury. *J Am Soc Nephrol* 8:582, 1997 (Abstract)

35. Inward CD, Howie AJ, Fitzpatrick MM, Rafaat F, Milford DV, Taylor CM: Renal histopathology in fatal cases of diarrhoea-associated haemolytic uraemic syndrome. British Association for Paediatric Nephrology. *Pediatr Nephrol* 11:556-559, 1997

36. van Setten PA, van Hinsbergh VW, van den Heuvel LP, Preyers F, Dijkman HB, Assmann KJ, van der Velden TJ, Monnens LA: Monocyte chemoattractant protein-1 and interleukin-8 levels in urine and serum of patents with hemolytic uremic syndrome. *Pediatr Res* 43:759-767, 1998

37. Inward CD, Varagunam M, Adu D, Milford DV, Taylor CM: Cytokines in haemolytic uraemic syndrome associated with verocytotoxin-producing Escherichia coli infection. *Arch Dis Child* 77:145-147, 1997

38. Matussek A, Lauber J, Bergau A, Hansen W, Rohde M, Dittmar KE, Gunzer M, Mengel M, Gatzlaff P, Hartmann M, Buer J, Gunzer F: Molecular and functional analysis of Shiga toxin-induced response patterns in human vascular endothelial cells. *Blood* 102:1323-1332, 2003

39. Noris M, Ruggenenti P, Todeschini M, Figliuzzi M, Macconi D, Zoja C, Paris S, Gaspari F, Remuzzi G: Increased nitric oxide formation in recurrent thrombotic microangiopathies: a possible mediator of microvascular injury. *Am J Kidney Dis* 27:790-796, 1996

40. Remuzzi G, Galbusera M, Salvadori M, Rizzoni G, Paris S, Ruggenenti P: Bilateral nephrectomy stopped disease progression in plasma-resistant hemolytic uremic syndrome with neurological signs and coma. *Kidney Int* 49:282-286, 1996

41. Tsai HM, Sussman, II, Nagel RL: Shear stress enhances the proteolysis of von Willebrand factor in normal plasma. *Blood* 83:2171-2179, 1994

42. Ruggeri ZM: von Willebrand factor. *J Clin Invest* 99:559-564, 1997

43. Byzova TV, Rabbani R, D'Souza SE, Plow EF: Role of integrin alpha(v)beta3 in vascular biology. *Thromb Haemost* 80:726-734, 1998

44. Cheresh DA: Human endothelial cells synthesize and express an Arg-Gly-Asp-directed adhesion receptor involved in attachment to fibrinogen and von Willebrand factor. *Proc Natl Acad Sci U S A* 84:6471-6475, 1987

45. Perrault C, Lankhof H, Pidard D, Kerbiriou-Nabias D, Sixma JJ, Meyer D, Baruch D: Relative importance of the glycoprotein Ib-binding domain and the RGD sequence of von Willebrand factor for its interaction with endothelial cells. *Blood* 90:2335-2344, 1997

46. Pysher TJ, Siegler RL, Tesh VL, Taylor FB, Jr.: von Willebrand Factor expression in a Shiga toxin-mediated primate model of hemolytic uremic syndrome. *Pediatr Dev Pathol* 5:472-479, 2002

47. Wagner DD: P-selectin chases a butterfly. *J Clin Invest* 95:1955-1956, 1995

48. Frenette PS, Johnson RC, Hynes RO, Wagner DD: Platelets roll on stimulated endothelium in vivo: an interaction mediated by endothelial P-selectin. *Proc Natl Acad Sci U S A* 92:7450-7454, 1995

49. Chong BH, Murray B, Berndt MC, Dunlop LC, Brighton T, Chesterman CN: Plasma P-selectin is increased in thrombotic consumptive platelet disorders. *Blood* 83:1535-1541, 1994

50. Simon M, Cleary TG, Hernandez JD, Abboud HE: Shiga toxin 1 elicits diverse biologic responses in mesangial cells. *Kidney Int* 54:1117-1127, 1998

51. Hughes AK, Stricklett PK, Schmid D, Kohan DE: Cytotoxic effect of Shiga toxin-1 on human glomerular epithelial cells. *Kidney Int* 57:2350-2359, 2000

52. Ergonul Z, Clayton F, Fogo AB, Kohan DE: Shigatoxin-1 binding and receptor expression in human kidneys do not change with age. *Pediatr Nephrol* 18:246-253, 2003

53. Hughes AK, Stricklett PK, Kohan DE: Shiga toxin-1 regulation of cytokine production by human glomerular epithelial cells. *Nephron* 88:14-23, 2001

54. Schmid DI, Kohan DE: Effect of shigatoxin-1 on arachidonic acid release by human glomerular epithelial cells. *Kidney Int* 60:1026-1036, 2001

55. Kaneko K, Kiyokawa N, Ohtomo Y, Nagaoka R, Yamashiro Y, Taguchi T, Mori T, Fujimoto J, Takeda T: Apoptosis of renal tubular cells in Shiga-toxin-mediated hemolytic uremic syndrome. *Nephron* 87:182-185, 2001

56. Takeda T, Dohi S, Igarashi T, Yamanaka T, Yoshiya K, Kobayashi N: Impairment by verotoxin of tubular function contributes to the renal damage seen in haemolytic uraemic syndrome. *J Infect* 27:339-341, 1993

57. Hughes AK, Stricklett PK, Kohan DE: Cytotoxic effect of Shiga toxin-1 on human proximal tubule cells. *Kidney Int* 54:426-437, 1998

58. Taguchi T, Uchida H, Kiyokawa N, Mori T, Sato N, Horie H, Takeda T, Fujimoto J: Verotoxins induce apoptosis in human renal tubular epithelium derived cells. *Kidney Int* 53:1681-1688, 1998

CHAPTER 2

THE ROLE OF THE ENDOTHELIUM IN HEMOLYTIC UREMIC SYNDROME

C. Zoja, M. Morigi, G. Remuzzi

J Nephrol 2001; 14: S58-62

The role of the endothelium in hemolytic uremic syndrome

Carla Zoja[1], Marina Morigi[1], Giuseppe Remuzzi[1,2]

[1] Mario Negri Institute for Pharmacological Research, Bergamo - Italy
[2] Unit of Nephrology and Dialysis, Bergamo Hospital, Bergamo - Italy

ABSTRACT: Hemolytic uremic syndrome (HUS), which is the most common cause of acute renal failure in children, is caused by Shiga toxin-producing *Escherichia coli* infection. This infection leads to renal and other organ microvascular thrombosis. Endothelial injury has been recognized as the trigger event in the development of microangiopathic process. Evidence suggests that leukocyte as well as platelet activation participate in endothelial damage. Intrinsic abnormalities of the complement system may also play a role in HUS.

Key words: *Verotoxin, Endothelium, Platelets, Leukocytes, Complement*

INTRODUCTION

Hemolytic uremic syndrome (HUS) is a disease comprising non-immune hemolytic anemia, thrombocytopenia and renal failure due to platelet thrombi in the microcirculation of the kidney and other organs (1, 2). The characteristic lesion, thrombotic microangiopathy, is unique to this syndrome. It consists of vessel wall thickening, with swelling and detachment of endothelial cells from the basement membrane and accumulation of fluffy material in the subendothelium (3). In its typical presentation, HUS manifests as an acute disease, with gastrointestinal or respiratory tract prodromes. Recovery without sequelae occurs in 80 to 90% of cases, either spontaneously (as in most cases of childhood HUS) or following plasma infusion or exchange (as in adult or severe forms of HUS). Typical HUS is triggered by environmental factors, drugs or infective agents such as verotoxin or Shiga-toxin-producing *E. coli*; systemic immune disorders or cancer may also cause the disease (1, 2). These forms of HUS may subside when the underlying condition has been treated or removed. However, there are rare forms, often occurring in families, which frequently relapse even after complete recovery of the presenting episode, with death or permanent neurological or renal sequelae being the final outcome in the large majority of cases. These atypical forms are considered to be supported by a genetic background of predisposition to microvascular thrombosis. Both autosomal recessive and autosomal dominant mode of inheritance have been recognized, with precipitating events such as pregnancy, virus-like disease or sepsis being identified in some but not in all series.

SHIGA TOXIN AS FOSTERER OF HUS

In 90% of cases of typical diarrhea-associated (D+) HUS in children, infection with *E. coli* producing a verotoxin (VT) also termed Shiga toxin (Stx), especially serotype O157:H7, has been strongly implicated as the most common causative agent of this disease (1, 4-6). Undercooked meat, unpasteurized milk, apple juice, radish sprouts and sausages have all been implicated in the transmission of *E. coli*. (7). Water-born as well as person to person transmission in either sporadic cases or outbreaks have also been reported. It is estimated that following exposition to *E. coli* O157:H7, 38% to 61% of persons develop hemorrhagic colitis, and 2% to 7% of these patients progress to overt HUS. Endothelial injury has been recognized as the trigger event in the development of microangiopathic process of HUS and evidence points to Shiga toxins as critical determinants for the development of vascular lesions (1, 2, 5, 8, 9). Stx-1 and Stx-2 or (VT-1 and VT-2) consist of a biologically active subunit A and five B subunits that allow binding of the toxin to a specific

glycosphingolipid globotriaosyl ceramide (Gb3) receptors on the endothelial cell surface. The binding is followed by internalization in the cytosol of the A subunit, which inhibits protein synthesis by inactivating ribosomal subunits and causes cell death (10) or apoptosis (11). After the ingestion of contaminated food or water, *E.coli* binds to specific receptors on the colonic mucosa, multiplies and causes cell death. This normally leads to diarrhea, but strains that produce Stx damage the vasculature of the mucosa, causing hemorrhagic colitis. Microvascular damage develops at target organs when the toxin gains access to the systemic circulation. Recent studies have contributed to clarify how Stx/VT, once it has reached the circulation, is transferred to the kidney (12). It has been shown that when VT-1 is incubated in whole blood *in vitro* it binds rapidly and completely to human polymorphonuclear leukocytes (PMN). Binding studies with ^{125}I-VT-1 showed a single class of binding sites on freshly isolated, non stimulated human PMN. Interestingly, the Kd of the high affinity receptor for VT on PMN was 100-fold less than that found for the functional receptor for VT, Gb3, on glomerular microvascular endothelial cells (GMVEC), which facilitated transfer of the toxin from PMN to GMVEC. Indeed, incubation of PMN, that had bound fluoresceinated VT with GMVEC resulted in passing of VT to GMVEC and subsequent inhibition of protein synthesis and cell death. Stimulating the GMVEC with inflammatory mediators, such as TNFα or LPS, upregulated the VT receptor Gb3 on cell surface and favored transfer of VT-1 from PMN. These *in vitro* data were further supported by the detection of VT-2 in the circulation of 9 out of 10 patients with the epidemic form of HUS, bound exclusively to PMN (13). The detection of VT-2 bound to PMN was associated with diarrhea at the time the blood samples were obtained.

It has been demonstrated that *in vitro* purified human monocytes bound VT significantly after activation by LPS, and that after toxin challenge the monocytes released cytokines like IL-1 and TNF that remarkably potentiated sensitivity of vascular endothelial cells to VT by upregulating endothelial Gb3 receptors (10, 14).

Shiga toxin and endothelial cell injury through leukocyte activation

The interaction between leukocytes and endothelial cells is instrumental to the development of microvascular injury in Stx-associated HUS as documented by experimental and clinical evidence. First, the number of neutrophils is elevated in HUS, and it was suggested that it is a predictive factor for the outcome of the disease (15). In addition, Fitzpatrick et al (16) described that neutrophils of HUS patients were activated as indicated by the fact that plasma concentrations of α1-antitrypsin-complexed elastase and the chemokine interleukin-8 (IL-8) – a potent activator of neutrophils-were remarkably higher in the acute phase of the disease. Neutrophils from children with acute phase of HUS adhered to endothelial cells *in vitro* more than normal neutrophils and induced endothelial injury by degrading endothelial cell fibronectin, possibly depending on the release of neutrophil-specific proteases (17). A preliminary report showed that glomerular endothelial cells exposed to Stx became more susceptible to neutrophil-mediated oxidant injury (18). Some years ago we demonstrated for the first time that Stx-1 promoted a massive leukocyte adhesion to cultured human umbilical vein endothelial cells (HUVEC) under flow conditions, by upregulating endothelial expression of the adhesive proteins E-selectin, ICAM-1 and VCAM-1 (19). The adhesion of leukocytes was enhanced by pre-exposure of endothelial cells to TNFα. Stx-1 was able to inhibit the process of rolling that normally precedes adhesion of cells to the endothelium.

Histological examination of kidney specimens from HUS children with evidence of Stx-producing *E.coli* infection, revealed a conspicuous infiltration of mononuclear and polymorphonuclear cells within the glomeruli, along with microvascular injury (20,21). In those patients urinary levels of IL-8 and monocyte chemoattractant protein-1 (MCP-1), potent attractants of neutrophils, and monocytes/macrophages and T-lymphocytes, respectively, were elevated during the acute phase of the disease, and gradually declined until recovery. This implied a role for these chemokines in the recruitment of inflammatory cells at glomerular level (21,22). Recently, we showed that Stx-induced leukocyte adhesion was followed by transmigration of leukocytes across the endothelium, under flow conditions, and that IL-8 and MCP-1 were implicated in the adhesive phenomena (23). The expression of IL-8 and MCP-1 mRNAs were upregulated after exposure of endothelial cells to subtoxic concentrations of Stx-2. Increased levels of chemokine transcripts were preceded by activation of the transcription factor NF-kB as revealed by electrophoretic mobility shift assay. Blocking of endothelial IL-8 and MCP-1 with corresponding antibodies significantly inhibited Stx-induced leukocyte adhesion and transmigration.

Among the inflammatory mediators that are released from adherent neutrophils, reactive oxygen species have been shown to exert a direct cytotoxic effect on vascular endothelium. Neutrophils from patients with HUS produced excessive superoxide anion (O_2^-), which suggested that oxygen radicals caused neutrophil-induced endothelial damage in these patients (24). Injured endothelium changes its normal throm-

boresistant phenotype and becomes thrombogenic initiating microvascular thrombus formation.

Shiga toxin and endothelial cell injury through platelet activation

We have recently demonstrated that Stx is a potent promoter of platelet adhesion and thrombus formation on cultured endothelial cells perfused with whole blood in a flow chamber system under high shear stress levels that mimic the ones encountered in the microcirculation (25). The effect of Stx was superior to that of other known thrombogenic agonists such as thrombin and cytokines. Microvascular endothelial cells of dermal origin demonstrated a remarkably greater sensitivity to the thrombogenic effect of Stx than endothelium derived from large vessels (HUVEC), possibly due to the higher expression of Stx receptors (20-fold more). In the attempt to identify the adhesive proteins involved in platelet-endothelial cell interactions elicited by Stx, which resulted in thrombus formation on microvascular endothelial cells, we first focused on the von Willebrand factor (vWF), which is the indispensable adhesive substrate to promote platelet thrombus formation in high shear stress environments (26). Changes in shear stress, the tractive force produced by blood flowing over the endothelial surface, have a profound influence on vWF handling by enhancing its susceptibility to proteolytic cleavage (27). vWF under conditions of high shear stress undergoes conformational changes and serves as a bridge between subendothelial matrix and glycoprotein (GP) Ib expressed on platelet membrane (26). The engagement of this receptor promotes activation of platelet $\alpha_{IIb}{}^{\beta}{}_{3}$ (GPIIb/IIIa) complex that binds to the RGD sequence of vWF leading to thrombus formation. We found that polymeric aurin tricarboxylic acid (ATA), an inhibitor of vWF-platelet GPIb interaction, completely prevented the deposition of thrombi (25). Furthermore, blockade of $\alpha_{IIb}{}^{\beta}{}_{3}$ on activated platelets by chimeric 7E3 Fab also abrogated platelet adhesion and thrombus formation, suggesting the involvement of vWF-platelet interaction at high shear stress in this phenomenon. Other experiments showed that functional blockade of endothelial β_3 integrin subunit, vitronectin receptor, P-selectin and PECAM-1 with specific antibodies was associated with a significant decrease of the endothelial area covered by thrombi (25). In addition, confocal microscopy studies revealed that Stx increased the expression of vitronectin receptor and P-selectin, and redistributed PECAM-1 away from cell-cell border of endothelial cells, thus indicating that the above endothelial adhesion molecules are directly involved and possibly determine the effect of Stx of enhancing platelet adhesion and thrombus formation in microvascular endothelium. In conclusion, these results might be relevant to understanding why thrombi in HUS localize in microvessels rather than in larger ones. They may also provide insights on the molecular events involved in the process of microvascular thrombosis associated with D+HUS.

Complement and HUS

Apart from Stx other agents potentially toxic to the vascular endothelium - such as certain viruses, bacteria, immunecomplexes and cytotoxic drugs - have been proposed as possible triggers of microvascular thrombosis of HUS. Independently from its causative agent, local thrombosis amplifies the inflammatory injury by promoting complement deposition within capillary vessels through formation of the C3bBb convertase of the alternative pathway of complement activation. Evidence implicating the complement system, and in particular the alternative pathway, exists for all forms of HUS. Low C3 levels were first described in D+HUS in the early 1970s and it has also been reported that persistently low levels are predictive of a poor prognosis (28). Hypocomplementemia was also found in sporadic and familial forms of HUS (29). Granular C3 deposits in glomeruli and arterioles of HUS patients and evidence of C3 breakdown products in HUS sera document that low C3 concentrations probably reflect complement consumption in the microvasculature. At variance with typical and sporadic forms in which hypocomplementemia subsides with remission of the disease, in recurrent and familial cases serum C3 levels are often consistently and remarkably depressed even during remission. This was initially attributed to an inherited defect in C3 synthesis, but much more convincing data are now available indicating that low C3 in HUS derives from either lack or altered function of factor H, a regulatory component of the alternative pathway of the complement system (30). By multivariated analysis on 35 cases of familial HUS from 10 families, we showed that decreased C3 levels correlated with history of disease and were associated with a 16.6-fold increased relative risk of developing HUS within the families (29). In this series low C3 levels also correlated with factor H deficiency. In addition, a recent report documented that an area on chromosome 1q, where factor H is mapped, segregates with HUS; in one family a mutation in factor H gene was found, consisting in a C to G transversion causing an arginine to glycine change in Short Consensus Repeat 20 (SCR20) (31). The same authors also described a nonsense mutation, located in SCR1 of factor H, in a sporadic case with late onset (31). In a large series of patients with familial history of HUS, we

found four new heterozygous mutations in factor H gene (32). Three of the mutations were observed in families with dominant transmission, the fourth was found in a single case of a patient who experienced disease recurrence on the renal allograft. Another study reported an apparent mutation in factor H (a C to T transition in SCR 20) in a family with HUS with a recessive mode of inheritance and severely depressed factor H levels (33). However, two independent groups subsequently documented that the apparent mutation was an artifact caused by coamplification of a factor H-related gene. They demonstrated that the real mutation in this family is an A to T transversion and a 24 bp deletion that was present in homozygosity in affected member patients and in heterozygosity in the healthy carriers (34, 35). Altogether, these data provide compelling molecular evidence that genetic alterations in factor H are involved in both autosomal dominant and recessive HUS. Data showing that following exposure to Stx producing *E. coli*, only 2 to 7% of patients progress to overt HUS suggest that a genetic predisposition may have a role also in typical D+ forms. Polymorphisms in the promoter and in the coding regions of factor H gene have been recently described. It is intriguing to speculate that some of these polymorphic variants confer a genetic predisposition to Stx-induced HUS.

Correspondence to:
Giuseppe Remuzzi, M.D.
"Mario Negri" Institute for Pharmacological Research
Via Gavazzeni, 11
24125 Bergamo, Italy
gremuzzi@marionegri.it

References

1. Remuzzi G, Ruggenenti P. The hemolytic uremic syndrome. Kidney Int 1995; 47: 2-19.
2. Ruggenenti P, Noris M, Remuzzi G. Thrombotic microangiopathy, hemolytic uremic syndrome, and thrombotic thrombocytopenic purpura. Kidney Int 2001; 60: 831-46.
3. Remuzzi G, Ruggenenti P, Bertani T. Thrombotic microangiopathies. In Tisher, CC, Brenner BM Eds. Renal Pathology. With Clinical and Functional Correlations. Philadelphia: J.B. Lippincott Company 1994; 1154-84.
4. Karmali MA, Petric M, Lim C, Fleming PC, Arbus GS, Lior M. The association between idiopathic hemolytic uremic syndrome and infection by verotoxin-producing *Escherichia coli*. J Infect Dis 1985; 151: 775-82.
5. Arbus GS. Association of verotoxin-producing *E. coli* and verotoxin with hemolytic uremic syndrome. Kidney Int 1997; 51: S-91-6.
6. Andreoli SP. The pathophysiology of the hemolytic uremic syndrome. Curr Opin Nephrol Hypertens 1999; 8: 459-64.
7. Mead PS, Griffin PM. *Escherichia coli* 0157:H7. Lancet 1998; 352: 1207-12.
8. Zoja C, Remuzzi G. The pivotal role of the endothelial cell in the pathogenesis of HUS. In Kaplan BS, Trompeter RS, Moake JL Eds. Hemolytic uremic syndrome and thrombotic thrombocytopenic purpura. New York: Marcel Dekker 1992; 389.
9. Obrig TG. Pathogenesis of shiga toxin (verotoxin)-induced endothelial cell injury. In Kaplan BS, Trompeter RS, Moake JL Eds. Hemolytic uremic syndrome and thrombotic thrombocytopenic purpura. New York: Marcel Dekker 1992; 405.
10. van de Kar NCAJ, Monnens LAH, Karmali MA, van Hinsbergh VWM. Tumor necrosis factor and interleukin-1 induce expression of the verocytotoxin receptor globotriaosylceramide on human endothelial cells: implications for the pathogenesis of the hemolytic uremic syndrome. Blood 1992; 80: 2755-64.
11. Pijpers AH, van Setten PA, Van den Heuvel LP. Verocytotoxin-induced apoptosis of human microvascular endothelial cells. J Am Soc Nephrol 2001; 12: 767-78.
12. Te Loo DM, Monnens LA, van der Velden TJ. Binding and transfer of verocytotoxin by polymorphonuclear leukocytes in hemolytic uremic syndrome. Blood 2000; 95: 3396-402.
13. Te Loo DM, Van Hinsbergh VW, Van den Heuvel LP, Monnens LA. Detection of verototoxin bound to circulating polymorphonuclear leukocytes of patients with hemolytic uremic syndrome. J Am Soc Nephrol 2001; 12: 800-6.
14. van Setten PA, Monnens LAH, Verstraten RGG, van den Heuvel LPWJ, van Hinsbergh VWM. Effects of verocytotoxin-1 on nonadherent human monocytes: binding characteristics, protein synthesis, and induction of cytokine release. Blood 1996; 88: 174-83.
15. Milford DV, Staten J, MacGreggor I, Dawes J, Taylor CM, Hill FG. Prognostic markers in diarrhoea-associated haemolytic-uremic syndrome: initial neutrophil count, human neutrophil elastase and von Willebrand factor antigen. Nephrol Dial Transplant 1991; 6: 232-7.
16. Fitzpatrick MM, Shah V, Trompeter RS, Dillon MJ, Barratt TM. Interleukin-8 and polymorphoneutrophil leukocyte activation in hemolytic uremic syndrome of childhood. Kidney Int 1992; 42: 951-6.
17. Forsyth KD, Simpson AC, Fitzpatrick MM, Barratt TM, Levinsky RJ. Neutrophil-mediated endothelial injury in haemolytic uremic syndrome. Lancet 1989; 2: 411-4.
18. Andreoli SP, Green DF. Verotoxin 1 promotes nitric oxide (NO) generation in glomerular endothelial cells (GEC) and accelerates PMN mediated GEC injury. J Am Soc Nephrol 1997; 8: 582A-5820.(Abstract)
19. Morigi M, Micheletti G, Figliuzzi M. Verotoxin-1 promotes leukocyte adhesion to cultured endothelial cells under physiologic flow conditions. Blood 1995; 86: 4553-8.
20. Inward CD, Howie AJ, Fitzpatrick MM. Renal histopathology in fatal cases of diarrhoea-associated haemolytic uremic syndrome. Pediatr Nephrol 1997; 11: 556-9.

21. van Setten PA, van Hinsbergh VWM, van den Heuvel LPWJ. Monocyte chemoattractant protein-1 and interleukin-8 levels in urine and serum of patients with hemolytic uremic syndrome. Pediatr Res 1998; 43: 759-67.
22. Inward CD, Varagunam M, Adu D, Milford DV, Taylor CM. Cytokines in haemolytic uremic syndrome associated with verocytotoxin-producing *Escherichia coli* infection. Arch Dis Child 1997; 77: 145-7.
23. Zoja C, Morigi M, Donadelli R. Verotoxin-2 induces subendothelial leukocyte transmigration via upregulation of MCP-1 and IL-8. J Am Soc Nephrol 1999; 10: 595A. (Abstract)
24. Noris M, Ruggenenti P, Todeschini M. Increased nitric oxide formation in recurrent thrombotic microangiopathies: a possible mediator of microvascular injury. Am J Kidney Dis 1996; 27: 790-6.
25. Morigi M, Galbusera M, Binda E. Verotoxin-1-induced upregulation of adhesive molecules renders microvascular endothelial cells thrombogenic at high shear stress. Blood 2001; 98: 1828-35.
26. Ruggeri ZM. Perspectives series: Cell adhesion in vascular biology. von Willebrand Factor. J Clin Invest 1997; 99: 559-64.
27. Tsai H-M, Sussman II, Nagel RL. Shear stress enhances the proteolysis of von Willebrand factor in normal plasma. Blood 1994; 83: 2171-9.
28. Stuhlinger W, Kourilsky O, Kanfer A, Sraer JD. Hemolytic-uremic syndrome: evidence for intravascular C3 activation. Lancet 1974; 2: 788-9.
29. Noris M, Ruggenenti P, Perna A, et al. Hypocomplementemia discloses genetic predisposition to hemolytic uremic syndrome and thrombotic thrombocytopenic purpura: role of factor H abnormalities. Italian Registry of Familial and Recurrent Hemolytic Uremic Syndrome/Thrombotic Thrombocytopenic Purpura. J Am Soc Nephrol 1999; 10: 281-93.
30. Zipfel PF. Hemolytic uremic syndrome: how do factor H mutants mediate endothelial damage? Trends Immunol 2001; 22: 345-8.
31. Warwicker P, Goodship TH, Donne RL. Genetic studies into inherited and sporadic hemolytic uremic syndrome. Kidney Int 1998; 53: 836-44.
32. Caprioli J, Bettinaglio P, Zipfel PF. The molecular basis of familial hemolytic uremic syndrome: mutation analysis of factor H gene reveals a hot spot in short consensus repeat 20. J Am Soc Nephrol 2001; 12: 297-307.
33. Ying L, Katz Y, Schlesinger M. Complement factor H gene mutation associated with autosomal recessive atypical hemolytic uremic syndrome. Am J Hum Genet 1999; 65: 1538-46.
34. Buddles MR, Donne RL, Richards A, Goodship J, Goodship TH. Complement factor H gene mutation associated with autosomal recessive atypical hemolytic uremic syndrome. Am J Hum Genet 2000; 66: 1721-2.
35. Caprioli J, Bettinaglio P, Vasile B. Factor H (HF) gene mutation in familial hemolytic uremic syndrome (HUS). J Am Soc Nephrol 2000; 11: 404A (Abstract).

CHAPTER 3

VEROTOXIN-1 PROMOTES LEUKOCYTE ADHESION TO CULTURED ENDOTHELIAL CELLS UNDER PHYSIOLOGIC FLOW CONDITIONS

M. Morigi, G. Micheletti, M. Figliuzzi, B.Imberti, M.A. Karmali, A. Remuzzi, G. Remuzzi, and C. Zoja

Blood 1995; 86: 4553-4558

Verotoxin-1 Promotes Leukocyte Adhesion to Cultured Endothelial Cells Under Physiologic Flow Conditions

By Marina Morigi, Gianluca Micheletti, Marina Figliuzzi, Barbara Imberti, Mohamed A. Karmali, Andrea Remuzzi, Giuseppe Remuzzi, and Carla Zoja

Hemolytic uremic syndrome (HUS), which is the most common cause of acute renal failure in infants and small children, is caused by verotoxin (VT)-producing *Escherichia coli* infection. Endothelial injury determines microvascular thrombosis and evidence is available from recent studies that suggests that leukocyte activation participates in endothelial damage. We studied here the effect of VT-1 on leukocyte adhesion to vascular endothelium under physiologic flow conditions. Human umbilical vein endothelial cells (HUVECs) were incubated for 24 hours with VT-1 (0.1, 1, and 10 pmol/L) and then exposed to a total leukocyte suspension in a parallel plate flow chamber under laminar flow conditions (1.5 dynes/cm²). Adherent cells were counted by digital image processing. Results showed that VT-1 dose-dependently increased the number of adhering leukocytes to HUVECs as compared with unstimulated cells. The adhesive response elicited by VT-1 was comparable to that of interleukin-1β (IL-1β), one of the most potent inducers of endothelial cell adhesiveness. Exposure of HUVECs to VT-1 did not affect the number of rolling leukocytes, which was similar to that of control values. To examine the role of adhesion molecules in VT-1–induced leukocyte adhesion, HUVECs were incubated with mouse monoclonal antibodies against E-selectin, intercellular adhesion molecule-1 (ICAM-1), and vascular cell adhesion molecule-1 (VCAM-1) before adhesion assay. Functional blocking of E-selectin, ICAM-1, and VCAM-1 on endothelial cells significantly inhibited VT-1–induced increase in leukocyte adhesion. In some experiments, before VT-1 incubation, HUVECs were pretreated for 24 hours with tumor necrosis factor α (TNFα; 100 U/mL), which is known to increase VT receptor expression on HUVECs. The number of adhering leukocytes on HUVECs exposed to TNFα and VT-1 significantly increased as compared with HUVECs incubated with VT-1 and TNFα alone. These results suggest that VT-1 modulates leukocyte-endothelium interaction, thus increasing leukocyte adhesion and upregulating adhesive proteins on endothelial surface membrane.

RESEARCH IN THE last few years has established a link between enteric infection with verotoxin (VT)-producing *Escherichia coli* (VTEC) and hemolytic uremic sindrome (HUS),[1-3] a disorder of thrombocytopenia, microangiopathic hemolytic anemia, and acute renal failure that mainly affects infants and small children.[4]

VT (or Shiga-like toxins, a family of *E coli*-derived toxins)[5] bind to a specific receptor identified as the glycosphingolipid globotriaosylceramide (Gb_3)[6,7] on leukocytes and endothelial cells of target organs, and cell susceptibility to VT damage is a function of Gb_3 expression on cell membranes.[8,9] In North America and Western Europe, 90% of children with epidemic diarrhea-associated HUS have evidence of VTEC infection.[3,10] It is now clear that vascular endothelial cell injury is central to the full development of microangiopatic lesions,[11] but the complex mechanism(s) underlying endothelial perturbation and damage in this disease is far from being defined. The toxicity of VT-1 on vascular endothelial cells in culture is remarkably potentiated by leukocyte-derived tumor necrosis factor α (TNFα), which also contributes to upregulate Gb_3 receptors on endothelial cells.[9,12] TNFα-induced upregulation of VT-1 receptors on endothelial cells depends on galactosyl transferase induction[13] by a mechanism independent of protein kinase C activation. Endothelial surface expression of VT-1 receptor then orients subsequent localization of microvascular damage, as documented by animal experiments.[14] Thus, TNFα appears a crucial molecule in the sequence of events leading to endothelial damage in VTEC-associated forms of childhood HUS. Finding that circulating inflammatory cells including macrophages (the main source of TNFα in humans) constitutively express VT-1 receptors and release TNFα in vitro upon VT-1 binding to its specific receptors[15] led investigators to consider the possibility that, in HUS, interaction between activated leukocytes and endothelial cells is indeed instrumental to the development of microvascular injury. Preliminary data have suggested that endothelial damage might critically depend on neutrophil-specific proteases, particularly elastases, released by activated hyperadherent leukocytes.[16] Consistent with this possibility are findings that levels of plasma leukocyte elastase were remarkably higher than normal in children with diarrhea-associated HUS, which presumably reflected leukocyte activation in vivo.[17]

The present study was designed to clarify whether VT-1 directly modulated leukocyte adhesion to endothelial cells. Experiments were planned to address (1) the effect of VT-1 on leukocyte adhesion to cultured endothelial cells exposed to flow conditions that mimic postcapillary venule circulation; (2) the molecular determinants of VT-1–induced leukocyte adhesion; and (3) the possible role of TNFα of amplifying VT-1–induced leukocyte adhesion to endothelial cells.

MATERIALS AND METHODS

Endothelial cell culture. Endothelial cells were obtained from human umbilical veins (HUVECs) by collagenase digestion according to the method of Jaffe et al.[18] The cells were grown in Medium 199 (GIBCO, Grand Island, NY) supplemented with 10% newborn calf serum (GIBCO), 10% human serum, and antibiotics. Cultures were grown at 37°C in 5% CO_2-95% air. Confluent HU-

From the Mario Negri Institute for Pharmacological Research, Bergamo, Italy; the Division of Nephrology and Dialysis, Ospedali Riuniti di Bergamo, Bergamo, Italy; and the Department of Microbiology, The Hospital for Sick Children, Toronto, Ontario, Canada.

Submitted June 12, 1995; accepted August 7, 1995.

Address reprint requests to Marina Morigi, Biol SciD, Mario Negri Institute for Pharmacological Research, Via Gavazzeni 11, 24125 Bergamo, Italy.

The publication costs of this article were defrayed in part by page charge payment. This article must therefore be hereby marked "advertisement" in accordance with 18 U.S.C. section 1734 solely to indicate this fact.

0006-4971/95/8612-0005$3.00/0

VECs were routinely used for experiments between the first and fifth passage. Cultured cells were identified as endothelial by their cobblestone morphology and the presence of von Willebrand factor, using indirect immunofluorescence microscopy. HUVECs were plated on 60- × 20-mm plastic coverslips (Thermanox; Nunc, Naperville, IL) coated with bovine gelatin and used 2 days after reaching confluence. HUVECs were incubated for 24 hours with control medium (M199 plus 10% fetal calf serum) or VT-1 (0.1, 1, and 10 pmol/L). Purified VT-1 was prepared in the laboratory of Dr M.A. Karmali (1.2 mg protein/mL; CD50 vero-cells: titer, 10^{-8} to 10^{-9}).[8] Endotoxin content of the VT-1 preparation was determined to less than 0.05 EU/mL using Limulus amoebocyte lysate assay (E-Toxic; Sigma Chemicals, St Louis, MO) at detection levels of 0.05 to 0.10 EU/mL. HUVECs stimulated for 4 hours with recombinant human interleukin-1β (IL-1β; 100 U/mL; 5×10^7 U/mg protein; Boheringer Mannheim, Mannheim, Germany) were used as positive control. Endotoxin contamination of VT-1 preparation was ruled out as a cause of VT-1–induced leukocyte adhesion by experiments in which HUVECs were incubated for 24 hours with endotoxin (Bacto Lipopolysaccharide [LPS]; *Escherichia coli* 0111:B4; Difco Laboratories, Detroit, MI) at a concentration that approximated that present in 10 pmol/L VT-1. In some experiments, after VT-1 incubation, HUVECs were treated with mouse monoclonal antibody (MoAb)-adhesion blockade anti–E-selectin (BBIG-E4; British Bio-Technology Products Ltd, Abingdon, Oxon, UK), anti–intercellular adhesion molecule-1 (ICAM-1) (BBIG-I1) or anti–vascular cell adhesion molecule-1 (VCAM-1) (BBIG-V1) at 10 μg/200 μL or with a mouse isotype-matched MoAb (IgG1, clone 2H4; British Bio-Technology) for 20 minutes before the adhesion assay. At the end of incubation, cells were exposed to human total leukocytes in a parallel-plate flow chamber for adhesion assay. In additional experiments, HUVECs were pretreated for 24 hours with human recombinant TNFα (100 or 300 U/mL; 6.1×10^7 U/mg protein; gift from BASF KNOLL, Ludwigshafen, Germany) before incubation for 24 hours with VT-1 (10 pmol/L).

Parallel-plate flow chamber. For adhesion experiments, we used a parallel-plate flow chamber as previously described.[19-21] Briefly, the chamber is composed of two parallel surfaces, a coverslip coated with HUVECs at confluence and a flat surface machined from polymethylmethacrylate, separated by a 250-μm thick silicon rubber gasket, leaving a rectangular surface (30 × 13 mm) exposed to flow. An inlet and an outlet channel distribute the fluid uniformly along the entrance side of the adhesion surface. After assembling with the HUVEC monolayer, the chamber is placed on the stage of an inverted phase-contrast microscope with a termostated hood to maintain the temperature at 37°C. The microscope is connected with a videorecording system (VHS; Panasonic, Osaka, Japan).

Adhesion assay under flow conditions. Before adhesion experiments, a leukocyte suspension was prepared from fresh venous blood collected on EDTA (final concentration, 5 mmol/L) and diluted with an equal volume of cold saline solution. The blood samples were centrifuged at 200*g* for 10 minutes at 4°C, the cell pellet was resuspended in 4 vol of Emagel (Behringwerke AG, Marburg, Germany), and erythrocytes were sedimented at 4°C for 40 minutes. Supernatant was removed and centrifuged at 500*g* for 7 minutes at 4°C, and the pellet washed twice by centrifugation with saline. Remaining erythrocytes were removed by ammonium chloride lysis at 4°C and centrifugation. After this procedure, the cell viability, measured by trypan blue exclusion, was greater than 95%. Cells were then resuspended in culture medium at a final concentration of 10^6 cells/mL.

Leukocyte suspension was pumped through the chamber on HUVEC monolayers, at controlled flow rates, using a syringe pump (Harvard Apparatus Inc, South Natick, MA). After an initial perfusion of the flow chamber at 0.6 dynes/cm^2 for 2 minutes for equilibration, the total leukocyte suspension was perfused through the chamber at a constant flow rate (1.5 dynes/cm^2) and images recorded using a video recording system. After 10 minutes of perfusion, the flow rate of the cell suspension was increased so that wall shear stress increased from 1.5 to 3.0 dynes/cm^2 to measure the number of cells rolling on the HUVEC surface. At this flow rate, leukocytes rolling on the adhesion surface are easily distinguishable from cells freely flowing in the suspension that move much faster. Images of adhering leukocytes on the HUVEC surface were digitized and processed on a personal computer using general purpose image processing software (NIH Image, v. 1.43, Bethesda, MD). The number of rolling cells on HUVEC surface at 3.0 dynes/cm^2 was determined on a series of 16 consecutive images digitized during a 10-second interval. Adherent leukocytes were identified and counted at the end of 13 minutes of perfusion.[20,21] All images were then superimposed by digital processing so that moving cells could be distinguished from their wake.

Statistical analysis. Results are expressed as the mean ± SE. Statistical analysis was performed using analysis of variance and the Tukey-Cicchetti test for multiple group comparisons, as appropriate.[22] Statistical significance was defined as $P < .05$.

RESULTS

Effect of VT-1 on leukocyte adhesion to HUVECs under physiologic flow conditions. We have studied the adhesion of peripheral total leukocytes to control, VT-1–treated (0.1, 1, and 10 pmol/L), and IL-1β–treated (100 U/mL) HUVECs under flow conditions. We used VT-1 at concentrations (chosen according to previous studies[8,9]) that did not affect cell morphology (Fig 1) and cell count after 24 hours of incubation (VT-1 at 10 pmol/L: 69.4 ± 2.0 × 10^4 cells *v* control: 65.5 ± 2.5 × 10^4 cells). As shown in Fig 2, exposure of HUVECs for 24 hours to increasing concentrations of VT-1 dose-dependently increased the number of leukocytes adhering to HUVECs after 13 minutes of perfusion, as compared with unstimulated control cells. On average 62 ± 7 leukocytes/mm^2 adhered to unstimulated HUVECs. Exposure of HUVECs to 0.1 pmol/L VT-1 did not modify the number of adherent leukocytes, which averaged 62 ± 4 leukocytes/mm^2. VT-1 at 1 pmol/L concentration significantly ($P < .01$) increased the number of adhering leukocytes as compared with control cells; on average, 181 ± 30 leukocytes/mm^2 adhered on the HUVEC surface. A similar adhesive response was observed after incubation with 10 pmol/L VT-1, with the number of adherent cells averaging 186 ± 20 leukocytes/mm^2 ($P < .01$ *v* control). On IL-1β–stimulated HUVECs, the mean number of firmly attached cells reached 226 ± 29 leukocytes/mm^2.

The possibility that VT-1–induced leukocyte adhesion could be due to endotoxin contamination of VT-1 preparations was ruled out by experiments showing that the number of leukocytes adhering to HUVECs exposed for 24 hours to LPS was similar to that of control HUVECs (66 ± 9 *v* 58 ± 9 leukocytes/mm^2). Figure 3 depicts digitized images from a representative experiment at the end of 13 minutes of leukocyte perfusion. A limited number of leukocytes firmly adhered to control HUVECs. A more than threefold increase in leukocyte adhesion was observed on HUVEC monolayers exposed for 24 hours to VT-1 (10 pmol/L). A similar response was elicited by IL-1β, which is one of the most potent inducers of endothelial cell adhesive properties.

The number of leukocytes rolling at 3 dynes/cm^2 are re-

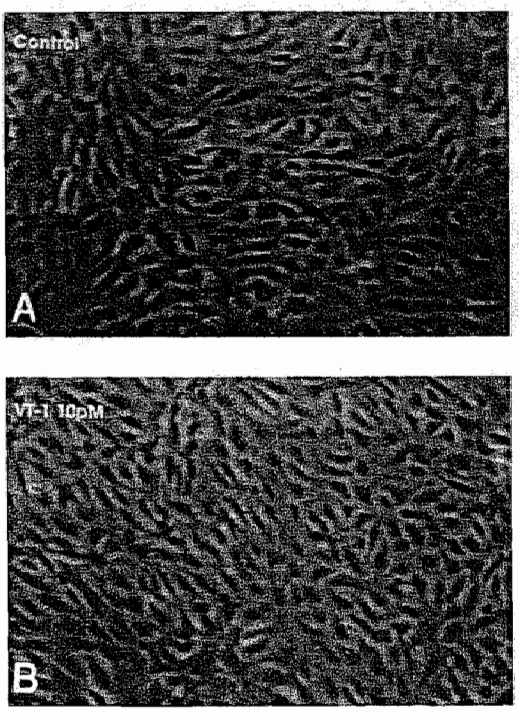

Fig 1. Effect of VT-1 on endothelial cell morphology. HUVECs were incubated for 24 hours with medium alone (control) or in the presence of VT-1 (10 pmol/L).

ported in Fig 4. On unstimulated static HUVECs, few rolling cells were detected averaging 2.3 ± 0.5 leukocytes/mm^2. Treatment of HUVECs for 24 hours with 1 or 10 pmol/L VT-1 did not affect the number of rolling leukocytes, which averaged 5.3 ± 2.1 and 3.4 ± 0.7 leukocytes/mm^2, respectively. However, on IL-1β–stimulated cells, the number of leukocytes rolling on endothelial surface significantly ($P <$ .01) increased compared with that rolling on control and VT-1–treated HUVECs (58 ± 6 leukocytes/mm^2).

Cell surface proteins involved in leukocyte adhesion to VT-1–stimulated HUVECs. To explore the molecular basis of VT-1–induced leukocyte adhesion to endothelial cells under flow, HUVECs exposed for 24 hours to VT-1 (10 pmol/L) were incubated for 20 minutes with MoAb anti–E-selectin, anti–ICAM-1, and anti–VCAM-1 immediately before performing leukocyte adhesion experiments. As shown in Fig 5, at the end of the perfusion assay the number of adherent leukocytes on HUVECs treated with VT-1 was significantly higher as compared with leukocytes adhering on control untreated HUVECs (191 ± 28 *v* 56 ± 6 leukocytes/mm^2, $P <$ .01). MoAb anti–E-selectin significantly inhibited VT-1 induced increase in leukocyte adhesion (73 ± 17 *v* 191 ± 28 leukocytes/mm^2, $P <$ .01). MoAb anti–ICAM-1 and anti–VCAM-1 also significantly reduced leukocyte adhesion to VT-1–treated HUVECs (100 ± 26 and 71 ± 15 leukocytes/mm^2, respectively; $P <$ .01 *v* VT-1). Noteworthy exposure of VT-1–treated HUVECs to MoAb anti–E-selectin and anti–VCAM-1 lowered the number of adhering leukocytes to control values (56 ± 6 leukocytes/mm^2). Treatment with irrelevant MoAb did not affect leukocyte adhesion on VT-1–treated HUVECs (207 ± 63 *v* 187 ± 56 leukocytes/mm^2).

The number of rolling leukocytes on VT-1–treated (10 pmol/L) HUVECs incubated with MoAb against E-selectin, ICAM-1, and VCAM-1 was similar to that observed on endothelial cells treated with VT-1 alone (3.4 ± 1.5; 4.8 ± 0.8; 3.1 ± 0.6 *v* 3.4 ± 0.7 leukocytes/mm^2).

Effect of TNF on VT-1–induced leukocyte adhesion to HUVECs under physiologic flow conditions. In some experiments, before VT-1 (10 pmol/L) incubation, HUVECs were pre-exposed for 24 hours to TNFα at the concentration of 100 U/mL, which was previously shown to increase VT-1 receptor expression on HUVECs[8] (Fig 6). VT-1 significantly enhanced leukocyte adhesion on HUVECs as compared with control cells (146 ± 15 *v* 45 ± 5 leukocytes/mm^2, $P <$ .01). The number of leukocytes adhering to HUVECs pre-exposed to TNFα before challenge with VT-1 were significantly higher than that of HUVECs exposed to VT-1 alone (300 ± 13 *v* 146 ± 15 leukocytes/mm^2, $P <$ .01). The number of leukocytes adhering on HUVECs exposed to TNFα (100 U/mL) alone averaged 201 ± 29 leukocytes/mm^2 ($P <$ .01 *v* TNFα + VT-1).

With additional experiments we established that leukocyte adhesion on HUVECs reached a plateau at a TNFα concentration of 300 U/mL (control, 71.2 ± 6.8; 100 U/mL TNFα, 162.4 ± 13.5; 300 U/mL TNFα, 286.2 ± 13.6; 500 U/mL TNFα, 268.0 ± 10.7 leukocytes/mm^2). When HUVECs pretreated with 300 U/mL TNFα were exposed to VT-1 (10

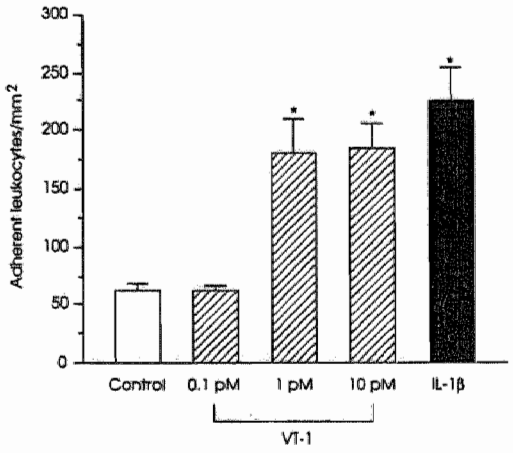

Fig 2. Adhesion of total leukocytes on unstimulated (control) or VT-1–stimulated HUVECs under conditions of flow. HUVECs were incubated for 24 hours with VT-1 (0.1, 1, 10 pmol/L). HUVECs activated with IL-1β (100 U/mL) were used as a positive control. Leukocyte adhesion was measured at the end of 13 minutes of perfusion. Data are expressed as the mean ± SE. *$P <$ .01 versus control.

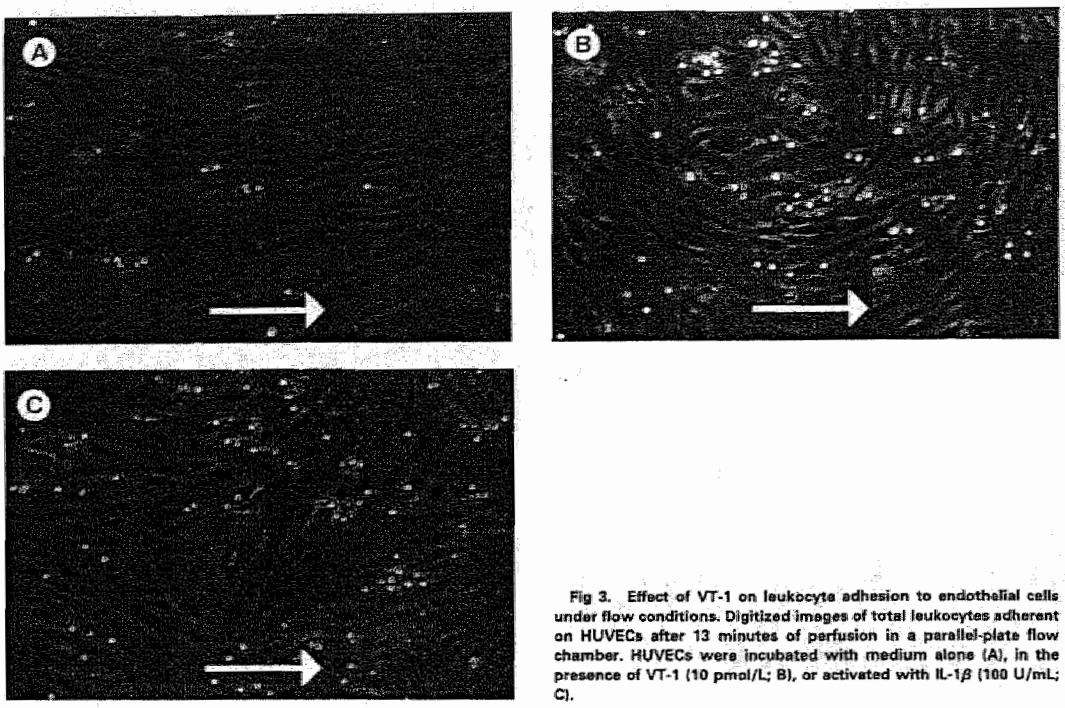

Fig 3. Effect of VT-1 on leukocyte adhesion to endothelial cells under flow conditions. Digitized images of total leukocytes adherent on HUVECs after 13 minutes of perfusion in a parallel-plate flow chamber. HUVECs were incubated with medium alone (A), in the presence of VT-1 (10 pmol/L; B), or activated with IL-1β (100 U/mL; C).

pmol/L), an additive effect of VT-1 on leukocyte adhesion was observed in only 4 of 8 experiments, with a percentage increase of 60.7% ± 8.3% over TNFα alone.

DISCUSSION

The present results show that VT-1 dose-dependently induced leukocyte adhesion to endothelial cells under flow conditions. The adhesive response elicited by VT-1 was quite comparable to that of IL-1β, one of the most potent inducers of leukocyte-endothelial cell adhesion. Because leukocyte attachment consistently induces granule content release,[23] the present study helps to clarify mechanism(s) by which VT-1 damages the endothelium. These results are in harmony with data that in vitro HUS neutrophils adhere to endothelium more than normal neutrophils.[16] Neutrophil-derived products (particularly elastase) that are released locally on neutrophil adhesion to endothelium degrade extracellular matrix, which would favor endothelial cell detachment from basement membrane, a typical feature of HUS.[11] Formal evidence that this may occur in HUS derives from data that enhanced adhesion of neutrophils from HUS patients to endothelium in vitro is followed by degradation of endothelial cell fibronectin.[16]

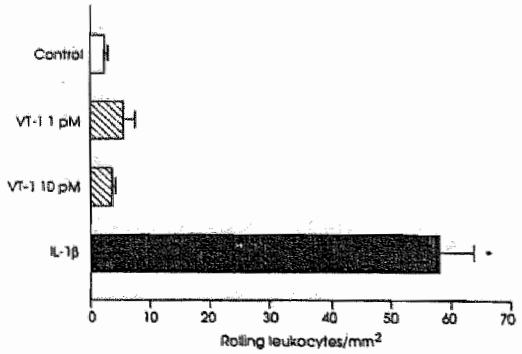

Fig 4. Rolling leukocytes on unstimulated (control) or VT-1–stimulated HUVECs under conditions of flow. HUVECs were incubated for 24 hours with VT-1 (1 and 10 pmol/L). HUVECs activated with IL-1β (100 U/mL) were used as a positive control. Leukocyte rolling was evaluated after 10 minutes of perfusion. Data are expressed as the mean ± SE. *$P < .01$ versus control and VT-1 (1 and 10 pmol/L).

Events that regulate recruitment of leukocytes and subsequent migration are critically dependent on adhesive molecules constitutively expressed on the surface of the endothelium and leukocytes or induced by cytokines or flow condition.[24-28,21] Early molecules involved in this process belong to the selectin family[29-32] and are expressed on endothelial cells upon cytokine activation. Subsequent firm adhesion of leukocytes implies the interactions of leukocyte β2 and β1 integrin receptors with specific endothelial ligand, ie, ICAM-1 and VCAM-1, constitutively expressed on endothelial surface, whose level is further increased by cytokine activation.[24,26,33,34]

With the present study we have established that functional

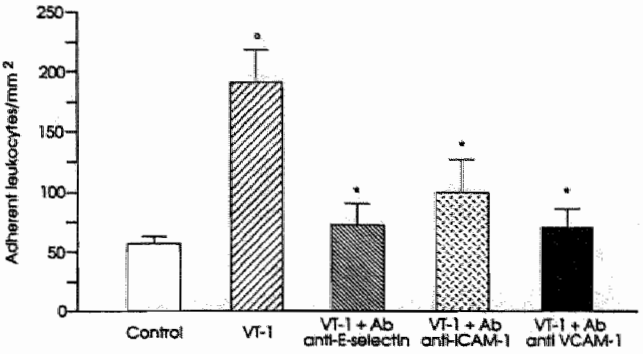

Fig 5. Effect of MoAb anti-E-selectin, anti-ICAM-1, or anti-VCAM-1 on VT-1-induced leukocyte adhesion on endothelial cells. Before the adhesion assay, VT-1-treated (10 pmol/L) HUVECs were incubated for 20 minutes with MoAb anti-E-selectin, anti-ICAM-1, or anti-VCAM-1. Data are expressed as the mean ± SE. °$P < .01$ versus control; *$P < .01$ versus VT-1.

blocking of E-selectin, ICAM-1, and VCAM-1 with respective antibodies significantly reduced VT-1-mediated leukocyte adhesion to endothelial cells exposed to flow. An additional finding of the present study was that VT-1 inhibited the process of rolling that normally precedes adhesion of cells to the endothelium. We observed a similar phenomenon in tumor cell adhesion to the endothelium under flow.[20] It was established that certain lines (ie, A375M and A2058 melanomas and the MG-63 osteosarcoma) firmly adhered on activated endothelial cells before any rolling could be seen, whereas other lines (HT-29M colon carcinoma and OVCAR-3 ovarian carcinoma) were capable of usual rolling before they adhered. It is tempting to speculate that VT-1 causes sudden expression of ICAM-1 and VCAM-1 at very high density on endothelial cell surface, which would promote immediate leukocyte adhesion not preceded by rolling. The last observation of the present study was that pre-exposure of HUVECs to TNFα before challenge with VT-1 significantly increased the number of adherent leukocytes under flow. This observation is consistent with several recent findings

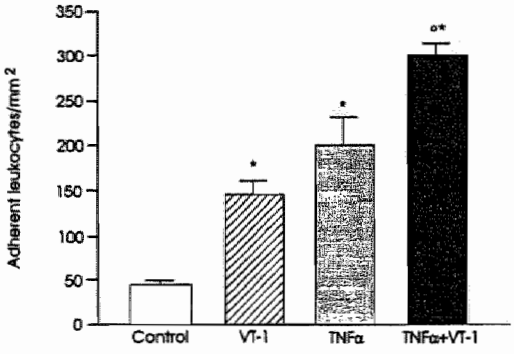

Fig 6. Effect of TNFα on VT-1-induced leukocyte adhesion on endothelial cells under flow conditions. HUVECs were incubated with medium alone, VT-1 (10 pmol/L), or TNFα (100 U/mL) before exposure to VT-1 (10 pmol/L). Data are expressed as the mean ± SE. *$P < .01$ versus control; °$P < .01$ versus VT-1 and TNFα.

that TNFα does promote upregulation of endothelial VT-Gb_3 receptor and supports VT-1 binding.[8,9]

That TNFα plays a major role in VT-1-induced microvascular injury is documented by findings that mice genetically defective in TNFα production were less sensitive to the lethal effects of VT-1.[35] These mice consistently had a longer mean time to death than did mice who were normally responsive. The molecular basis for the interaction between VT-1 and TNFα in determing extent and localization of microvascular lesions were recently addressed in an elegant experiment of mice bearing a chloroamphenicol acetyl-transferase (CAT) reporter gene that indicates TNFα synthesis.[36] Upon VT-1 injection to the above-mentioned mice, CAT activity was selectively induced in the kidney but not in other organs, indicating a distinct potential of VT-1 of upregulating TNFα gene expression not equally distributed within all organs, which fits well with the unique sensitivity of the kidney to microvascular damage in HUS.

In conclusion, our results indicate that (1) VT-1 is a potent promoter of leukocyte adhesion to endothelial cells under flow conditions; (2) VT-1-induced leukocyte-endothelial interaction depends on upregulation of adhesion molecules that include E-selectin, ICAM-1, and VCAM-1, as documented by inhibition studies with respective specific antibodies; and (3) VT-1-induced leukocyte adhesion is enhanced by TNFα.

Despite the potential limitations of these in vitro studies as far as their theoretical implication in vivo, the present findings might be relevant to understand the nature of microvascular lesions in children with VTEC-associated HUS and open exciting new perspectives for treatment.

ACKNOWLEDGMENT

This work is dedicated to Prof Alfredo Leonardi. We thank Drs Aldo Gambarini and Paola Rosaschino (Division of Obstetrics and Gynecology, Ospedale Bolognini, Seriate, Bergamo, Italy) for invaluable help in collecting umbilical samples.

REFERENCES

1. Karmali MA, Petric M, Lim C, Fleming PC, Arbus GS, Lior M: The association between idiopathic hemolytic uremic syndrome and infection by verotoxin-producing *Escherichia coli*. J Infect Dis 151:775, 1985

2. Karmali MA: The association of verocytotoxins and the classical hemolytic uremic syndrome, in Kaplan BS, Trompeter RS, Moake JL (eds): Hemolytic Uremic Syndrome and Thrombotic Thrombocytopenic Purpura. New York, NY, Marcel Dekker, 1992, p 199

3. Remuzzi G, Ruggenenti P: The hemolytic uremic syndrome. Kidney Int 47:2, 1995

4. Remuzzi G, Ruggenenti P, Bertani T: Thrombotic microangiopathy, in Tisher CC, Brenner BM (eds): Renal Pathology With Clinical and Functional Correlations. Philadelphia, Lippincott, 1994, p 1154

5. O'Brien AD, Holmes RK: Shiga and shiga-like toxins. Microbiol Rev 51:206, 1987

6. Lingwood CA, Law H, Richardson S, Petric M, Brunton JL, De Grandis S, Karmali MA: Glycolipid binding of purified and recombinant *Escherichia coli* produced verotoxin in vitro. J Biol Chem 262:8834, 1987

7. Lindberg AA, Brown JE, Stronberg N, Westling-Ryd M, Schultz JE, Karlsson K-A: Identification of the carbohydrate receptor for Shiga toxin produced by Shigella dysenteriae type 1. J Biol Chem 262:1779, 1987

8. Obrig TG, Louise CB, Lingwood CA, Boyd B, Barley-Maloney L, Daniel TO: Endothelial heterogeneity in Shiga Toxin receptors and responses. J Biol Chem 268:15484, 1993

9. van de Kar NCAJ, Monnens LAH, Karmali MA, van Hinsbergh VWM: Tumor necrosis factor and interleukin-1 induce expression of the verocytotoxin receptor globotriaosylceramide on human endothelial cells: Implications for the pathogenesis of the hemolytic uremic syndrome. Blood 80:2755, 1992

10. Kavi J, Wise R: Causes of the haemolytic uraemic syndrome: It might be verocytotoxin produced by *Escherichia coli*. Br Med J 298:65, 1989

11. Zoja C, Remuzzi G: The pivotal role of the endothelial cell in the pathogenesis of HUS, in Kaplan BS, Trompeter RS, Moake JL (eds): Hemolytic Uremic Syndrome and Thrombotic Thrombocytopenic Purpura. New York, NY, Marcel Dekker, 1992, p 389

12. Louise CB, Obrig TG: Shiga toxin-associated hemolytic-uremic syndrome: Combined cytotoxic effects of shiga toxin, interleukin-1β, and tumor necrosis factor alpha on human vascular endothelial cells in vitro. Infect Immunity 59:4173, 1991

13. van de Kar NCAJ, Kooistra T, Vermeer M, Lesslauer W, Monnens LAH, van Hinsbergh VWM: Tumor necrosis factor α induces endothelial galactosyl transferase activity and verocytotoxin receptors. Role of specific tumor necrosis factor receptors and protein kinase C. Blood 85:734, 1995

14. Zoja C, Corna D, Farina C, Sacchi G, Lingwood C, Doyle MP, Padhye VV, Abbate M, Remuzzi G: Verotoxin glycolipid receptors determine the localization of microangiopathic process in rabbits given verotoxin-1. J Lab Clin Med 120:229, 1992

15. van Setten PA, van de Heuvel LPWJ, Monnens LAH: Effects of verocytotoxin-1 on human monocytes. Binding characteristics and induction of cytokine release. J Am Soc Nephrol 4:639, 1993 (abstr)

16. Forsyth KD, Simpson AC, Fitzpatrick MM, Barratt TM, Levinsky RJ: Neutrophil-mediated endothelial injury in haemolytic uraemic syndrome. Lancet 2:411, 1989

17. Fitzpatrick MM, Shah V, Trompeter RS, Dillon MJ, Barratt TM: Interleukin-8 and polymorphoneutrophil leucocyte activation in hemolytic uremic syndrome of childhood. Kidney Int 42:951, 1992

18. Jaffe E, Nachman R, Becker C, Minick C: Culture of human endothelial cells derived from umbilical veins: Identification by morphologic and immunologic criteria. J Clin Invest 52:2745, 1973

19. Lawrence MB, McIntire LV, Eskin SG: Effect of flow on polymorphonuclear leukocyte/endothelial cell adhesion. Blood 70:1284, 1987

20. Giavazzi R, Foppolo M, Dossi R, Remuzzi A: Rolling and adhesion of human tumor cells on vascular endothelium under physiological flow conditions. J Clin Invest 92:3038, 1993

21. Morigi M, Zoja C, Figliuzzi M, Foppolo M, Micheletti G, Bontempelli M, Saronni M, Remuzzi G, Remuzzi A: Fluid shear stress modulates surface expression of adhesion molecules by endothelial cells. Blood 85:1696, 1995

22. Wallenstein S, Zucker CL, Fleiss JL: Some statistical methods useful in circulation research. Circ Res 47:1, 1980

23. Nathan CF: Neutrophil activation on biological surfaces. Massive secretion of hydrogen peroxide in response to products of macrophages and lymphocytes. J Clin Invest 80:1550, 1987

24 Brady HR: Leukocyte adhesion molecules and kidney diseases. Kidney Int 45:1285, 1994

25. Cronstein BN, Weissman G: The adhesion molecules of inflammation. Arthritis Rheum 36:147, 1993

26. Osborn L: Leukocyte adhesion to endothelium in inflammation. Cell 62:3, 1990

27. Nagel T, Resnick N, Atkinson WJ, Dewey CF Jr, Gimbrone MA Jr: Shear stress selectively upregulates intercellular adhesion molecule-1 expression in cultured human vascular endothelial cells. J Clin Invest 94:885, 1994

28. Ohtsuka A, Ando J, Korenaga R, Kamiya A, Toyama-Sorimachi N, Miyasaka M: The effect of flow on the expression of vascular adhesion molecule-1 by cultured mouse endothelial cells. Biochem Biophys Res Commun 193:303, 1993

29. Alon R, Rossiter H, Wang X, Springer TA, Kupper TS: Distinct cell surface ligands mediate T lymphocyte attachment and rolling on P and E selectin under physiological flow. J Cell Biol 127:1485, 1994

30. Ley K, Bullard DC, Arbonés ML, Bosse R, Vestweber D, Tedder TF, Beaudet AL: Sequential contribution of L- and P-selectin to leukocyte rolling in vivo. J Exp Med 181:669, 1995

31. Lawrence MB, Springer TA: Neutrophils roll on E-selectin. J Immunol 151:6338, 1993

32. Abbassi O, Kishimoto TK, McIntire LV, Anderson DC, Smith CW: E-selectin supports neutrophil rolling in vitro under conditions of flow. J Clin Invest 92:2719, 1993

33. Wuthrich RP: Intercellular adhesion molecules and vascular cell adhesion molecule-1 and the kidney. J Am Soc Nephrol 3:1201, 1992

34. Jones DA, McIntire LV, Smith CW, Picker LJ: A two-step adhesion cascade for T cell/endothelial cell interactions under flow conditions. J Clin Invest 94:2443, 1994

35. Barrett TJ, Potter ME, Strockbine NA: Evidence for participation of the macrophage in Shiga like toxin-II induced lethality in mice. Microb Pathog 9:95, 1990

36. Harel Y, Silva M, Giroir B, Weinberg A, Cleary TB, Beutler B: A reporter transgene indicates renal-specific induction of tumor necrosis factor (TNF) by Shiga-like toxin. J Clin Invest 92:2110, 1993

CHAPTER 4

SHIGA TOXIN-2 TRIGGERS ENDOTHELIAL LEUKOCYTE ADHESION AND TRANSMIGRATION VIA NF-KB DEPENDENT UP REGULATION OF IL-8 AND MCP-1.

C. Zoja, S. Angioletti, R. Donadelli, C. Zanchi, S. Tomasoni, E. Binda, B. Imberti, M. te Loo, L. Monnens, G. Remuzzi and M. Morigi

Kidney Int 2002; 62: 846-856

Kidney International, Vol. 62 (2002), pp. 846–856

Shiga toxin-2 triggers endothelial leukocyte adhesion and transmigration via NF-κB dependent up-regulation of IL-8 and MCP-1[1]

CARLA ZOJA, STEFANIA ANGIOLETTI, ROBERTA DONADELLI, CRISTINA ZANCHI, SUSANNA TOMASONI, ELENA BINDA, BARBARA IMBERTI, MAROESKA TE LOO, LEO MONNENS, GIUSEPPE REMUZZI, and MARINA MORIGI

Mario Negri Institute for Pharmacological Research, and Unit of Nephrology and Dialysis, Azienda Ospedaliera, Ospedali Riuniti di Bergamo, Bergamo, Italy; and Department of Pediatrics, University Hospital Nijmegen, Nijmegen, The Netherlands

Shiga toxin-2 triggers endothelial leukocyte adhesion and transmigration via NF-κB dependent up-regulation of IL-8 and MCP-1.

Background. Shiga toxin (Stx)-producing *E. coli* is a causative agent of the epidemic form of hemolytic uremic syndrome (HUS), the most common cause of acute renal failure in children. Endothelial injury and leukocyte activation are instrumental to the development of microangiopathic lesions. To obtain more insight into the mechanisms favoring endothelium-leukocyte interaction, we studied (*1*) the effect of Stx-2 on leukocyte adhesion and transmigration in human endothelial cells under flow; (*2*) the effect of Stx-2 on endothelial expression of monocyte chemoattractant protein-1 (MCP-1) and interleukin-8 (IL-8) and their functional role in the adhesive phenomena; and (*3*) the role of nuclear factor-κB (NF-κB) in endothelial chemokine expression.

Methods. For adhesion experiments, human umbilical vein endothelial cells (HUVEC) and human glomerular endothelial cells (GEC) were incubated for 24 hours with Stx-2 (25 pmol/L), with or without anti-IL-8 or MCP-1 antibodies, and then exposed to leukocyte suspension under flow (1.5 dynes/cm^2). IL-8 and MCP-1 expression was evaluated in Stx-2 treated endothelial cells (6 hours) by Northern blot. NF-κB activity was assessed by electrophoretic mobility shift assay. The role of NF-κB in Stx-induced chemokines was evaluated by transfecting HUVEC with an adenovirus coding for IκBα.

Results. Stx-2 significantly enhanced the number of leukocytes that adhered and then migrated across the endothelium. Stx-2 increased the expression of IL-8 and MCP-1, which was preceded by NF-κB activation. Blocking of endothelial IL-8 and MCP-1 with corresponding antibodies significantly inhibited Stx-induced leukocyte adhesion and migration either in HUVEC or GEC. Adenovirus-mediated gene transfer of IκBα down-regulated IL-8 and MCP-1 mRNA and also inhibited the adhesion and transmigration of leukocytes in Stx-treated HUVEC.

Conclusions. Stx-2 via a transcriptional activation mechanism specifically mediated by NF-κB up-regulates endothelial MCP-1 and IL-8. Both chemokines are important modulators of leukocyte adhesion and transmigration under flow. These findings might be relevant to understand the nature of microvascular lesions in HUS and open future perspectives for better treatment of microvascular thrombosis.

Sporadic hemolytic uremic syndrome (HUS) is a disease of thrombocytopenia, microangiopathic hemolytic anemia and acute renal failure that mainly affects infants and small children [1, 2]. Infection with Shiga toxin (Stx)-producing *Escherichia coli* has been strongly implicated as the most common causative agent [3–6]. *E. coli* 0157:H7 strains that are isolated from patients with HUS produce Stx-1 and Stx-2, and epidemiological data indicate that Stx-2 producing *E. coli* are more likely to cause HUS than the strains that produce only Stx-1 [5, 6].

After the ingestion of contaminated food or water [7], Shiga toxins gain access to the systemic circulation and rapidly and completely bind to specific receptors expressed on circulating cells, mainly polymorphonuclear leukocytes, which transport them to the kidney or other target organs [8, 9]. Endothelial damage is crucial to the subsequent development of microangiopathic lesions, and evidence is available that the interaction between leukocytes and endothelial cells serves to magnify the extent of endothelial injury [5, 6, 10, 11]. Shiga toxins can directly damage endothelial cells after binding to a specific glycosphingolipid globotriaosyl ceramide (Gb3) receptor expressed on the cell surface [11, 12]. The binding is followed by internalization in the cytosol of the toxin that exerts its cytotoxic effect via inhibition of protein

[1] See Editorial by Siegler and Pysher, p. 1088.

Key words: hemolytic uremic syndrome, chemokines, glomerular endothelial cells, gene transfer, flow, thrombocytopenia, acute renal failure.

Received for publication December 27, 2001
and in revised form March 22, 2002
Accepted for publication March 27, 2002

synthesis [4, 13, 14] and apoptosis [15]. Cytokines like interleukin-1 (IL-1) and tumor necrosis factor (TNF) released by monocytes/macrophages in response to Stxs [16] remarkably enhanced vascular sensitivity to the toxins by up-regulating the endothelial Gb3 receptor [13].

We have demonstrated that Stx-1 induced a massive leukocyte adhesion to cultured human endothelial cells under flow conditions, by up-regulating the adhesive proteins E-selectin, intracellular adhesion molecule-1 (ICAM-1), and vascular cell adhesion molecule-1 (VCAM-1) [17]. The adhesion of leukocytes was enhanced by pre-exposure of the endothelial cells to TNF-α. Moreover, neutrophils from children with the acute phase of HUS adhered to endothelial cells in vitro more than normal neutrophils and induced endothelial injury by local release of proteases [18]. Indeed, plasma concentrations of α1-antitrypsin–complexed elastase and the chemokine IL-8—a potent activator of neutrophils—were remarkably higher in the acute phase of the disease, which presumably reflected neutrophil activation and degranulation in vivo [19].

Kidney specimens from HUS children with evidence of Stx-producing *E. coli* infection revealed a conspicuous infiltration of polymorphonuclear and mononuclear cells within the glomeruli, along with microvascular injury [20, 21]. In those patients urinary levels of IL-8 and monocyte chemoattractant protein-1 (MCP-1), potent attractants of neutrophils, and monocytes/macrophages and T-lymphocytes, respectively, were elevated during the acute phase of the disease, and gradually declined until recovery, implying a role for these chemokines in the recruitment of inflammatory cells at the glomerular level [21, 22].

Evidence is available that IL-8 and MCP-1 can be released by endothelial cells stimulated by proinflammatory mediators, such as cytokines and lipopolysaccharide [23], depending on the activity of the transcription factor NF-κB [24]. NF-κB is present in an inactive form in the cell cytoplasm and is activated upon proteolytic degradation of the inhibitory protein IκB [25].

The present study investigated: (*1*) the effects of Stx-2 on leukocyte adhesion and transmigration through human endothelium human umbilical vein endothelial cells (HUVEC) and human glomerular endothelial cells (GEC)-under flow conditions; (*2*) the ability of Stx-2 to modulate the endothelial expression of the chemoattractant proteins IL-8 and MCP-1 and their functional role in the adhesive phenomena. Moreover, since IL-8 and MCP-1 are regulated by the transcription factor NF-κB, we also studied (*3*) whether Stx-2 induced the activation of NF-κB in endothelial cells and (*4*) whether transfection of endothelium with recombinant adenovirus coding for IκBα, the natural inhibitor of NF-κB, resulted in successful inhibition of chemokine up-regulation, and leukocyte adhesion and transmigration induced by Stx-2.

METHODS

Endothelial cell culture and incubation

Human umbilical vein endothelial cells (HUVEC were obtained by collagenase digestion according to th method of Jaffé et al [26]. The cells were grown in Me dium 199 (Gibco BRL, Gaithersburg, MD, USA) sup plemented with 10% newborn calf serum (Gibco) an 10% human serum, 5 mmol/L N-2-hydroxyethylpipera zine-N-2-ethanesulfonic acid (HEPES; Sigma Chemical St. Louis, MO, USA), 100 U/mL penicillin, 100 μg/mL streptomycin, 2.5 μg/mL fungizone, 2 mmol/L glutamine (Gibco), 15 U/mL heparin (Parke-Davis, Milan, Italy) and 50 μg/mL endothelial cell growth factor. Cultured cells were identified as endothelial by their cobblestone morphology and the presence of von Willebrand factor, using indirect immunofluorescence microscopy. Confluent cells were routinely used between the first and fifth passages. For adhesion experiments, HUVEC were plated on 60 × 20 mm plastic coverslips (Thermanox; Nunc Inc, Naperville, IL, USA) coated with bovine gelatin (0.2%, Sigma) and used two days after reaching confluence.

Human glomerular endothelial cells (GEC) were isolated from kidneys that were not suitable for transplantation because of anatomical anomalies or technical reasons, by collagenase digestion as previously described [27]. The cells were grown in Medium 199 supplemented with 10% newborn calf serum (Gibco) and 10% human serum, 2 mmol/L glutamine, 100 U/mL penicillin, 100 μg/mL streptomycin, 5 U/mL heparin and 150 μg/mL endothelial cell growth factor. Cells were characterized by indirect immunofluorescence with a panel of endothelial cell-specific antibodies, namely von Willebrand factor, platelet-endothelial cell adhesion molecule-1 (PECAM-1) and visceral epithelial (VE)-cadherin. To exclude contamination with epithelial and mesangial cells, indirect immunofluorescence with antibodies against anti-cytokeratin 20 and anti-α-smooth muscle actin were performed [27]. No immunoreactivity was observed in cells used for the experiments, indicating that pure GEC were used. Two different donors of GEC were used to perform experiments.

For adhesion experiments GEC were plated on 60 × 20-mm plastic coverslips (Thermanox) coated with porcine gelatin (1%; Fluka BioChemika, Buchs, Switzerland) and used two days after reaching confluence.

To investigate the effect of Stx-2 on leukocyte adhesion and transmigration, confluent HUVEC were incubated for 24 hours with medium alone (M-199 plus 10% fetal calf serum; Gibco), with Stx-2 at a subtoxic concentration (25 pmol/L; Toxin Technology Inc., Sarasota, FL, USA) or with TNF-α (100 U/mL; Knoll AG, Ludwigshafen, Germany), then endothelial cells were perfused at 1.5 dynes/cm^2 in a parallel plate flow chamber with total leukocyte suspension. Selected adhesion experi-

ments ($N = 3$) under flow were performed in GEC exposed for 24 hours to Stx-2 (25 pmol/L).

To elucidate whether Stx-2 modulated endothelial expression of IL-8 and MCP-1, HUVEC were exposed for six hours to different concentrations of Stx-2 (25 pmol/L, 50 pmol/L and 1 nmol/L), and then cells were processed for Northern blot analysis of IL-8 and MCP-1 mRNA.

The role of these chemokines in Stx-induced leukocyte adhesion and transmigration was evaluated by incubating HUVEC or GEC pre-treated 24 hours with 25 pmol/L Stx-2- with functional blocking rabbit polyclonal anti-human IL-8 antibody (10 μg/200 μL; Endogen, Woburn, MA, USA) or mouse monoclonal anti-human MCP-1 antibody (20 μg/200 μL; a kind gift by G. Peri, Mario Negri Institute, Milan, Italy) [28] or with rabbit or mouse isotype-matched IgG (10 μg/200 μL, Endogen; and 20 μg/200 μL, Camfolio, Becton Dickinson, San Jose, CA, respectively) as control, for 20 minutes at room temperature, before the adhesion assay.

To identify the leukocyte populations that adhered on Stx-treated endothelial cells in the presence or absence of anti-IL-8 and MCP-1 antibodies, HUVEC at the end of leukocyte perfusion under flow were stained by May-Grunwald/Giemsa. Cells were fixed in methyl alcohol for three minutes at room temperature and stained with 1:2 dilution of May-Grunwald solution in phosphate-buffered saline (PBS) for one minute. After two washings with distilled water, cells were incubated for five minutes with 1:3 dilution of Giemsa solution in PBS. Coverslips were washed twice and examined by microscope. Polymorphonuclear cells and mononuclear cells were identified and counted in several fields ($N = 10$) for each coverslip ($N = 4$ experiments).

The ability of Stx-2 to activate the transcription factor NF-κB was evaluated by electrophoretic mobility shift analysis (EMSA) of nuclear extracts from HUVEC exposed for one hour to Stx-2 (25 pmol/L, 50 pmol/L and 1 nmol/L).

Finally, to assess the involvement of NF-κB in Stx-induced IL-8 and MCP-1 mRNA up-regulation and leukocyte adhesion and transmigration, HUVEC were transfected (for 3 h) with recombinant adenovirus coding for IκBα, the natural inhibitor of NF-κB [29]. After transfection, cells were maintained for 24 hours in growth medium and then exposed (6 h) to 50 pmol/L Stx-2 for Northern blot experiments or to 25 pmol/L Stx-2 (24 h) for adhesion experiments.

Shiga toxin-2 preparation

Shiga toxin-2 was prepared by the manufacturer as follows: *E. coli* strain PMJ-100 was grown overnight in Brain Heart Infusion Broth, then centrifuged to collect the cells. The cells were extracted by freezing and then treating with lysing agent (B-PER; Pierce, Rockford, IL, USA). The extract was dialyzed and purified chromatographically (DEAE-anion exchange, Sephacryl-gel filtration). Purity was assessed using sodium dodecyl saline-polyacrylamide gel electrophoresis (SDS-PAGE) and activity was determined by a Vero cells-cytotoxicity assay.

Leukocyte isolation

Leukocyte suspension was prepared from human fresh venous blood collected from healthy volunteers on ethylenediaminetetraacetic acid (EDTA; final concentration 5 mmol/L) and diluted with an equal volume of cold saline solution as previously described [17]. The blood samples were centrifuged at 200 × *g* for 10 minutes at 4°C, the cell pellet was resuspended in 4 volumes of Emagel (Behringwerke AG, Marburg, Germany) and erythrocytes were allowed to sediment at 4°C for 40 minutes. Supernatant was removed, centrifuged at 500 × *g* for 10 minutes at 4°C and the pellet washed twice by centrifugation with saline. The remaining erythrocytes were removed by ammonium chloride lysis at 4°C and centrifugation. After this procedure the cell viability, measured by trypan blue exclusion, was greater than 95%. Cells were then resuspended in culture medium at a final concentration of 10^6 cells/mL.

Adhesion assay under flow conditions

For adhesion experiments we used a parallel-plate flow chamber and a perfusion system as previously described [30, 31]. Briefly, the chamber is composed of two parallel surfaces, a coverslip coated with HUVEC at confluence and a flat surface machined from polymethylmethacrylate. The two surfaces are separated by a 250 μm thick silicon rubber gasket, leaving a rectangular surface of 30 × 13 mm exposed to flow. An inlet and outlet channel distributed the fluid uniformly along the entrance side of the adhesion surface. Shear stress levels as a function of medium flow rate was calculated assuming fully developed laminar flow between the two parallel plates. After assembling with the HUVEC monolayer, the chamber is placed on the stage of an inverted phase-contrast microscope with a thermostated hood to maintain the temperature at 37°C. The microscope is connected with a video recording system (Panasonic, Osaka, Japan). Leukocyte suspension was pumped through the chamber, at controlled flow rates, using a syringe pump (Harvard Apparatus Inc., South Natick, MA, USA). After initial perfusion with cell free medium plus 0.5% bovine serum albumin at 0.6 dynes/cm^2 for two minutes for equilibration, the leukocyte suspension was perfused through the chamber at 1.5 dynes/cm^2 and images recorded thereafter. After 10 minutes, cell free medium was perfused at a flow rate of 3.0 dynes/cm^2 for evaluation of the number of leukocytes rolling on the HUVEC surface. At this flow rate the rolling leukocytes are easily distinguishable from cells freely flowing in the suspension that move much faster. After three minutes of perfu-

sion at 3.0 dynes/cm² several fields (>10) were observed for evaluation of the number of firmly adherent cells. Images acquired during the perfusion experiments were digitized and processed on a personal computer using general purpose image processing software (NIH Image, v. 1.59; NIH, Bethesda, MD, USA). Adherent leukocytes were identified and counted at the end of the 13 minute perfusion, as previously described in details [31]. The number of cells transmigrated across the HUVEC monolayer during the perfusion experiments was quantified by visual inspection of the videotape, since adherent cells that transmigrate under the endothelium change their color from white to black [32].

The shear stress of 1.5 dynes/cm², used to study leukocyte–endothelium interaction, mimics post-capillary venule circulation [30], but this same value of wall shear stress may be present also within the glomerular microcirculation. In a three-dimensional model of glomerular capillary [33], we estimated that a large fraction of glomerular capillary segments are exposed to wall shear stress values <5 dynes/cm².

Northern blot analysis

Total RNA was isolated from HUVEC by the guanidium isothiocyanate/cesium chloride procedure, as previously described [34]. Ten micrograms of total RNA were then fractionated on 1.6% agarose gel and blotted onto synthetic membranes (Zeta-probe; Bio-Rad, Richmond, CA, USA). IL-8 and MCP-1 cDNA probes were kindly provided by Dr. K. Matsushima (Laboratory of Molecular Immunoregulation, National Cancer Institute, Bethesda, MD, USA). IL-8 mRNA was detected by using a 300 base pair (bp) fragment of human IL-8 cDNA. For MCP-1 a 345 bp fragment of human MCP-1 cDNA was used to detect the MCP-1 mRNA transcript. The probes were labeled with α-^{32}P dCTP by random-primed method as previously described [35]. Hybridization was performed overnight at 60°C in 0.5 mol/L Na_2HPO_4, pH 7.2, 7% SDS. Filters were washed twice for 30 minutes with 40 mmol/L Na_2HPO_4, pH 7.2, 5% SDS and two times for 10 minutes with 40 mmol/L Na_2HPO_4, pH 7.2, 1% SDS at 65°C. Membranes were subsequently probed with a glyceraldehyde-3-phosphate dehydrogenase (GAPDH) cDNA, taken as internal standard of equal loading of the samples on the membrane. IL-8 and MCP-1 mRNA optical density was normalized to that of the constituently released GAPDH gene expression.

Preparation of nuclear extracts

Nuclear extracts were prepared from HUVEC using the NE-PER™ Nuclear and Cytoplasmic Extraction Reagents Kit (Pierce/Celbio, Pero, Italy) according to the manufacturer's instructions. To minimize proteolysis, all buffers contained protease inhibitor cocktail (Protease inhibitor cocktail tablets; Boehringer Mannheim, Mannheim, Germany). The protein concentration was determined by the Bradford assay using the Bio-Rad protein assay reagent.

Electrophoretic mobility shift and supershift assays. Electrophoretic mobility shift assays (EMSAs) were performed as previously described [36] using the kB DNA sequence of the immunoglobulin gene (5'-GGGACT TTCC). Nuclear extracts (2 μg) were incubated with 50 kcpm of ^{32}P labeled NF-κB oligonucleotide in a binding reaction mixture [10 mmol/L Tris-HCl, pH 7.5, 80 mmol/L NaCl, 1 mmol/L EDTA, 1 mmol/L dithiothreitol (DTT), 5% glycerol, 1.5 μg of poly(dI-dC)] for 30 minutes on ice. To assay the specificity of the binding reaction, a 100-fold molar excess of unlabeled NF-κB probe or an unlabeled nonspecific oligonucleotide (tissue plasminogen activator regulatory element, TRE) was added to the binding reaction mixture as indicated, prior to the addition of the labeled κB probe. For supershift assays, the reaction mixture minus the probe was incubated for one hour on ice with 1 μL of affinity-purified rabbit polyclonal antisera specific for p65 (sc-109), p50 (sc-114), RelB (sc-226), cRel (sc-71) and p52 (sc-298; Santa Cruz Biotechnology, Santa Cruz, CA, USA). The labeled NF-κB oligonucleotide was then added, and the incubation was continued at room temperature for 20 minutes.

Overexpression of adenovirally encoded IκBα in HUVEC. Subconfluent HUVEC were incubated with recombinant adenovirus coding for IκBα (a kind gift from Dr. R. de Martin, Department of Vascular Biology and Thrombosis Research, University of Vienna, Vienna, Austria) [29] or with a control adenovirus (Ad null control) at a multiplicity of infection (MOI) of 300 in M-199 without serum for three hours at 37°C. The adenovirus was washed off and cells were maintained in fresh growth medium for 24 hours. Then HUVEC were exposed to Stx-2 (25 or 50 pmol/L) for additional 24 hours and processed for IL-8 and MCP-1 mRNA expression (Northern blot) or leukocyte adhesion and transmigration experiments.

Statistical analysis

Results are expressed as mean ± SE. Data were analyzed by analysis of variance (ANOVA) followed by Tukey's test for multiple comparisons or by the nonparametric Kruskal-Wallis test for multiple comparisons. Statistical significance level was defined as $P < 0.05$.

RESULTS

Stx-2 promotes leukocyte adhesion and transmigration via up-regulation of IL-8 and MCP-1 mRNA in HUVEC

We previously showed that Stx-1 induced leukocyte adhesion to HUVEC under flow conditions [17]. Here,

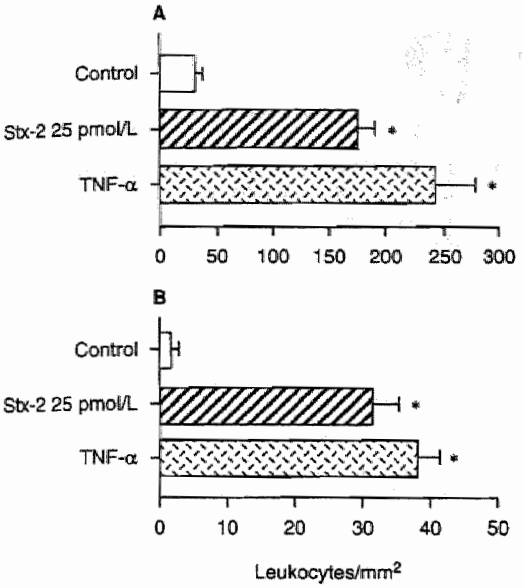

Fig. 1. Leukocyte adhesion (*A*) and transmigration (*B*) in human umbilical endothelial vein cells (HUVEC) treated with Shiga toxin-2 (Stx-2) under flow condition (1.5 dynes/cm²). Endothelial cells were exposed to control medium, Stx-2 (25 pmol/L, 24 hours) or tumor necrosis factor-α (TNF-α; 100 U/mL, 24 hours) as positive control. At the end of perfusion, the number of adherent and transmigrated leukocytes were quantified by digital analysis of videotapes of each experiment ($N = 9$ experiments). Data are expressed as mean ± SE. *$P < 0.01$ vs. control.

we investigated the effect of Stx-2 on subendothelial leukocyte transmigration and the role of IL-8 and MCP-1 expressed by the endothelium in these adhesive events. Consistent with our prior study [17], Stx-2 at a subtoxic concentration (25 pmol/L, 24 h) significantly ($P < 0.01$) increased the number of leukocytes that adhered on HUVEC with respect to unstimulated cells (175 ± 14 vs. 32 ± 6 leukocytes/mm²; Fig. 1). This response was similar to that elicited by TNF-α, one of the most potent inducers of endothelial cell adhesive properties, used as positive control (244 ± 34 leukocytes/mm²). As shown in Figure 1, a massive transmigration of leukocytes across the endothelium was elicited by Stx-2 (Stx-2, 33 ± 3 vs. control, 2 ± 1 leukocytes/mm², $P < 0.01$), which was as intense as that observed after cell activation with TNF-α (39 ± 2 leukocytes/mm²).

Scanning electron micrographs of Stx-2 treated HUVEC illustrate adherent and transmigrated leukocytes at different stages of activation in a sequence that resembles the multistep model of in vivo leukocyte-endothelial cell recognition and extravasation (Fig. 2) [23, 37]. As the initial step, some leukocytes attach to the endothelium through their membrane projections, others become activated and change shape (Fig. 2A) before transmigrating through the subendothelium (Fig. 2B).

The ability of Stx-2 to modulate the endothelial expression of IL-8 and MCP-1 was assessed by Northern blot experiments. The expression of IL-8 mRNA increased over control after 6 hour exposure of HUVEC to different concentrations of Stx-2 (Fig. 3A). Actually, Stx-2 at 25 pmol/L, the same concentration used in the adhesion experiments, promoted a twofold increase in IL-8 transcript levels as compared to control cells ($P < 0.01$), which was further enhanced by 50 pmol/L and maintained elevated by the highest concentration of 1 nmol/L (2.6- and 2.4-fold increase, $P < 0.01$). As shown in Figure 3B, up-regulation of MCP-1 mRNA also was induced by Stx-2 at all the concentrations studied ($P < 0.01$ vs. control).

To study the functional role of these chemokines in Stx-2–induced leukocyte adhesion and transmigration, HUVEC exposed for 24 hours to 25 pmol/L Stx-2 were treated with anti-IL-8 and anti-MCP-1 antibodies before performing the adhesion assay. Functional blocking of IL-8 significantly reduced the number of adhering leukocytes on Stx-2 treated HUVEC under flow conditions (Stx-2, 164 ± 12 vs. Stx-2 + anti-IL-8 Ab, 40 ± 2 leukocytes/mm², $P < 0.01$; Fig. 4). A remarkable inhibitory effect also was obtained by treating HUVEC with the anti-MCP-1 Ab (Stx-2 + anti-MCP-1 Ab, 80 ± 7 leukocytes/mm², $P < 0.01$; Fig. 4). As a consequence of the reduced leukocyte adhesion, the number of transmigrated cells through the endothelial monolayer was significantly lessened by both anti-IL-8 and anti-MCP-1 antibodies (Stx-2, 29 ± 1 vs. Stx-2 + anti-IL-8 Ab, 3 ± 1 and Stx-2 + anti-MCP-1 Ab, 6 ± 1 leukocytes/mm²; $P < 0.01$; Fig. 4). Treatment with the corresponding irrelevant antibodies did not affect leukocyte adhesion (irrelevant rabbit IgG, 154 ± 6 and irrelevant mouse IgG, 157 ± 13 leukocytes/mm² for anti-IL-8 and MCP-1 Abs, respectively) and transmigration induced by Stx-2 (irrelevant rabbit IgG, 30 ± 3 and irrelevant mouse IgG, 33 ± 4 leukocytes/mm² for anti- IL-8 and MCP-1 Abs, respectively).

By analyzing the leukocyte populations that adhered to the Stx-treated endothelial cells after flow exposure, we identified polymorphonuclear cells as the major subsets of adherent leukocytes (80.2 ± 4.2%). Mononuclear cells (19.3 ± 4.2%) also were present. Anti-IL-8 antibody reduced by 81.8 ± 2.8% and 69.5 ± 5.5% the adhesion of polymorphonuclear and mononuclear cells, respectively. As expected, a more pronounced inhibitory effect on adherent mononuclear cells was observed after treatment with anti-MCP-1 antibody (% inhibition, mononuclear cells, 90.2 ± 1.5 and polymorphonuclear cells, 27 ± 3.4%).

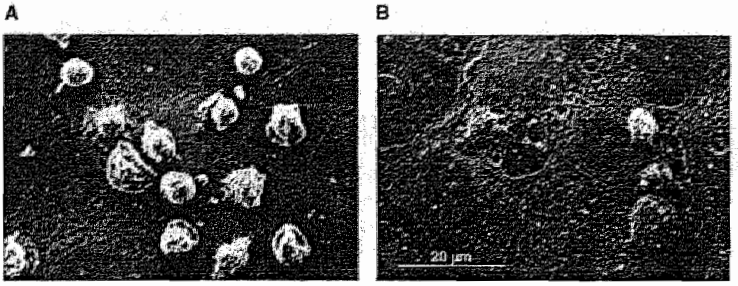

Fig. 2. Scanning electron micrograph of adherent and transmigrated leukocytes in HUVEC challenged with Stx-2. Micrographs show adherent (*A*) and transmigrated (*B*) leukocytes at different stages of activation in HUVEC treated with Stx-2 (25 pmol/L, 24 h).

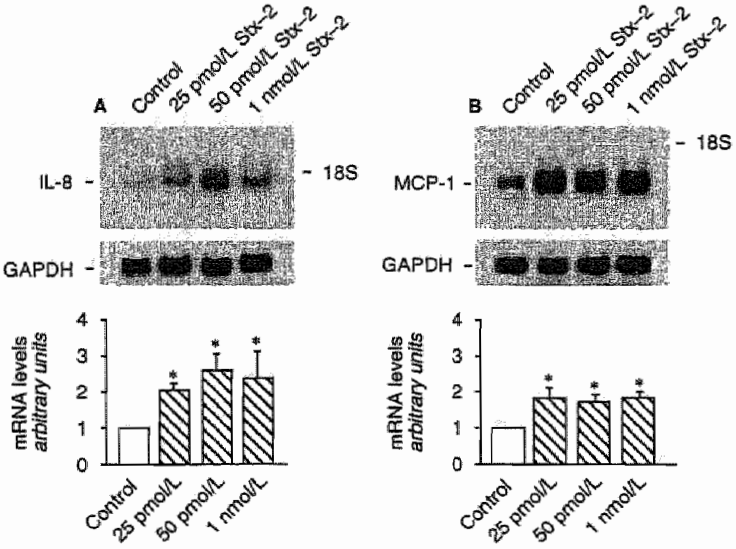

Fig. 3. Expression of interleukin-8 (IL-8; *A*) and monocyte chemoattractant protein-1 (MCP-1; *B*) mRNA in HUVEC exposed to Stx-2. (Top) Northern blot experiments were performed using total RNA isolated after a 6-hour period of culture with medium alone (control) or Stx-2 (25 pmol/L, 50 pmol/L and 1 nmol/L). Data shown are representative of $N = 5$ experiments. (Bottom) Densitometric analysis of autoradiographic signals for IL-8 and MCP-1. The optical density of the autoradiographic signals was quantified and calculated as the ratio of IL-8 or MCP-1 to GAPDH mRNA. Results (mean ± SE) are expressed as the fold increase over control (considered as 1) in densitometric arbitrary units. $^*P <$ 0.01 vs. control.

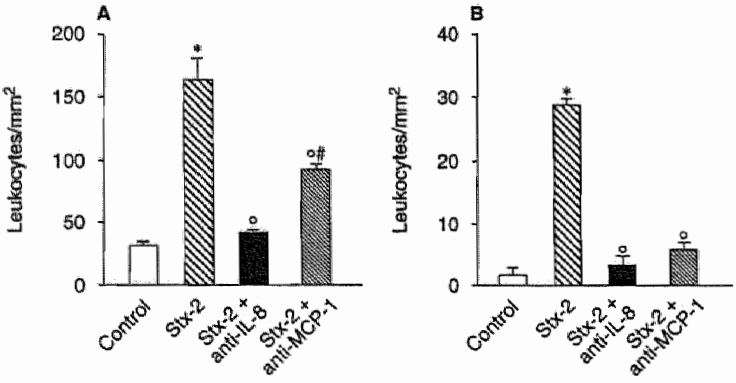

Fig. 4. Effect of anti-IL-8 or anti-MCP-1 antibodies on Stx-2 induced leukocyte adhesion and transmigration under flow. Before the adhesion assay, HUVEC treated for 24 hours with Stx-2 (25 pmol/L) were exposed for 20 minutes to anti-IL-8 or anti-MCP-1 antibodies. At the end of perfusion, the number of adherent and transmigrated leukocytes were quantified. Data are mean ± SE ($N = 7$ experiments). $^*P < 0.01$ vs. control, $^\circ P < 0.01$ vs. Stx-2, $\#P < 0.05$ vs. Stx-2 + anti IL-8 antibody.

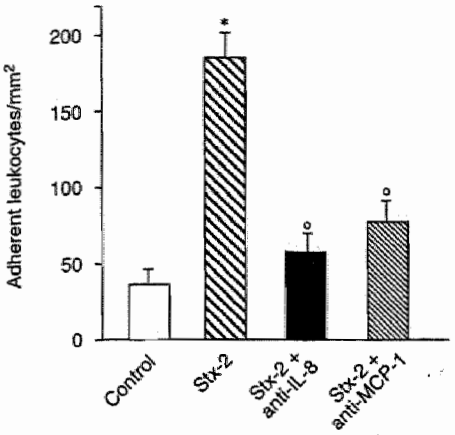

Fig. 5. Stx-2 induces leukocyte adhesion on glomerular endothelial cells (GEC) under flow. Effect of anti-IL-8 or anti-MCP-1 antibodies. GEC were treated for 24 hours with control medium or Stx-2 (25 pmol/L), and then cells were exposed or not to anti-IL-8 or anti-MCP-1 antibodies for 20 minutes. At the end of perfusion, the number of adherent leukocytes were quantified. Data are mean ± SE ($N = 3$ experiments). *$P < 0.01$ vs. control, °$P < 0.01$ vs. Stx-2.

Stx-2 enhances leukocyte adhesion and transmigration in glomerular endothelial cells through an IL-8 and MCP-1 dependent pathway

In selected experiments performed in human glomerular endothelial cells, Stx-2 (25 pmol/L, 24 h) promoted a massive adhesion of leukocytes on the endothelium under flow, at a comparable extent than HUVEC. As shown in Figure 5, on average 185 ± 16 leukocytes/mm² adhered to Stx-2 treated GEC compared with 36 ± 10 leukocytes/mm² to unstimulated cells ($P < 0.01$). Anti-IL-8 and anti-MCP-1 antibodies significantly limited the number of adherent leukocytes (Stx-2 + anti-IL-8 Ab, 57 ± 12; Stx-2 + anti-MCP-1 Ab, 77 ± 14 leukocytes/mm²; $P < 0.01$ vs. Stx-2). Similar to what was observed in HUVEC, leukocyte adhesion induced by Stx-2 on GEC was followed by transendothelial migration, which was reduced by the functional blockade of IL-8 and MCP-1.

Stx-2 activates the transcription factor NF-κB

Based on the evidence that both the IL-8 and MCP-1 genes have a consensus sequence in their promoter for the transcription factor NF-κB [38, 39], we studied the effect of Stx-2 on NF-κB activation. As shown in Figure 6, the nuclear extracts from control cells displayed two constitutive bands: an upper complex (complex I) and a faster migrating lower complex (complex II). Treatment of HUVEC for one hour with increasing concentrations of Stx-2 elicited a substantial rise in NF-κB binding activity that was already evident at 25 pmol/L (Fig. 6A). The specificity of the binding reaction was confirmed in competition experiments by the ability of excess unlabeled (cold) NF-κB oligonucleotide to inhibit binding. Moreover, when excess unlabeled TRE oligonucleotide was used as irrelevant probe, it did not affect the binding of the specific κB probe to nuclear proteins.

Since NF-κB complexes may constitute a variety of different homo- and heterodimers, the subunit compositions of the Stx-induced DNA complexes were analyzed by supershift assay (Fig. 6B). Rabbit polyclonal antisera specific for p65, p50, cRel, RelB, and p52 were added to nuclear extracts of Stx-treated HUVEC. The upper band, complex I consisted of p65/p50 heterodimer, since pre-incubation of the cells with anti-p50 antibody consistently reduced the intensity of the complex, while anti-p65 antibody abolished it. Both antibodies caused further gel retardation (supershift). Complex II was inhibited by anti-p50 antibody, suggesting that the complex II represented p50/p50 homodimer.

Adenoviral overexpression of IκBα inhibits Stx-induced IL-8 and MCP-1 mRNA and leukocyte adhesion and transmigration

We explored the possibility that up-regulation of endothelial IL-8 and MCP-1 mRNA in response to Stx-2 was dependent on NF-κB. Since NF-κB activity is regulated by IκB inhibitor proteins, which sequester NF-κB into cytoplasm and avoid its translocation to the nucleus, overexpression of IκBα was achieved through infection of HUVEC with a replication-deficient recombinant adenovirus encoding IκBα. In non-stimulated cells, complex formation with IκBα inhibited constitutive expression of IL-8 and MCP-1. Moreover, delivery of IκBα resulted in a remarkable reduction of Stx-induced IL-8 and MCP-1 mRNA transcript levels (Fig. 7), thus indicating that activated NF-κB is responsible for chemokine up-regulation.

The consequence of inhibiting NF-κB by adenovirus-mediated gene transfer of IκBα was investigated further in the adhesion assay. As shown in Figure 8, leukocyte adhesion induced by Stx-2 was reduced by 60% on HUVEC overexpressing IκBα versus noninfected cells ($P < 0.05$). A similar inhibition (70%; $P < 0.05$) was observed in leukocyte transmigration. No difference was observed in unstimulated cells infected with the control adenovirus (Ad null control) with respect to unstimulated cells transfected with rAd IκBα.

DISCUSSION

Endothelial dysfunction is crucial to the development of microvascular lesions in HUS [5, 6], and increasing evidence suggests that Shiga toxins, by favoring interaction of endothelial cells with leukocytes [17, 18] and platelets [40], serve to amplify and extend the injury at renal level. As a follow-up of previous studies [17], here

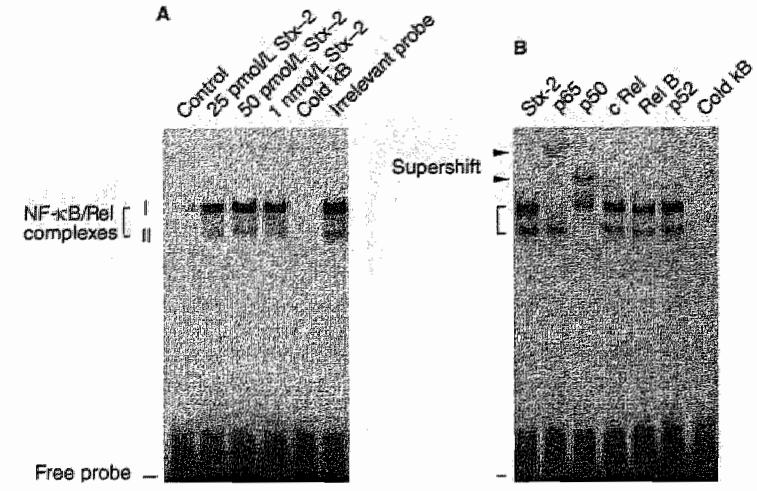

Fig. 6. Stx-2 activates the transcription factor NF-κB. (*A*) EMSA for NF-κB activity was performed in nuclear extracts from HUVEC exposed for 1 hour to Stx-2 (25 pmol/L, 50 pmol/L and 1 nmol/L). Complexes I and II denote the inducible κB specific DNA-protein complexes. A 100-fold molar excess unlabeled (cold) or an unlabeled nonspecific oligonucleotide (irrelevant probe) was added to nuclear extracts from HUVEC treated with Stx-2 (50 pmol/L). The results shown are representative of three independent experiments employing different nuclear extracts. (*B*) Subunit composition of NF-κB activated by Stx-2. Nuclear extracts from HUVEC treated with Stx-2 (50 pmol/L, 1 hour) were incubated with antibodies against p65, p50, cRel, RelB and p52 subunits. Antibody supershifts produced by binding of the antibody to the DNA-protein complex are indicated.

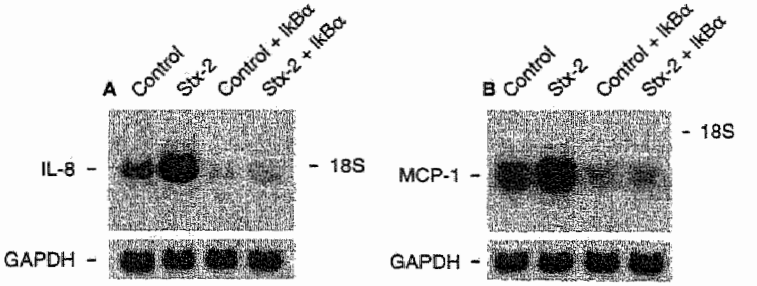

Fig. 7. Expression of IL-8 and MCP-1 mRNA induced by Stx-2 is inhibited by adenovirus-mediated gene transfer of IκBα. Endothelial cells were left untreated or infected with rAd.IkBα for 3 hours, then cells were exposed to medium alone or to Stx-2 (50 pmol/L, 6 hours). Results shown are representative of $N = 3$ Northern blot experiments.

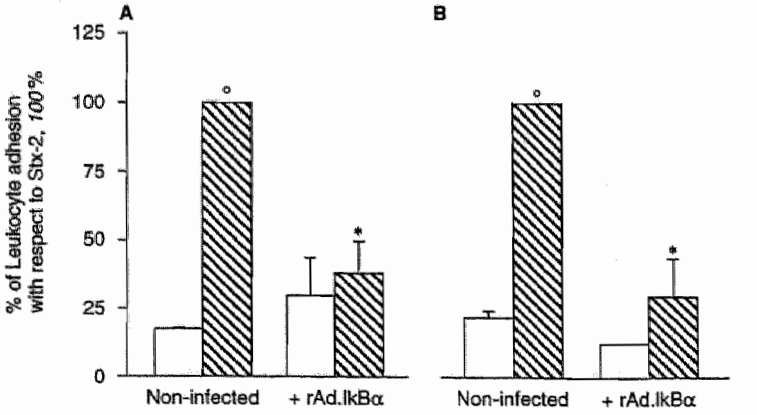

Fig. 8. Leukocyte adhesion and transmigration induced by Stx-2 are regulated by endothelial activation of NF-κB dependent genes. Endothelial cells were left untreated or infected with rAd.IκBα for 3 hours, then cells were exposed to medium alone (control; □) or to Stx-2 (25 pmol/L, 24 h; Stx-2; ▨). At the end of incubation, HUVEC were perfused with total leukocyte suspension and the number of leukocytes that adhered and transmigrated were quantified. Data are expressed as mean ± SE ($N = 3$ experiments). °$P < 0.05$ vs. control; *$P < 0.05$ vs. non infected Stx-2.

we characterized the adhesive phenomena triggered by Stx-2, studying the adhesion and transmigration of leukocytes in human endothelial cells exposed to Stx-2, under flow conditions. We found that sub-toxic concentrations of Stx-2 [17, 40] induced a significant increase in the number of leukocytes adhering to HUVEC, followed by a massive transmigration through the endothelial monolayer. The adhesion elicited by Stx-2, that is, sixfold increase over control, was comparable to that of TNF-α (8-fold increase), one of the most potent inducers of leukocyte-endothelial cell adhesiveness known to date. The major subset of leukocytes that adhered on Stx-treated endothelial cells consisted of polymorphonuclear cells (80%) while mononuclear cells represented 20%.

A relevant finding was that exposure to Stx-2 under flow induced massive adhesion and transmigration of leukocytes in glomerular endothelial cells, to a similar extent as that for HUVEC. Thus, both types of endothelial cells at confluence showed a similar sensitivity to a Stx-2 concentration that did not affect cell viability, but stimulated intracellular pathways resulting in the enhanced adhesive phenomena.

Contrasting data are available in the literature regarding the differential sensitivity of HUVEC and renal microvascular endothelial cells to Stxs. Confluent HUVEC were little susceptible to the cytotoxic effect of Stx-1, unless they were pretreated with cytokines that up-regulate Gb3 receptors [13]. Renal microvascular endothelial cells had greater sensitivity to the toxic effects of Stx-1 than HUVEC, because they constitutively expressed 50-times more Stx receptor [41]. At variance, purified glomerular endothelial cells, such as those used in our study, similarly to HUVEC, responded to Stx and underwent cell death and inhibition of protein synthesis only when they were sub-confluent. At confluence, they instead required pre-exposure to cytokines [15].

The concept that leukocytes are crucial to the pathogenesis of microvascular lesions in Stx-associated HUS is based on evidence that the number of polymorphonuclear cells is elevated and may be a predictive factor for the outcome of the disease [42]. Ultrastructural studies showed polymorphonuclear and mononuclear cell infiltrates in the glomeruli of patients with sporadic HUS [20, 21]. In addition, during the acute phase of the disease neutrophils are activated [19], become more adhesive than normal, and damage the endothelium by producing elastase [18] and superoxide [43]. More recently, in vitro and in vivo studies pointed to an additional role of neutrophils as the cells responsible for binding and transfer of Stx from intestine to the kidney endothelium [8, 9].

In the present study we sought to understand cellular and molecular mechanisms responsible for the recruitment of leukocytes into the kidney of HUS, which have never been clarified.

Interleukin-8 and MCP-1 were significantly increased in the urine of HUS patients during the acute phase of the disease and returned to normal in remission [21, 22]. Here we found that IL-8 and MCP-1 mRNA expression was increased after a six hour exposure of endothelial cells to Stx-2. That both chemokines can actually have a functional role in the adhesive process triggered by Stx-2 rests on the evidence that specific antibodies against IL-8 and MCP-1 limited to a remarkable extent the leukocyte adhesion and subendothelial transmigration in HUVEC as well as glomerular endothelial cells treated with Stx-2. Of note, anti-IL-8 antibody had a more pronounced inhibitory effect as compared to anti-MCP-1 antibody. Actually, anti-IL-8 antibody markedly decreased both adherent polymorphonuclear and mononuclear cells (82% and 70% inhibition, respectively). This finding is consistent with recent data that IL-8, thought to act predominantly on neutrophils, instead had the ability to promote the adhesion of monocytes to vascular endothelium under flow [44]. Anti-MCP-1 antibody almost completely abolished mononuclear cell adhesion to Stx-treated endothelium (90% inhibition) and decreased polymorphonuclear cells by 27%.

Chemokines trigger adhesion and migration of distinct leukocyte subsets either as soluble chemoattractants or as immobilized molecules bound to heparan sulfate proteoglycans of the endothelial surface of post-capillary venules and small veins [23, 37, 45]. In an in vitro flow-based adhesion assay and video microscopy, exposure of endothelial cells to hypoxia and re-oxygenation resulted in neutrophil attachment and migration due to the action of IL-8 expressed on the endothelium, as documented by the inhibitory effect of an anti-IL-8 antibody [46]. In a model of monocytes rolling on adenovirally E-selectin transduced endothelial cells under flow, MCP-1 and IL-8 caused firm adhesion of monocytes to the endothelium through the activation of leukocyte integrins [44].

Since IL-8 and MCP-1 genes have in their promoter a consensus sequence for the transcription factor NF-κB [38, 39], we verified whether NF-κB activation could be a candidate pathway of Stx-2-induced chemokine expression in endothelial cells. NF-κB belongs to Rel family comprising different members, including RelA (p65), cRel, RelB, p50 and p52, which form homo- or heterodimers with different affinities for variants of a decameric consensus binding site [25, 47]. NF-κB exists in an inactive form in the cytoplasm of cells bound to the inhibitory IκB subunit and upon activation by different stimuli NF-κB translocates into the nucleus for binding to DNA motifs in gene promoters [25]. Here we found that exposure of endothelial cells to Stx-2 increased NF-κB-DNA binding activity and that the protein subunits involved were p65/p50 heterodimer and p50/p50 homodimer. These results are in line with a previous study showing that treatment of cultured human monocytes with Stx-1

induced nuclear translocation of NF-κB complexes and IκB degradation [48].

As a proof of the concept that Stx-induced IL-8 and MCP-1 genes are regulated by NF-κB, we inhibited endothelial response to Stx-2 by inducing overexpression of an NF-κB specific inhibitor, IκBα. Delivery of IκBα to HUVEC followed by Stx-2 stimulation fully suppressed IL-8 and MCP-1 mRNA up-regulation. As expected, Stx-2-induced leukocyte adhesion and transmigration were strongly reduced in IκB transfected HUVEC, suggesting that such adhesive processes are selectively modulated by activation of NF-κB dependent genes. Our findings are consistent with the recent observation that adenoviral transfer of IκBα suppressed the endothelial expression of adhesive molecules required for the adhesion and transmigration of monocytes on endothelium activated by TNF-α under flow [49].

In conclusion, the results of the present study documented that (*1*) under flow Stx-2 induces a massive adhesion and transmigration of leukocytes on HUVEC and glomerular endothelial cells, through the up-regulation of IL-8 and MCP-1; (*2*) this phenomenon involves the activation of NF-κB, to the extent that endothelial cell overexpression of a specific inhibitor IκBα, using a recombinant adenovirus, fully prevents leukocyte adhesion and transmigration.

Despite the potential limitations in extrapolating results from in vitro studies, our findings might be relevant to understand the role of chemokines in promoting leukocyte-endothelium interaction which favors microvascular lesions in Stx-associated HUS, and could help to find innovative treatments.

ACKNOWLEDGMENTS

Part of this work was presented at the 32nd Annual Meeting of the American Society of Nephrology (Miami Beach, Florida, November 1-8, 1999). The contribution of Dr. Ariela Benigni, Head Department of Molecular Medicine, and Dr. Andrea Remuzzi, Head Department of Biomedical Engeneering, is greatly acknowledged. The Authors thank Dr. Rainer de Martin (Department of Vascular Biology and Thrombosis Research, University of Vienna, Vienna, Austria) for kindly providing recombinant adenovirus expressing IκBα, and Dr. Giuseppe Peri (Mario Negri Institute, Milan, Italy), for providing anti-MCP-1 monoclonal antibody.

Reprint requests to Carla Zoja, Ph.D., 'Mario Negri' Institute for Pharmacological Research, Via Gavazzeni 11, 24125 Bergamo, Italy
E-mail: zoja@marionegri.it

REFERENCES

1. Remuzzi G, Ruggenenti P: The hemolytic uremic syndrome. *Kidney Int* 47:2–19, 1995
2. Siegler RL: Hemolytic uremic syndrome in children. *Curr Opin Pediatr* 7:159–163, 1995
3. Karmali MA, Petric M, Lim C, *et al*: The association between idiopathic hemolytic uremic syndrome and infection by verotoxin-producing *Escherichia coli*. *J Infect Dis* 151:775–782, 1985
4. Arbus GS: Association of verotoxin-producing *E. coli* and verotoxin with hemolytic uremic syndrome. *Kidney Int* 51(Suppl 58):S91–S96, 1997
5. Andreoli SP: The pathophysiology of the hemolytic uremic syndrome. *Curr Opin Nephrol Hypertens* 8:459–464, 1999
6. Ruggenenti P, Noris M, Remuzzi G: Thrombotic microangiopathy, hemolytic uraemic syndrome, and thrombotic thrombocytopenic purpura. *Kidney Int* 60:831–846, 2001
7. Mead PS, Griffin PM: *Escherichia coli* 0157:H7. *Lancet* 352:1207–1212, 1998
8. Te Loo DM, Monnens LA, van der Velden TJ: et al Binding and transfer of verocytotoxin by polymorphonuclear leukocytes in hemolytic uremic syndrome. *Blood* 95:3396–3402, 2000
9. Te Loo DM, Van Hinsbergh VW, Van den Heuvel LP, Monnens LA: Detection of verotoxin bound to circulating polymorphonuclear leukocytes of patients with hemolytic uremic syndrome. *J Am Soc Nephrol* 12:800–806, 2001
10. Zoja C, Remuzzi G: The pivotal role of the endothelial cell in the pathogenesis of HUS, in *Hemolytic Uremic Syndrome and Thrombotic Thrombocytopenic Purpura*, edited by Kaplan BS, Trompeter RS, Moake JL, New York, Marcel Dekker, 1992, p 389
11. Obrig TG: Pathogenesis of shiga toxin (verotoxin)-induced endothelial cell injury, in *Hemolytic Uremic Syndrome and Thrombotic Thrombocytopenic Purpura*, edited by Kaplan BS, Trompeter RS, Moake JL, New York, Marcel Dekker, 1992, p 405
12. Lingwood CA: Role of verotoxin receptors in pathogenesis. *Trends Microbiol* 4:147–153, 1996
13. van de Kar NCAJ, Monnens LAH, Karmali MA, van Hinsbergh VWM: Tumor necrosis factor and interleukin-1 induce expression of the verocytotoxin receptor globotriaosylceramide on human endothelial cells: implications for the pathogenesis of the hemolytic uremic syndrome. *Blood* 80:2755–2764, 1992
14. Obrig TG: Shiga toxin mode of action in *E. coli* 0157:H7 disease. *Front Biosci* 2:635–642, 1997
15. Pijpers AH, van Setten PA, Van den Heuvel LP, *et al*: Verocytotoxin-induced apoptosis of human microvascular endothelial cells. *J Am Soc Nephrol* 12:767–778, 2001
16. van Setten PA, Monnens LAH, Verstraten RGG, *et al*: Effects of verocytotoxin-1 on nonadherent human monocytes: Binding characteristics, protein synthesis, and induction of cytokine release. *Blood* 88:174–183, 1996
17. Morigi M, Micheletti G, Figliuzzi M, *et al*: Verotoxin-1 promotes leukocyte adhesion to cultured endothelial cells under physiologic flow conditions. *Blood* 86:4553–4558, 1995
18. Forsyth KD, Simpson AC, Fitzpatrick MM, *et al*: Neutrophil-mediated endothelial injury in haemolytic uraemic syndrome. *Lancet* ii:411–414, 1989
19. Fitzpatrick MM, Shah V, Trompeter RS, *et al*: Interleukin-8 and polymorphoneutrophil leukocyte activation in hemolytic uremic syndrome of childhood. *Kidney Int* 42:951–956, 1992
20. Inward CD, Howie AJ, Fitzpatrick MM, *et al*: Renal histopathology in fatal cases of diarrhea-associated haemolytic uraemic syndrome. *Pediatr Nephrol* 11:556–559, 1997
21. van Setten PA, van Hinsbergh VWM, van den Heuvel LPWJ, *et al*: Monocyte chemoattractant protein-1 and interleukin-8 levels in urine and serum of patents with hemolytic uremic syndrome. *Pediatr Res* 43:759–767, 1998
22. Inward CD, Varagunam M, Adu D, *et al*: Cytokines in haemolytic uraemic syndrome associated with verocytotoxin-producing *Escherichia coli* infection. *Arch Dis Child* 77:145–147, 1997
23. Luster AD: Chemokines-chemotactic cytokines that mediate inflammation. *N Engl J Med* 338:436–445, 1998
24. Schlöndorff D, Nelson PJ, Luckow B, Banas B: Chemokines and renal disease. *Kidney Int* 51:610–621, 1997
25. Tak PP, Firestein GS: NF-κB: A key role in inflammatory diseases. *J Clin Invest* 107:7–11, 2001
26. Jaffe E, Nachman R, Becker C, Minick C: Culture of human endothelial cells derived from umbilical veins; identification by morphologic and immunologic criteria. *J Clin Invest* 52:2745–2756, 1973
27. van Setten PA, van Hinsbergh VWM, van der Velden TJAN, *et al*: Effects of TNF-α on verocytotoxin cytotoxicity in purified human glomerular microvascular endothelial cells. *Kidney Int* 51: 1245–1256, 1997
28. Peri GC, Milanese C, Matteucci C, *et al*: A new monoclonal antibody (5D3–F7) which recognizes human monocyte-chemotactic protein-1 but not related chemokines. Development of a sand-

wich ELISA and in situ detection of producing cells. *J Immunol Meth* 174:249–257, 1994
29. WRIGHTON CJ, HOFER-WARBINEK R, MOLL T, *et al*: Inhibition of endothelial cell activation by adenovirus-mediated expression of IκBα, an inhibitor of the transcription factor NF-κB. *J Exp Med* 183:1013–1022, 1996
30. LAWRENCE MB, MCINTIRE LV, ESKIN SG: Effect of flow on polymorphonuclear leukocyte/endothelial cell adhesion. *Blood* 70:1284–1290, 1987
31. MORIGI M, ZOJA C, FIGLIUZZI M, *et al*: Fluid shear stress modulates surface expression of adhesion molecules by endothelial cells. *Blood* 85:1696–1703, 1995
32. MORIGI M, ZOJA C, COLLEONI S, *et al*: Xenogeneic serum promotes leukocyte-endothelium interaction under flow through two temporally distinct pathways: Role of complement and nuclear factor-κB. *J Am Soc Nephrol* 10:2197–2207, 1999
33. REMUZZI A, BRENNER BM, PATA V, *et al*: Three-dimensional reconstructed glomerular capillary network: blood flow distribution and local filtration. *Am J Physiol* 23:F562–F572, 1992
34. RAMBALDI A, YOUNG DC, GRIFFIN JD: Expression of the M-CSF (CSF-1) gene by human monocytes. *Blood* 69:1409–1413, 1987
35. ZOJA C, LIU X-H, DONADELLI R, *et al*: Renal expression of monocyte chemoattractant protein-1 in lupus autoimmune mice. *J Am Soc Nephrol* 8:720–729, 1997
36. ZOJA C, DONADELLI R, COLLEONI S: *et al*: Protein overload stimulates RANTES production by proximal tubular cells depending on NF-κB activation. *Kidney Int* 53:1608–1615, 1998
37. ROVIN BH, PHAN LT: Chemotactic factors and renal inflammation. *Am J Kidney Dis* 31:1065–1084, 1998
38. KUNSCH C, ROSEN CA: NF-Kappa B subunit-specific regulation of the interleukin-8 promoter. *Mol Cell Biol* 10:6137–6146, 1993
39. UEDA A, OKUDA K, OHNO S, *et al*: NF-kappa B and Sp1 regulate transcription of the human monocyte chemoattractant protein-1 gene. *J Immunol* 153:2052–2063, 1994
40. MORIGI M, GALBUSERA M, BINDA E, *et al*: Verotoxin-1-induced up-regulation of adhesive molecules renders microvascular endothelial cells thrombogenic at high shear stress. *Blood* 98:1828–1835, 2001
41. OBRIG TG, LOUISE CB, LINGWOOD CA, *et al*: Endothelial heterogeneity in shiga toxin receptors and responses. *J Biol Chem* 268: 15484–15488, 1993
42. MORRIS KP, COULTHARD MG, MATTHEWS JN: Predicting outcome after childhood hemolytic uremic syndrome. *Clin Nephrol* 36:263–264, 1991
43. KING AJ, SUNDARAM S, CENDOROGIO M, *et al*: Shiga toxin induces superoxide production in polymorphonuclear cells with subsequent impairment of phagocytosis and responsiveness to phorbol esters. *J Infect Dis* 179:503–507, 1999
44. GERSZTEN RE, GARCIA-ZEPEDA EA, LIM YC, *et al*: MCP-1 and IL-8 trigger firm adhesion of monocytes to vascular endothelium under flow conditions. *Nature* 398:718–723, 1999
45. WEBB LM, EHRENGRUBER MU, CLARK-LEWIS I, *et al*: Binding to heparan sulfate or heparin enhances neutrophil responses to interleukin 8. *Proc Natl Acad Sci USA* 90:7158–7162, 1993
46. RAINGER GE, FISHER AC, NASH GB: Endothelial-borne platelet-activation factor and interleukin-8 rapidly immobilize rolling neutrophils. *Am J Physiol* 272:H114–H122, 1997
47. BALDWIN AS: The transcription factor NF-κB and human disease. *J Clin Invest* 107:3–6, 2001
48. SAKIRI R, RAMEGOWDA B, TESH VL: Shiga toxin type 1 activates tumor necrosis factor-α gene transcription and nuclear translocation of the transcription activators nuclear factor-κB and activator protein-1. *Blood* 92:558–566, 1998
49. WEBER KS, DRAUDE G, ERL W, *et al*: Monocyte arrest and transmigration on inflamed endothelium in shear flow is inhibited by adenovirus-mediated gene transfer of IκB-α. *Blood* 93:3685–3693, 1999

CHAPTER 5

VEROTOXIN-1-INDUCED UP-REGULATION OF ADHESIVE MOLECULES RENDERS MICROVASCULAR ENDOTHELIAL CELLS THROMBOGENIC AT HIGH SHEAR STRESS

M. Morigi, M. Galbusera, E. Binda, B. Imberti, S. Gastaldi, A. Remuzzi, C. Zoja, and G. Remuzzi

Blood 2001; 98:1828-1835

Verotoxin-1–induced up-regulation of adhesive molecules renders microvascular endothelial cells thrombogenic at high shear stress

Marina Morigi, Miriam Galbusera, Elena Binda, Barbara Imberti, Sara Gastoldi, Andrea Remuzzi, Carla Zoja, and Giuseppe Remuzzi

Verotoxin-1 (VT-1)–producing *Escherichia coli* is the causative agent of postdiarrheal hemolytic uremic syndrome (D+HUS) of children, which leads to renal and other organ microvascular thrombosis. Why thrombi form only on arterioles and capillaries is not known. This study investigated whether VT-1 directly affected endothelial antithrombogenic properties promoting platelet deposition and thrombus formation on human microvascular endothelial cell line (HMEC-1) under high shear stress. Human umbilical vein endothelial cells (HUVECs) were used for comparison as a large-vessel endothelium. HMEC-1 and HUVECs were pre-exposed for 24 hours to increasing concentrations of VT-1 (2-50 pM) and then perfused at 60 dynes/cm^2 with heparinized human blood prelabeled with mepacrine. Results showed that VT-1 significantly increased platelet adhesion and thrombus formation on HMEC-1 in comparison with unstimulated control cells. An increase in thrombus formation was also observed on HUVECs exposed to VT-1, but to a remarkably lower extent. The greater sensitivity of HMEC-1 to the toxin in comparison with HUVECs was at least in part due to a higher expression of VT-1 receptor (20-fold more) as documented by FACS analysis. The HMEC-1 line had a comparable susceptibility to the thrombogenic effect of VT-1 as primary human microvascular cells of the same dermal origin (HDMECs). The adhesive molecules involved in VT-induced thrombus formation were also studied. Blocking the binding of von Willebrand factor to platelet glycoprotein Ib by aurintricarboxylic acid (ATA) or inhibition of platelet $\alpha_{IIb}\beta_3$-integrin by chimeric 7E3 Fab resulted in a significant reduction of VT-1–induced thrombus formation, suggesting the involvement of von Willebrand factor–platelet interaction at high shear stress in this phenomenon. Functional blockade of endothelial β_3-integrin subunit, vitronectin receptor, P-selectin, and PECAM-1 with specific antibodies was associated with a significant decrease of the endothelial area covered by thrombi. Confocal microscopy studies revealed that VT-1 increased the expression of vitronectin receptor and P-selectin and redistributed PECAM-1 away from the cell-cell border of HMEC-1, as well as of HDMECs, thus indicating that the above endothelial adhesion molecules are directly involved and possibly determine the effect of VT-1 on enhancing platelet adhesion and thrombus formation in microvascular endothelium. These results might help to explain why thrombi in HUS localize in microvessels rather than in larger ones and provide insights on the molecular events involved in the process of microvascular thrombosis associated with D+HUS. (Blood. 2001;98:1828-1835)

Introduction

Verotoxin (VT)–producing *Escherichia coli* infection has been strongly implicated as the causative agent for most cases of postdiarrheal hemolytic uremic syndrome (D+HUS), a disorder of microangiopathic hemolytic anemia, thrombocytopenia, and acute renal failure that mainly affects infants and small children.[1-3] The characteristic lesion, thrombotic microangiopathy, consists of swelling and detachment of endothelial cells from the basement membrane and deposition of platelet thrombi that occlude the microcirculation of the kidneys and other organs.[4] Why thrombi form only in arterioles and capillaries is not known.

It is now clear that endothelial dysfunction plays a crucial role in the sequence of events leading to the microangiopathic processes, and evidence points to VT-1 and VT-2 as critical determinants for the development of vascular lesions. Verotoxins (also called Shiga toxins) are formed by a biologically active A subunit and a number of B subunits by which the toxin binds to a specific glycosphingolipid globotriaosyl ceramide (Gb3) receptor on the endothelial surface.[2,5] After binding, the toxin penetrates the cytosol by endocytosis and exerts its cytotoxic effect by inhibiting protein synthesis and causing cell death.[6-8] Monocytes/macrophages in response to VT release cytokines such as interleukin-1 (IL-1) and tumor necrosis factor (TNF) that remarkably potentiate sensitivity of vascular endothelial cells to VT by up-regulating endothelial Gb3 receptor.[9] Evidence also shows that renal microvascular endothelial cells have a higher sensitivity to the cytotoxic effect of VT as compared to endothelial cells derived from large vessels.[7,8]

The interaction between leukocytes and endothelial cells is instrumental in the development of microvascular injury in VT-associated HUS. Thus, evidence suggests that neutrophils isolated from children in the acute phase of D+HUS adhered to endothelial cells in culture more than normal neutrophils and induced endothelial injury by local release of proteases.[10] We have demonstrated in vitro that VT-1 directly induced a massive leukocyte adhesion to

From the Mario Negri Institute for Pharmacological Research, Bergamo, Italy, and the Division of Nephrology and Dialysis, Azienda Ospedaliera, Ospedali Riuniti di Bergamo, Bergamo, Italy.

Submitted May 2, 2000; accepted May 15, 2001.

E.B. is a recipient of a fellowship from "Foppolo aiuta i bambini."

Reprints: Marina Morigi, Mario Negri Institute for Pharmacological Research, Via Gavazzeni 11, 24125 Bergamo, Italy; e-mail: morigi@marionegri.it.

The publication costs of this article were defrayed in part by page charge payment. Therefore, and solely to indicate this fact, this article is hereby marked "advertisement" in accordance with 18 U.S.C. section 1734.

cultured endothelial cells under flow conditions, by up-regulating the adhesive proteins E-selectin, intercellular adhesion molecule-1 (ICAM-1), and vascular cell adhesion molecule-1 (VCAM-1).[11] Furthermore, a preliminary report has shown that glomerular endothelial cells exposed to VT became more susceptible to neutrophil-mediated oxidant injury.[12] Taken together these studies indicate that VT causes cell injury by altering cell adhesive properties and by increasing endothelial susceptibility to leukocyte-mediated injury. The resulting injured endothelium changes its normal thromboresistant phenotype and becomes thrombogenic, initiating microvascular thrombus formation.

In HUS, structural damage of microvessels associated with narrowing of the lumina determines major changes in fluid shear stress, which would favor persistent endothelial damage, platelet activation, and progression of microvascular thrombosis.[13] Changes in shear stress, the tractive force produced by blood flowing over the endothelial surface, have a profound influence on von Willebrand factor (vWF) handling by enhancing its susceptibility to proteolytic cleavage.[14] Under conditions of high shear stress, vWF undergoes conformational changes and serves to bridge the subendothelial matrix to glycoprotein (GP) Ib expressed on platelet membranes.[15] The engagement of this receptor promotes activation of the platelet $\alpha_{IIb}\beta_3$ (GPIIb/IIIa) complex that binds to the RGD (Arg-Gly-Asp) sequence of vWF leading to thrombus formation.[15] Via the RGD sequence, vWF may also bind vitronectin receptor ($\alpha_v\beta_3$), the major integrin expressed on endothelial cells[16] that promotes endothelial cell adhesion to the vascular matrix.[17] GPIb is also expressed on endothelial cells; however, controversial results about its function have been reported so far.[18,19]

Several distinct endothelial cell molecules have been reported to be involved in the binding of platelets to endothelial cells. P-selectin, which is stored in intracellular granules of platelets and endothelial cells together with vWF and which rapidly mobilizes to the cell surface on stimulation,[20] is required for platelet rolling and adhesion on activated endothelium.[21] Increased plasma levels of P-selectin have been measured in patients with HUS, possibly reflecting activation/damage of platelets and endothelial cells.[22] Evidence also indicates that platelet-endothelial cell adhesion molecule-1 (PECAM-1) expressed on endothelial cells[23] contributes to platelet adhesion and aggregation at sites of injured endothelium, as documented by the finding that anti-PECAM-1 antibody injection delayed thrombus formation in laser-induced microvessel injury of mouse brain.[24]

In the present study, we sought to (1) assess whether VT-1 directly affected the antithrombogenic properties of the endothelium under high shear stress; (2) evaluate whether microvascular endothelium had a higher sensitivity to VT-1–induced thrombus formation, as compared to endothelium derived from large vessels; and (3) identify platelet and endothelial cell adhesive proteins involved in the thrombotic process promoted by VT-1.

Materials and methods

Endothelial cell culture and incubation

The human microvascular endothelial cell line of dermal origin (HMEC-1)[25] was a kind gift from Dr Francisco J. Candal (Centers for Disease Control and Prevention, Atlanta, GA). The growth medium consisted of MCDB 131 (Gibco, Grand Island, NY) supplemented with 10% fetal bovine serum (Gibco), 1 μg/mL hydrocortisone, 100 U/mL penicillin, 100 μg/mL streptomycin, 2 mM glutamine (Gibco), and 50 μg/mL endothelial cell growth factor prepared as described.[26]

Human umbilical vein endothelial cells (HUVECs) were obtained by collagenase digestion according to the method of Jaffe and coworkers.[27] The cells were grown in Medium 199 (Gibco) supplemented with 10% newborn calf serum (Gibco) and 10% human serum, 5 mM *N*-2-hydroxyethylpiperazine-*N*-2-ethanesulfonic acid (HEPES; Sigma Chemical, St Louis, MO), 100 U/mL penicillin, 100 μg/mL streptomycin, 2.5 μg/mL fungizone, 2 mM glutamine (Gibco), 15 U/mL heparin (Parke-Davis, Milan, Italy), and 50 μg/mL endothelial cell growth factor. Cultured cells were identified as endothelial by their cobblestone morphology and the presence of vWF, using indirect immunofluorescence microscopy. Confluent HUVECs were used for experiments between the first and fifth passage.

Primary human microvascular endothelial cells of dermal origin (HDMECs) (Promocell, Heidelberg, Germany) were cultured in endothelial cell growth medium MV plus SupplementMix (Promocell). HDMECs were used between the second and sixth passage.

For the experiments, endothelial cells were plated on 60 × 20-mm plastic coverslips (Thermanox; Nunc, Naperville, IL) and used 1 day after reaching confluence.

To study the effect of VT-1 in inducing platelet adhesion and thrombus formation, HMEC-1 and HUVECs were pre-exposed for 24 hours in static condition to 2, 10, and 50 pM VT-1 (kindly provided by Dr M. A. Karmali, Hospital for Sick Children, Toronto, ON, Canada; endotoxin content <0.05 EU/mL using Limulus amoebocyte lysate assay) in medium plus 2% fetal calf serum (Hyclone Laboratories, Logan, UT); then cells were perfused at 60 dynes/cm^2 in a parallel plate flow chamber with human blood. Blood was drawn from an antecubital vein through a 19-gauge needle (infusion set) directly into a polypropylene tube and prelabeled for 5 minutes with fluorescent dye mepacrine (10 μM, quinacrine dihydrochloride BP; Sigma Chemical). Blood was then transferred (5-mL aliquots) to test tubes and not disturbed until assay. The percentage of the surface occupied by thrombi was calculated by analysis of fluorescent thrombus images acquired by confocal microscopy.

The concentrations of VT-1 used for the adhesion experiments did not affect cell count after 24 hours of incubation either in HMEC-1 (10 pM: $75 \pm 0.5 \times 10^4$, 50 pM: $75 \pm 5 \times 10^4$ versus control: $70 \pm 5 \times 10^4$ cells) or in HUVECs (10 pM: $38.2 \pm 1.1 \times 10^4$, 50 pM: $37.4 \pm 0.7 \times 10^4$ versus control: $36.5 \pm 0.5 \times 10^4$ cells).

To evaluate endothelial integrity, HMEC-1 pre-exposed for 24 hours to VT-1 (10 pM) were perfused with blood without mepacrine and then fixed with 0.5% glutaraldehyde (Fluka, Milan, Italy), dehydrated with methyl alcohol, and stained with May-Grunwald Giemsa technique (Carlo Erba Reagents, Milan, Italy).

By selected experiments we verified whether the HMEC-1 cell line exhibited a similar sensitivity to VT-1—as for the VT effect to induce thrombus formation—compared with primary HDMECs. For this purpose HMEC-1 and HDMECs were exposed to VT-1 (10 pM) for 24 hours. HUVECs were studied in parallel.

To compare the effect of VT-1 with respect to other thrombogenic stimuli, HMEC-1 and HUVECs were exposed to thrombin (2 U/mL, 10 minutes; Biosciences, La Jolla, CA), TNF-α (100 U/mL, 4 hours; BASF KNOLL, Ludwigshafen, Germany), IL-1β (100 U/mL, 4 hours; Becton Dickinson, Milan, Italy), or VT-1 (10 pM, 24 hours) and perfused with blood at 60 dynes/cm^2.

To identify platelet receptors involved in VT-induced thrombus formation, HMEC-1 treated for 24 hours with VT-1 (10 pM) were perfused with human blood preincubated with inhibitors of GPIb and $\alpha_{IIb}\beta_3$ receptor binding. We used polymeric aurin tricarboxylic acid (ATA; ATA trisodium salt, Aldrich Chemical, Milwaukee, WI) that interacts with vWF and inhibits its binding to platelet receptor GPIb.[28] Because the most effective inhibitors of vWF are ATA polymers of molecular weight greater than 2500 d,[29] the higher molecular weight polymers of ATA were separated from the lower molecular weight ones by a 30-kd cutoff dialysis membrane concentrators (Centricon 30, Amicon, Beverly, MA). For experiments blood samples were incubated with ATA (100 μg/mL) for 5 minutes at 37°C before perfusion on VT-treated HMEC-1. The platelet receptor $\alpha_{IIb}\beta_3$ was blocked by incubating blood samples with chimeric 7E3 Fab anti-$\alpha_{IIb}\beta_3$

(20 μg/mL; Abciximab, Reopro; Eli Lilly, Indianapolis, IN)[30] for 5 minutes at 37°C before blood perfusion.

To determine the endothelial adhesive proteins involved in VT-induced thrombus formation, HMEC-1 pretreated with VT-1 (10 pM) for 24 hours were incubated with chimeric 7E3 Fab (20 μg/mL) for 20 minutes, mouse monoclonal antibody (mAb) antihuman vitronectin receptor LM609 (10 μg/mL; Chemicon International, Temecula, CA) for 10 minutes, mouse mAb anti-GPIbα LJ-Ib1 (100 μg/mL, a kind gift from Dr Zaverio M. Ruggeri, The Scripps Research Institute, La Jolla, CA)—a competitive inhibitor of vWF binding—for 20 minutes,[31] mouse mAb antihuman P-selectin (50 μg/mL; Endogen, Woburn, MA) for 20 minutes, or mouse mAb antihuman PECAM-1 (25 μg/mL, Endogen) for 10 minutes; then the adhesion assay was performed. Appropriate concentration and incubation time for each antibody were identified by preliminary experiments. Irrelevant antibody of mouse IgG1 (CAMfolio, Becton Dickinson) at concentrations of 10, 25, and 50 μg/mL were used.

The involvement of P-selectin and PECAM-1 in VT-1–induced thrombus formation on HDMECs was also assessed, using the same experimental condition described above for HMEC-1.

Adhesion assay under flow conditions and fluorescence confocal microscopy

Platelet adhesion assay was performed with whole blood perfused in a chamber using a syringe pump. A flow chamber regulated at 37°C was used, in which one surface of the perfusion channel was a coverslip (Thermanox; Nunc, Naperville, IL) seeded with a monolayer of endothelial cells. The chamber dimensions (30 × 1 mm and 150 μm in thickness) allow us to obtain a wide range of shear rates using low flow rates of blood. The flow conditions are well characterized for this geometry and are predicted to be laminar with very low Reynolds number (< 10); precise estimation of shear stress conditions on the adhesion surface was also performed using the computational fluid dynamic analysis (CFD package FIDAP, Fluid Dynamic International, Evanston, IL) to verify the inlet and outlet effect on flow velocity profiles. The system was filled with 10 mM phosphate-buffered saline (PBS) at pH 7.3; then the slide seeded with the endothelial monolayer was mounted in the flow chamber. Heparinized whole blood was incubated with the fluorescent dye mepacrine (10 μM). Mepacrine concentrates in the dense granules of platelets and in the granules of leukocytes. At this concentration it has no effect on normal platelet function.[32] Any fluorescence within the erythrocytes is quenched by hemoglobin. Blood preincubated for 5 minutes at 37°C was then perfused into the chamber at constant flow rate of 1500 l/sec (60 dynes/cm^2). After 3 minutes, perfusion was stopped and the slide with the endothelial cell monolayer was dehydrated and fixed in acetone for 20 minutes.

Images of platelet thrombi on endothelial cell surface were acquired by a confocal inverted laser microscope (InSight plus; Meridian Instruments, Okemos, MI). An argon laser emission filter at 488 nm was used to excite specimens. Fifteen fields, systematically digitized along the adhesion surface, were acquired using a computer-based image analysis system. The area occupied by thrombi was evaluated by automatic edge detection using built-in specific functions of the software Image 1.61 (National Institutes of Health, Bethesda, MD), and expressed as μm^2/field analyzed (total area: 474 473 μm^2/field).

Scanning electron microscopy

For scanning electron microscopy analysis HMEC-1 grown on coverslips were treated with VT-1 (10 pM, 24 hours), perfused with blood, and then fixed overnight at 4°C with 2.5% glutaraldehyde in 0.1 M sodium cacodylate buffer, pH 7.4. The slides were rinsed in 0.1 M sodium cacodylate buffer, osmicated for 1 hour, and then dehydrated in an ascending series of ethanol. The dehydration series concluded with 2 × 15-minute exchanges in 100% ethanol. After drying, the slides were coated with gold and examined in a scanning electron microscope (Stereoscan 200, Cambridge Instruments, Cambridge, MA).

Flow cytometry analysis

The surface expression of VT-1 receptor on HMEC-1 and HUVECs was evaluated by flow cytometry analysis (FACS; FACSort, Becton Dickinson). Endothelial cells in suspension were incubated for 45 minutes at room temperature with 1 μg/100 μL fluorescein isothiocyanate (FITC)–labeled albumin (Sigma Chemical) as control or 1 μg/100 μL FITC-labeled VT-1B subunit (a kind gift from Dr C. A. Lingwood, The Hospital for Sick Children, Toronto, ONT),[33] washed 3 times, fixed with 2% paraformaldehyde, and assayed within 1 hour.

Fluorescence confocal microscopy

The HMEC-1 line and HDMECs grown on coverslips were incubated with medium alone or VT-1 (10 pM) for 24 hours and then fixed in 3% paraformaldehyde plus 2% sucrose in PBS, pH 7.4, for 15 minutes at room temperature. After 3 washings (5 minutes) with PBS plus 3% bovine serum to prevent nonspecific antibody binding, cells were treated with anti-P-selectin antibody (50 μg/mL) or antivitronectin receptor antibody LM609 (10 μg/mL). For PECAM-1 assessment, cells were permeabilized with Triton X-100 (0.1% in PBS; Sigma Chemical) for 4 minutes before incubation with anti-PECAM-1 antibody (10 μg/mL). Then cells were incubated with FITC-conjugated F(ab')$_2$ goat antimouse IgG + IgM (Jackson Immunoresearch Laboratories, West Grove, PA).

Negative control experiments with FITC-conjugated antibody alone were performed. Coverslips were washed, mounted in 1% *N*-propyl-gallate in 50% glycerol, 0.1 M Tris-HCl, pH 8, and examined under confocal inverted laser microscopy. Representative fields were digitized with millions of colors and printed.

Statistical analysis

Results are expressed as mean ± SE. Statistical analysis was performed using ANOVA followed by the Tukey test for multiple comparisons, as appropriate.[34] Statistical significance was defined as P less than .05.

Results

VT-1 promotes platelet adhesion and thrombus formation on endothelial cells

We studied the effect of VT-1 on platelet adhesion and thrombus formation under laminar flow at high shear rate on HMEC-1. HUVECs were used for comparison as large-vessel endothelium. Heparinized blood was prelabeled with mepacrine and perfused at 60 dynes/cm^2 over resting or VT-1–treated endothelial cells; then thrombus formation was quantified by analyzing images acquired by confocal microscopy. On resting HMEC-1 only limited platelet deposits were observed, usually less than 0.3% of the total perfused area, corresponding to about 1200 μm^2/field analyzed. Exposure of HMEC-1 to VT-1 for 24 hours led to a significant ($P < .01$) increase in platelet adhesion and thrombus formation in comparison to control cells, with a maximum effect at 10 pM (2 pM: 7754 ± 1592; 10 pM: 10 090 ± 2246; 50 pM: 8244 ± 2874 versus control: 1077 ± 140 μm^2 area covered by thrombi) (Figure 1).

In these experimental conditions the endothelial cell integrity was preserved as indicated by staining with May-Grunwald Giemsa of HMEC-1 treated with VT-1 (10 pM) and then perfused with blood.

As shown in Figure 1, VT-1 also promoted platelet adhesion and thrombus formation on HUVECs but to a remarkably lower extent than on HMEC-1 (2 pM: 3406 ± 297; 10 pM: 3849 ± 540; 50 pM: 2497 ± 99 versus control: 1311 ± 263 μm^2).

Figure 2 depicts digitized images from a representative experiment acquired by confocal fluorescent microscopy showing an

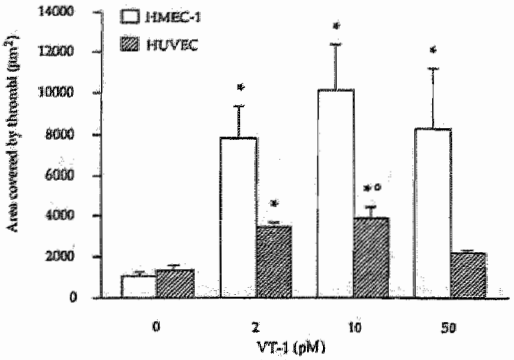

Figure 1. Effect of VT-1 on platelet adhesion and thrombus formation on HMEC-1 and HUVECs. HMEC-1 and HUVECs were treated for 24 hours with VT-1 (0, 2, 10, 50 pM) and then perfused with mepacrine-labeled blood at high shear stress (60 dynes/cm²). The area occupied by thrombi was measured on images acquired by confocal fluorescence microscopy, as described in "Materials and methods." Data are expressed as mean ± SE of area covered by thrombi (n = 8 experiments). *$P < .01$ versus untreated cells; °$P < .05$ HUVEC + VT-1(10 pM) versus HMEC-1 + VT-1 (10 pM).

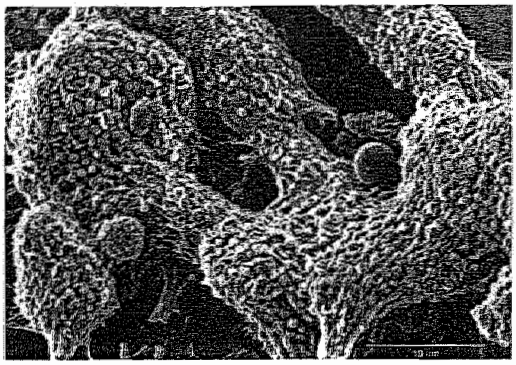

Figure 3. Scanning electron micrograph of thrombi on HMEC-1. HMEC-1 treated with VT-1 (10 pM) reveal organized thrombi with entrapped leukocytes at different stages of activation.

increase in the number of mepacrine-labeled thrombi on HMEC-1 exposed to VT-1 in comparison to HUVECs.

Scanning electron microscopy evaluation of VT-treated HMEC-1 illustrates the attachment of platelets to the endothelial cell monolayer to form organized thrombi in which leukocytes at different stages of activation are entrapped (Figure 3).

In selected experiments, the behavior of the HMEC-1 cell line in response to the thrombogenic effect of VT-1 was compared with that of primary microvascular endothelial cells of similar dermal origin. VT-1 (10 pM) induced thrombus formation on the HMEC-1 line and primary HDMEC to a similar extent (HMEC-1: 11 831 ± 1303; HDMEC: 9226 ± 1979 μm² area covered by thrombi). HUVECs used in these settings for comparison were significantly less susceptible to the effects of VT-1 (4061 ± 553 μm², $P < .01$ versus HMEC-1 and $P < .05$ versus HDMECs).

VT-1 is more thrombogenic than thrombin and cytokines

We compared the capability of VT-1 to induce thrombus formation on HMEC-1 and HUVECs with other thrombogenic agonists like thrombin, TNF-α, and IL-1β. As shown in Figure 4, thrombin and cytokines were less effective in promoting platelet deposition than VT-1 in both endothelial cell types. The superior thrombogenic effect of VT-1 translated in larger thrombus size with respect to thrombin, TNF-α, and IL-1β, indicating a selective pattern of endothelial activation implemented by VT-1 (mean area of thrombi, HMEC-1 + VT-1: 2584 ± 511 μm²; HMEC-1 + thrombin: 1140 ± 132 μm²; HMEC-1 + TNF-α: 1204 ± 588 μm²; HMEC-1 + IL-1β: 950 ± 362 μm²; and HUVEC + VT-1: 1748 ± 399 μm²; HUVEC + thrombin: 637 ± 128 μm²; HUVEC + TNF-α: 427 ± 149 μm²; HUVEC + IL-1β: 1406 ± 618 μm²).

VT-1 receptor expression on endothelial cells

To investigate whether the higher sensitivity of HMEC-1 to VT-1 with respect to HUVECs was due to a different expression of VT-1 receptors, FACS studies were performed using fluorescent VT-1B subunit. Surface expression of VT-1 receptor, as a percentage of fluorescent cells, is depicted in Figure 5. The percentage of resting HMEC-1 stained with fluorescent VT-1B subunit was approximately 20-fold higher than that observed for HUVECs. FITC-albumin, used as control, bound to HMEC-1 and HUVECs at comparable extents (1% ± 0.08% and 0.9% ± 0.1% of fluorescent cells, respectively).

Effect of functional blockade of platelet and endothelial adhesive molecules on VT-1–induced thrombus formation in HMEC-1

To identify adhesive proteins involved in thrombus formation induced by VT-1 at high shear rate, we first evaluated the effect of

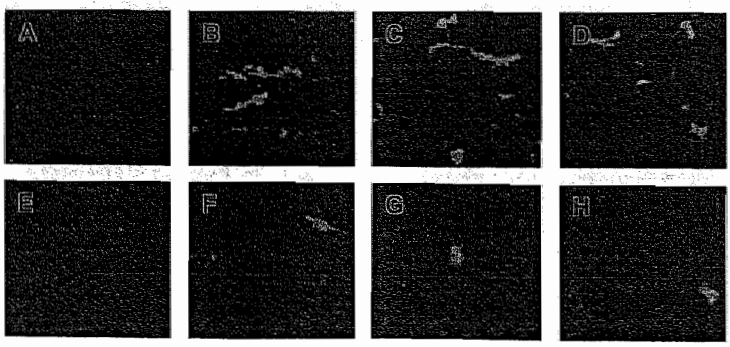

Figure 2. Thrombi formed after treatment with VT-1. Micrographs show thrombi formed on HMEC-1 (A-D) and HUVEC (E-H) treated with VT-1. Cells were incubated with control medium (A,E) or with VT-1 at 2 pM (B,F), 10 pM (C,G), 50 pM (D,H) for 24 hours, perfused with blood at 60 dynes/cm², and examined by confocal microscopy. Digitized representative fields are shown.

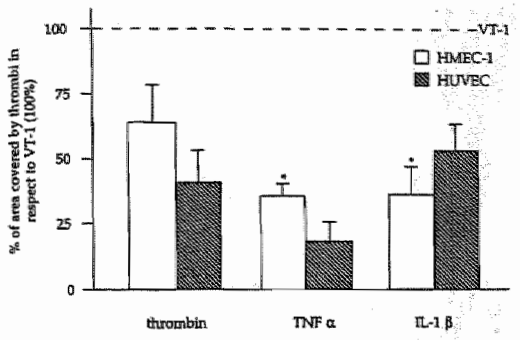

Figure 4. Effect of thrombin, TNF-α, and IL-1β on thrombus formation on HMEC-1 and HUVEC compared with VT-1. Endothelial cells were incubated with thrombin (2 U/mL, 10 minutes), TNF-α (100 U/mL, 4 hours), IL-1β (100 U/mL, 4 hours), or VT-1 (10 pM, 24 hours), perfused with blood at 60 dynes/cm², and examined under confocal microscopy. Data are expressed as mean ± SE of percent of area covered by thrombi in respect to VT-1 (100%) (n = 3 experiments). *$P < .01$ versus VT-1.

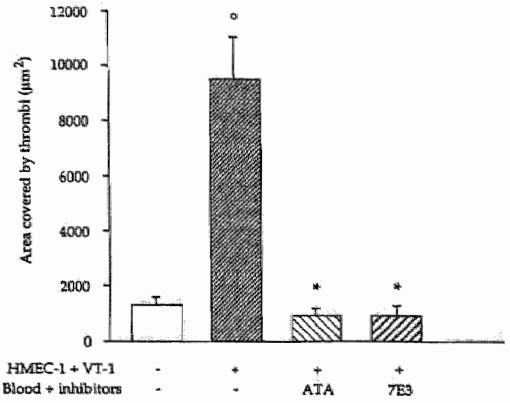

Figure 6. Effect of blockade of vWF binding to platelet GPIb or $\alpha_{IIb}\beta_3$ with specific inhibitors on VT-1–induced thrombus formation on HMEC-1. ATA (100 μg/mL), which inhibits vWF binding to GPIb, or 7E3 Fab (20 μg/mL), an anti-$\alpha_{IIb}\beta_3$, was added to blood 5 minutes before perfusion over HMEC-1. Data are expressed as mean ± SE (n = 6 experiments). *$P < .01$ versus control; *$P < .01$ versus VT-1.

blocking the interaction between vWF and platelet receptors GPIb and $\alpha_{IIb}\beta_3$. As shown in Figure 6, ATA, which inhibits vWF-GPIb interaction, completely prevented platelet deposition and thrombus formation induced by VT-1 (10 pM) on HMEC-1 surface (VT-1 + ATA: 919 ± 256 μm² versus VT-1: 9502 ± 1475 μm,² $P < .01$). A similar significant ($P < .01$) reduction in the area occupied by thrombi was observed by blocking the platelet receptor $\alpha_{IIb}\beta_3$ with the chimeric 7E3 Fab (VT-1 + 7E3: 952 ± 278 μm²).

Considering that GPIb is also expressed on endothelial cells, we investigated the role of this receptor on VT-1–induced thrombus formation in HMEC-1. Functional blocking of GPIb with LJ-Ib1 mAb did not affect thrombus formation in response to VT-1 (VT-1 + anti-GPIb: 12 096 ± 2716 μm² versus VT-1: 12 696 ± 1677 μm²), suggesting that in this experimental setting endothelial GPIb was not involved in vWF-induced thrombi at high shear stress.

Because it is known that vWF, besides binding extracellular matrix proteins, can interact with endothelial β_3-integrin subunit via RGD sequence, we assessed the role of β_3-integrin and more specifically of $\alpha_v\beta_3$ in the thrombotic process induced by VT-1 in HMEC-1. As shown in Figure 7, blocking of β_3-integrin subunit by 7E3 or inhibition of $\alpha_v\beta_3$-integrin complex by LM609 both resulted in a significant ($P < .01$) reduction of the area covered by thrombi (VT-1 + 7E3: 2477 ± 515 μm²; VT-1 + LM609: 3096 ± 972 μm² versus VT-1: 11 609 ± 1961 μm²).

To investigate endothelial adhesive proteins that can directly interact with platelet receptors, HMEC-1 preincubated for 24 hours with VT-1 were exposed to anti-P-selectin and anti-PECAM-1 antibodies. Anti-P-selectin antibody almost completely ($P < .01$) prevented platelet adhesion (VT-1 + anti-P selectin: 2386 ± 826 μm²). Blocking of PECAM-1 had a less pronounced but still significant ($P < .05$) inhibitory effect on VT-1–induced thrombus formation with the area covered by thrombi averaging 4553 ± 532 μm² (Figure 7). Irrelevant antibody did not significantly modify VT-1–induced platelet deposition (percent of reduction in area covered by thrombi compared with VT-1 alone: 10 μg/mL, 2%; 25 μg/mL, 9%; and 50 μg/mL, 15%).

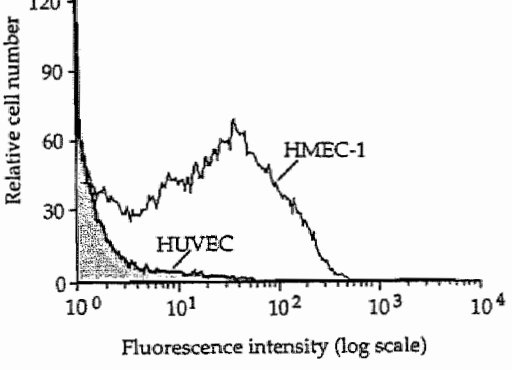

Figure 5. Flow cytometric analysis of VT-1 receptor expression on unstimulated HMEC-1 and HUVECs using FITC-labeled VT-1B subunit. Percentage of fluorescent HMEC-1 cells was 34% and of fluorescent HUVEC cells, 2%.

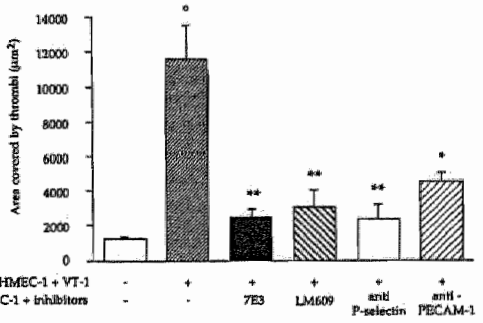

Figure 7. Effect of functional blockade of endothelial adhesion molecules on VT-1–induced thrombus formation on HMEC-1. Cells pretreated with VT-1 (10 pM, 24 hours) were incubated with the following adhesion blocking antibodies: anti-β_3-integrin subunit (7E3 Fab 20 μg/mL for 20 minutes), anti-$\alpha_v\beta_3$ (LM609 10 μg/mL for 10 minutes), anti-P-selectin (50 μg/mL for 20 minutes), and anti-PECAM-1 (25 μg/mL for 10 minutes) before blood perfusion at 60 dynes/cm². Data are expressed as mean ± SE (n = 6 experiments). *$P < .01$ versus untreated cells. **$P < .05$, **$P < .01$ versus VT-1.

The involvement of P-selectin and PECAM-1 in platelet deposition elicited by VT-1 was also confirmed on primary microvascular endothelial cells by using functional blocking antibodies that reduced by 79% ± 7% and 86% ± 4%, respectively, the area covered by thrombi ($P < .01$ versus VT-1).

Endothelial adhesive proteins involved in VT-1–induced thrombus formation

We characterized by confocal fluorescence microscopy the distribution on the endothelial surface of the adhesive molecules found in the above experiments to be implicated in the thrombotic process induced by VT-1. As shown in Figure 8A,B, HMEC-1 treated with VT-1 (10 pM, 24 hours) exhibited an increased expression of vitronectin receptor, as small diffuse granules on the luminal surface, in comparison to unstimulated cells.

The HMEC-1 cell line in a resting condition did not stain for P-selectin on the apical surface (Figure 8C). In contrast, on VT-1 challenge a strong fluorescence was observed with the P-selectin staining pattern of granules distributed on the apical side (Figure 8D).

PECAM-1 localized to the cell-cell border of adjacent unstimulated HMEC-1 as a linear staining (Figure 8E). After treatment with VT-1 PECAM-1 redistributed away from intercellular junctions and formed irregular patches of staining along the periphery of the cell or diffuse granules on the luminal surface and/or at the intracellular level (Figure 8F).

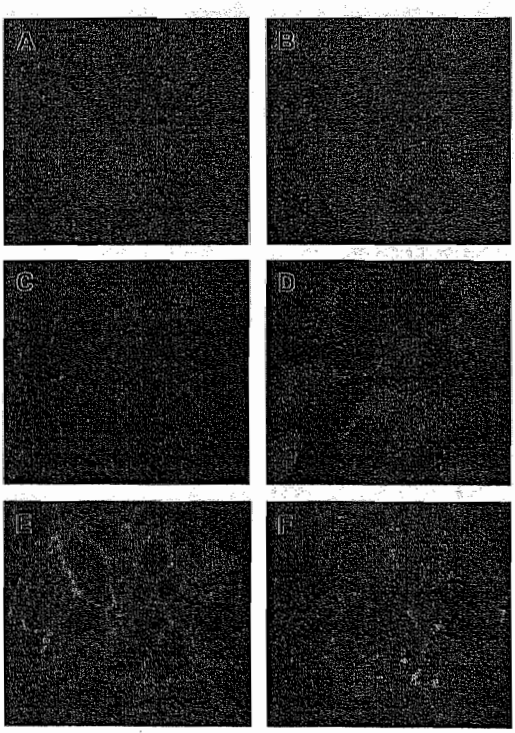

Figure 8. Expression of adhesive molecules in HMEC-1 treated with VT-1. Micrographs of HMEC-1 treated with control medium (A,C,E) or VT-1 (10 pM, 24 hours; B,D,F) and stained for vitronectin receptor $\alpha_v\beta_3$ (A,B), P-selectin (C,D), and PECAM-1 (E,F). HMEC-1 exposed to VT-1 showed an increased surface expression of vitronectin receptor and P-selectin as a diffuse granular pattern. PECAM-1 appeared redistributed away from the cell junctions after VT-1 treatment (n = 3 experiments).

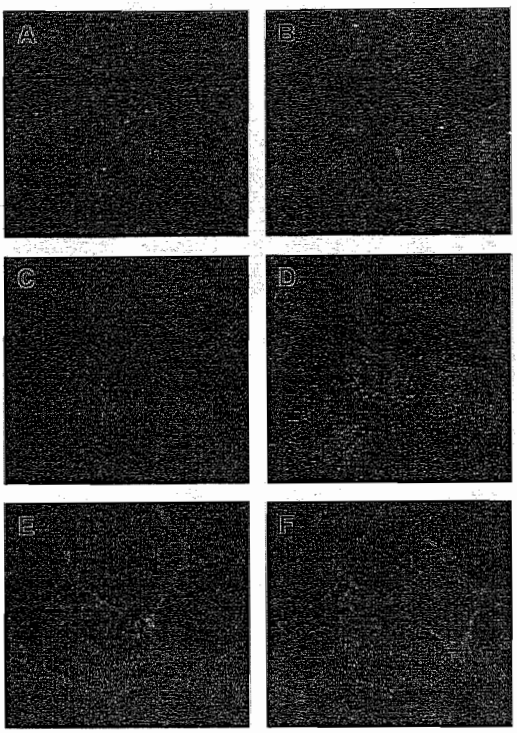

Figure 9. Expression of adhesive molecules in HDMECs treated with VT-1. Micrographs of HDMEC treated with control medium (A,C,E) or VT-1 (10 pM, 24 hours; B,D,F) and stained for vitronectin receptor $\alpha_v\beta_3$ (A,B), P-selectin (C,D), and PECAM-1 (E,F). HDMEC exposed to VT-1 showed an increased surface expression of vitronectin receptor and P-selectin as a diffuse granular pattern. PECAM-1 appeared redistributed away from the cell-cell border and irregular patches of staining were evident along the periphery of the cells after VT-1 treatment (n = 3 experiments).

By studying the effect of VT-1 on the expression of these adhesive proteins in primary HDMECs we observed a distribution similar to that of the HMEC-1 line (Figure 9A-F).

Discussion

Verotoxin-producing *E coli*, the causative agent of D+HUS, activates endothelial cells to acquire a prothrombotic phenotype with corresponding lesions confined to microvessels mostly of renal glomeruli.[1-4]

In this report we show for the first time that VT-1 directly induces platelet adhesion and thrombus formation on cultured endothelial cells perfused with whole blood in a flow chamber system under shear stress levels high enough to mimic the ones encountered in the microcirculation. The effect of VT-1 was superior to that of other known thrombogenic agonists such as thrombin and cytokines.

The area occupied by thrombi was more pronounced on VT-1–treated endothelial cells of microvascular (HMEC-1) in comparison with large-vessel (HUVEC) origin. The HMEC-1 line

had a similar sensitivity to the thrombogenic effect of VT-1 as HDMECs.

That microvascular endothelium is indeed more susceptible to the prothrombotic activity of VT-1 is consistent with previous findings. Thus, renal microvascular endothelial cell viability, as well as their protein synthesis capacity, were reduced by VT concentrations that were instead not cytotoxic for HUVECs.[7] Basal Gb3 levels in renal microvascular endothelial cells were 50-fold higher than in HUVECs, which suggested a relationship between the degree of VT sensitivity and the amount of Gb3 receptor expressed by these cells.[7] Similar to renal microvascular endothelial cells, we found that HMEC-1 expressed about 20-fold more VT-1 receptors than HUVECs, which might account for the different sensitivity of different vascular beds to VT-mediated disease.

In the attempt to identify the adhesive proteins involved in platelet-endothelial cell interactions elicited by VT-1, which eventually resulted in thrombus formation on HMEC-1, we first focused on vWF, which is the indispensable adhesive substrate to promote platelet thrombus formation in high shear stress environments.[15] We found that ATA, an inhibitor of vWF-platelet GPIb interaction, completely prevented the deposition of thrombi. Furthermore, blockade of $\alpha_{IIb}\beta_3$ on activated platelets by chimeric 7E3 Fab also abrogated platelet adhesion and thrombus formation. These observations extend to our experimental condition what has been documented in other settings,[15,35] that is, at high shear stress the mechanism supporting platelet adhesion and thrombus formation requires binding of platelet GPIb to vWF. The engagement of this receptor then promotes activation of platelet receptor $\alpha_{IIb}\beta_3$ that mediates irreversible adhesion by interacting with the RGD sequence of vWF. Therefore, the inhibition of one of these steps with ATA or 7E3 would result in a complete blocking of thrombus formation.

It has been widely described that interaction of vWF with platelet GPIb/$\alpha_{IIb}\beta_3$ is instrumental in mediating platelet adhesion to subendothelial matrix at high shear rates.[15] Here, we provide a series of observations indicating that vWF-mediated platelet adhesion on VT-1 challenge occurred mainly on the endothelial surface rather than in the subendothelium. First, we have verified by light microscopy that the integrity of the endothelial layer was still preserved after blood perfusion at high shear stress. Moreover, based on the evidence that vWF via the RGD sequence[17] binds vitronectin receptor ($\alpha_v\beta_3$), the major integrin expressed on endothelial cells,[16] we have documented by confocal fluorescence microscopy that vitronectin receptors were up-regulated and/or redistributed on the apical aspect of HMEC-1 after VT-1 exposure. Finally, functional blocking of endothelial vitronectin receptor $\alpha_v\beta_3$ with LM609 almost completely abrogated thrombus formation. Altogether these data indicate that VT-1 alters endothelial thromboresistance by inducing changes in the surface expression of vitronectin receptor that leads to platelet deposition via a vWF-dependent bridging mechanism. These findings are in line with recent studies showing that prothrombotic mediators such as α-thrombin and IL-1β induced on the luminal surface of endothelial cells up-regulation of vitronectin receptors that in turn promoted platelet adhesion through an RGD-dependent pathway.[36]

Our finding that treatment of endothelial cells with anti-GPIb antibody did not inhibit thrombus formation induced by VT-1 suggested that GPIb expressed on endothelium is not engaged in the interaction with soluble vWF in a high shear stress environment.

The endothelial adhesive molecules P-selectin[20] and PECAM-1[23] have been involved in the process of platelet deposition on activated or damaged endothelium by their direct binding to platelets.[21,24,37] Thus, it has been shown by intravital fluorescence microscopy that ischemia/reperfusion injury caused overexpression of P-selectin on intestinal microvascular endothelial cells, in association with platelet rolling and adhesion.[37] Antibodies against P-selectin significantly reduced microvascular thrombosis, which implied a direct role of this endothelial adhesive molecule in platelet deposition under flow conditions.[37] We have found that inhibition of P-selectin with a specific antibody caused a significant decrease in VT-induced thrombus formation on HMEC-1. These data, along with our observation of a strong expression of P-selectin on the apical surface of HMEC-1 after VT-1 challenge, provide evidence for the involvement of P-selectin in the thrombotic process elicited by VT-1 at high shear stress.

As for endothelial PECAM-1, its contribution to platelet deposition was proved in a model of laser-induced endothelial injury in mouse brain arterioles by the observation that anti–PECAM-1 antibody reduced microvascular thrombosis over damaged but not denuded endothelium.[24] Our present study showed that functional blocking of PECAM-1 resulted in a significant reduction of the area covered by thrombi in HMEC-1 exposed to VT-1. In addition, confocal microscopy experiments revealed that VT-1 induced a redistribution of this protein away from cell junctions, a pattern similar to that described in human endothelial cells after cytokine stimulation.[38] We speculate that PECAM-1 once redistributed on the endothelial surface may undergo phosphorylation,[23] which would render this adhesive receptor available for platelet interaction.

In primary microvascular endothelial cells treated with VT-1, expression of vitronectin receptor, P-selectin, and PECAM-1 was similar to that observed in the HMEC-1 line. Moreover, as in HMEC-1, blockade of P-selectin and PECAM-1 by specific antibodies markedly limited VT-1–induced thrombus formation, thus suggesting that thrombotic response elicited by VT-1 involved activation of the same endothelial adhesive proteins in both line and primary microvascular endothelial cells.

In conclusion, our results indicate for the first time that (1) VT-1 is a potent promoter of platelet adhesion and thrombus formation on endothelial cells under high shear stress; (2) microvascular endothelial cells demonstrate a remarkably greater sensitivity to the thrombogenic effect of VT-1 than endothelium derived from large vessels, possibly due to the higher expression of VT-1 receptor; (3) at high shear stress interaction of vWF with platelet GPIb/$\alpha_{IIb}\beta_3$ supports VT-1–induced platelet deposition through the binding to vitronectin receptor on the endothelial luminal surface; and (4) up-regulation and/or redistribution of endothelial vitronectin receptors, P-selectin, and PECAM-1 appear instrumental in the process of thrombus formation induced by VT-1.

These findings might help to clarify why thrombi in HUS preferentially localize in microvessels and provide insights on the determinants possibly involved in the process of microvascular thrombosis associated with D+HUS.

Acknowledgments

We are indebted to Prof Giuseppe Silva and Piero Pellini for helpful cooperation during scanning electron microscopy evaluations (Politecnico di Milano, Italy). We thank Dr Anna Falanga (Unit of Hematology, Azienda Ospedaliera, Ospedali Riuniti di Bergamo, Italy) for kind cooperation, and Stefania Angioletti, Chiara Rossi, and Federica Casiraghi for technical assistance.

References

1. Remuzzi G, Ruggenenti P. The hemolytic uremic syndrome. Kidney Int. 1995;47:2-19.
2. Arbus GS. Association of verotoxin-producing *E. coli* and verotoxin with hemolytic uremic syndrome. Kidney Int. 1997;51(suppl.58):S91–S96.
3. Andreoli SP. The pathophysiology of the hemolytic uremic syndrome. Curr Opin Nephrol Hypertens. 1999;8:459-464.
4. Ruggenenti P, Remuzzi G. Thrombotic microangiopathy. In: Suki WN, Massry SG, eds. Suki and Massry's Therapy of Renal Diseases and Related Disorders. Boston: Kluwer Academic Publishers; 1998:513-527.
5. Lingwood CA. Role of verotoxin receptors in pathogenesis. Trends Microbiol. 1996;4:147-153.
6. van de Kar NCAJ, Monnens LAH, Karmali MA, van Hinsbergh VWM. Tumor necrosis factor and interleukin-1 induce expression of the verocytotoxin receptor globotriaosylceramide on human endothelial cells: implications for the pathogenesis of the hemolytic uremic syndrome. Blood. 1992;80:2755-2764.
7. Obrig TG, Louise CB, Lingwood CA, Boyd B, Barley-Maloney L, Daniel TO. Endothelial heterogeneity in Shiga toxin receptors and responses. J Biol Chem. 1993;268:15484-15488.
8. van Setten PA, van Hinsbergh VWM, van der Velden TJAN, et al. Effects of TNFα on verocytotoxin cytotoxicity in purified human glomerular microvascular endothelial cells. Kidney Int. 1997;51: 1245-1256.
9. van Setten PA, Monnens LAH, Verstraten RGG, van den Heuvel LPWJ, van Hinsbergh VWM. Effects of verocytotoxin-1 on nonadherent human monocytes: binding characteristics, protein synthesis, and induction of cytokine release. Blood. 1996;88:174-183.
10. Forsyth KD, Simpson AC, Fitzpatrick MM, Barratt TM, Levinsky RJ. Neutrophil-mediated endothelial injury in haemolytic uraemic syndrome. Lancet. 1989;ii:411-414.
11. Morigi M, Micheletti G, Figliuzzi M, et al. Verotoxin-1 promotes leukocyte adhesion to cultured endothelial cells under physiologic flow conditions. Blood. 1995;86:4553-4558.
12. Andreoli SP, Green DF. Verotoxin 1 promotes nitric oxide (NO) generation in glomerular endothelial cells (GEC) and accelerates PMN mediated GEC injury [abstract]. J Am Soc Nephrol. 1997;8: 582A.
13. Remuzzi G, Galbusera M, Salvadori M, Rizzoni G, Perle S, Ruggenenti P. Bilateral nephrectomy stopped disease progression in plasma-resistant hemolytic uremic syndrome with neurological signs and coma. Kidney Int. 1996;49:282-286.
14. Tsai H-M, Sussman II, Nagel RL. Shear stress enhances the proteolysis of von Willebrand factor in normal plasma. Blood. 1994;83:2171-2179.
15. Ruggeri ZM. Perspectives series: cell adhesion in vascular biology. von Willebrand factor. J Clin Invest. 1997;99:559-564.
16. Byzova TV, Rabbani R, D'Souza SE, Plow EF. Role of integrin $\alpha_v\beta_3$ in vascular biology. Thromb Haemost. 1998;80:726-734.
17. Cheresh DA. Human endothelial cells synthesize and express an Arg-Gly-Asp-directed adhesion receptor involved in attachment of fibrinogen and von Willebrand factor. Proc Natl Acad Sci U S A. 1987;84:6471-6475.
18. Wu G, Essex DW, Meloni FJ, et al. Human endothelial cells in culture and in vivo express on their surface all four components of the glycoprotein Ib/IX/V complex. Blood. 1997;90:2660-2669.
19. Perrault C, Lankhof H, Pidard D, et al. Relative importance of the glycoprotein Ib-binding domain and the RGD sequence of von Willebrand factor for its interaction with endothelial cells. Blood. 1997;90:2335-2344.
20. Wegner DD. P-selectin chases a butterfly [editorial]. J Clin Invest. 1995;95:1955-1956.
21. Frenette PS, Johnson RC, Hynes RO, Wagner DD. Platelets roll on stimulated endothelium in vivo: an interaction mediated by endothelial P-selectin. Proc Natl Acad Sci U S A. 1995;92:7450-7454.
22. Chong BH, Murray B, Berndt MC, Dunlop LC, Brighton T, Chesterman CN. Plasma P-selectin is increased in thrombotic consumptive platelet disorders. Blood. 1994;83:1535-1541.
23. Newman PJ. Perspectives series: cell adhesion in vascular biology. The biology of PECAM-1. J Clin Invest. 1997;99:3-8.
24. Rosenblum WI, Nelson GH, Wormley B, Werner P, Wang J, Shih CC-Y. Role of platelet-endothelial cell adhesion molecule (PECAM) in platelet adhesion/aggregation over injured but not denuded endothelium in vivo and ex vivo. Stroke. 1996;27: 709-711.
25. Ades EW, Candal FJ, Swerlick RA, et al. HMEC-1: establishment of an immortalized human microvascular endothelial cell line. J Invest Dermatol. 1992;99:683-690.
26. Maciag T, Cerundolo J, Ilsley S, Kelley PR, Forand R. An endothelial cell growth factor from bovine hypothalamus: identification and partial characterization. Proc Natl Acad Sci U S A. 1979; 76:5674-5678.
27. Jaffe E, Nachman R, Becker C, Minick C. Culture of human endothelial cells derived from umbilical veins; identification by morphologic and immunologic criteria. J Clin Invest. 1973;52:2745-2756.
28. Phillips MD, Moake JL, Nolasco L, Turner N. Aurin tricarboxylic acid: a novel inhibitor of the association of von Willebrand factor and platelets. Blood. 1988;72:1898-1903.
29. Weinstein M, Vosburgh E, Phillips M, Turner N, Chute-Rose L, Moake J. Isolation from commercial aurintricarboxylic acid of the most effective polymeric inhibitors of von Willebrand factor interaction with platelet glycoprotein Ib. Comparison with other polyanionic and polyaromatic polymers. Blood. 1991;78:2291-2298.
30. The EPIC Investigators. Use of a monoclonal antibody directed against the platelet glycoprotein IIb/IIIa receptor in high-risk coronary angioplasty. N Engl J Med. 1994;330:956-961.
31. Handa M, Titani K, Holland LZ, Roberts JR, Ruggeri ZM. The von Willebrand factor-binding domain of platelet membrane glycoprotein Ib. J Biol Chem. 1986;261:12579-12585.
32. Alevriadou BR, Moake JL, Turner NA, et al. Real-time analysis of shear-dependent thrombus formation and its blockade by inhibitors of von Willebrand factor binding to platelets. Blood. 1993;81: 1263-1276.
33. Lingwood CA. Verotoxin-binding in human renal sections. Nephron. 1994;66:21-28.
34. Wallenstein S, Zucker CL, Fleiss JL. Some statistical methods useful in circulation research. Circ Res. 1980;47:1-9.
35. Kroll MH, Hellums D, McIntire LV, Schafer AI, Moake JL. Platelets and shear stress. Blood. 1996;88:1525-1541.
36. Gawaz M, Neumann F-J, Dickfeld T, et al. Vitronectin receptor ($\alpha_v\beta_3$) mediates platelet adhesion to the luminal aspect of endothelial cells. Implications for reperfusion in acute myocardial infarction. Circulation. 1997;96:1809-1818.
37. Massberg S, Enders G, Leiderer R, et al. Platelet-endothelial cell interactions during ischemia/reperfusion: the role of P-selectin. Blood. 1998; 92:507-515.
38. Romer LH, McLean NV, Yan H-C, Daise M, Sun J, DeLisser HM. IFN-γ and TNF-α induce redistribution of PECAM-1 (CD31) on human endothelial cells. J Immunol. 1995;154:6582-6592.

CHAPTER 6

IN RESPONSE TO PROTEIN LOAD PODOCYTES REORGANIZE CYTOSKELETON AND MODULATE ET-1 GENE: IMPLICATION FOR PERMSELECTIVE DYSFUNCTION OF CHRONIC NEPHROPATHIES

M. Morigi, S. Buelli, S. Angioletti, C. Zanchi, L. Longaretti, C. Zoja, M. Galbusera, S. Gastoldi, P. Mundel, G. Remuzzi and A. Benigni

Am J Pathol 2005; 166: 1309-1320

American Journal of Pathology, Vol. 166, No. 5, May 2005

Cardiovascular, Pulmonary and Renal Pathology

In Response to Protein Load Podocytes Reorganize Cytoskeleton and Modulate Endothelin-1 Gene

Implication for Permselective Dysfunction of Chronic Nephropathies

Marina Morigi,* Simona Buelli,* Stefania Angioletti,* Cristina Zanchi,* Lorena Longaretti,* Carla Zoja,* Miriam Galbusera,* Sara Gastoldi,* Peter Mundel,† Giuseppe Remuzzi,*‡ and Ariela Benigni*

From the 'Mario Negri' Institute for Pharmacological Research, Bergamo, Italy; the Division of Nephrology and Dialysis,† Azienda Ospedaliera, Ospedali Riuniti di Bergamo, Bergamo, Italy; and the Department of Medicine,‡ Albert Einstein College of Medicine, New York, New York*

Effacement of podocyte foot processes occurs in many proteinuric nephropathies and is accompanied by rearrangement of the actin cytoskeleton. Here, we studied whether protein overload affects intracellular pathways, leading to cytoskeletal architecture changes and ultimately to podocyte dysfunction. Mouse podocytes bound and endocytosed both albumin and IgG via receptor-specific mechanisms. Protein overload caused redistribution of F-actin fibers instrumental to up-regulation of the prepro-endothelin (ET)-1 gene and production of the corresponding peptide. Increased DNA-binding activity for nuclear factor (NF)-κB and Ap-1 nuclear proteins was measured in nuclear extracts of podocytes exposed to excess proteins. Both Y27632, which inhibits Rho kinase-dependent stress fiber formation, and jasplakinolide, an F-actin stabilizer, decreased NF-κB and Ap-1 activity and reduced ET-1 expression. This suggested a role for the cytoskeleton, through activated Rho, in the regulation of the ET-1 peptide. Focal adhesion kinase (FAK), an integrin-associated nonreceptor tyrosine kinase, was phosphorylated by albumin treatment via Rho kinase-triggered actin reorganization. FAK activation led to NF-κB- and Ap-1-dependent ET-1 expression. These data suggest that reorganization of the actin cytoskeletal network in response to protein load is implicated in modulation of the ET-1 gene via Rho kinase-dependent FAK activation of NF-κB and Ap-1 in differentiated podocytes. Increased ET-1 generation might alter glomerular permselectivity and amplify the noxious effect of protein overload on dysfunctional podocytes. *(Am J Pathol 2005, 166:1309–1320)*

Glomerulosclerosis, key lesion of progressive renal disease, consists of extracellular matrix accumulation and progressive obliteration of glomerular capillaries with loss of glomerular filtration capacity. Permissive factors include high intraglomerular capillary pressure, hypertrophy, and the filtration of excess amounts of plasma proteins across the capillary barrier.[1–6] A crucial component of the glomerular filter is the podocyte, a highly specialized epithelial cell endowed with foot processes. Podocytes possess a contractile structure, composed of actin and associated proteins and connected to the glomerular basement membrane at focal contacts via $\alpha_3\beta_1$ integrin, that stabilizes glomerular architecture by counteracting the distension of the glomerular basement membrane.[7,8] The contractile apparatus of the foot processes responds to vasoactive hormones to control glomerular capillary surface area and in turn ultrafiltration coefficient.

Recent experimental and clinical evidence seems to imply an important role of podocytes in the pathophysiology of glomerular damage and progressive renal dysfunction.[9–14] In this context, repeated injections of albumin in rats are followed by glomerular epithelial cell swelling, cytoplasmic protein droplets in podocytes, and extensive foot process effacement. Such events culminate in podocyte detachment from the basement mem-

Accepted for publication January 20, 2005.

Part of this work was presented at the American Society of Nephrology/International Society of Nephrology World Congress of Nephrology (San Francisco, CA, October 10 to 17, 2001).

Address reprint requests to Dr. Marina Morigi, 'Mario Negri' Institute for Pharmacological Research, Via Gavazzeni 11, 24125 Bergamo, Italy. E-mail: morigi@marionegri.it.

brane.[15] Evidence of a causal link between podocyte protein deposition and progressive damage rests on the demonstration that in rats with renal mass reduction protein accumulation in podocytes preceded dedifferentiation and injury, documented as loss of synaptopodin and increase in desmin expression.[16] Podocyte abnormalities were accompanied by transforming growth factor-β mRNA up-regulation. Concomitantly, *in vitro* experiments indicated that albumin overload in cultured podocytes caused loss of the synaptopodin differentiation marker, and enhanced transforming growth factor-β1 mRNA and protein.[16] Whether protein overload also affects the generation of other mediators of renal damage in podocytes is ill defined.

Endothelin-(ET) 1, a highly potent vasoconstrictor peptide,[17] has been implicated in the pathogenesis of glomerulosclerosis[18] by virtue of its action on cell proliferation, chemotaxis, and extracellular matrix accumulation.[19] Among renal cells, glomerular epithelial cells constitutively express preproET-1 mRNA and synthesize the mature peptide[20,21] whose generation is markedly up-regulated by transforming growth factor-β, C5b-9, and thrombin.[20] Stringent control of ET-1 gene expression is achieved through a highly regulated promoter containing consensus sequences for the binding sites of the nuclear factor-1, the activating protein-1 (Ap-1), dimers Jun-Fos, GATA-2, and nuclear factor (NF)-κB.[22–24] Activating protein-1 transcriptional activation is regulated by Rho-related small GTPases[25] involved in the remodeling of actin cytoskeleton.[26,27] Finding that overexpression of dominant-negative mutants of RhoA and RhoB led to a significant reduction in pre-pro-ET-1 promoter activity indicates that Rho proteins modulate basal expression of ET-1 gene in endothelial cells.[28] No evidence is available as for the regulation of ET-1 gene transcription and related intracellular mechanisms in podocytes.

Here we test the hypothesis that protein overload alters the F-actin-based contractile podocyte apparatus resulting in modulation of ET-1 gene expression and production of the vasoactive peptide. We also provide evidence for relevant intracellular signaling evoked by cytoskeletal changes ultimately leading to ET-1 gene expression.

Materials and Methods

Cell Culture and Incubation

Immortalized mouse podocytes were grown according to the method described by Mundel and colleagues.[29] Briefly, cells were cultured under growth-permissive conditions on rat tail collagen type I-coated plastic dishes (BD Bioscience, Bedford, MA), at 33°C in RPMI 1640 medium (Invitrogen, Gaithersburg, MD) supplemented with 10% fetal bovine serum (Invitrogen), 10 U/ml mouse recombinant γ-interferon (Sigma Chemical Co., Saint Louis, MO), and 100 U/ml penicillin plus 0.1 mg/ml streptomycin (Sigma). To induce differentiation, podocytes were maintained in nonpermissive conditions at 37°C without γ-interferon for 14 days and used for the experiments. In this culture condition, cells stopped proliferating and were identified as differentiated podocytes by their arborized morphology and the presence of high levels of synaptopodin, using indirect immunofluorescence microscopy. Cells were routinely maintained for 24 hours in serum-free medium before all of the experiments.

Experimental Design

We first addressed whether albumin and IgG bind to podocytes through a receptor-mediated mechanism. Binding and uptake studies were performed as previously described[30] using human serum albumin (HSA, low endotoxin, Sigma) labeled with 5(6)-carboxyfluorescein-*N*-hydroxysuccinimide ester (FLUOS) or fluorescein isothiocyanate (FITC)-conjugated human IgG (IgG, Sigma). To investigate the effect of protein overload on F-actin cytoskeletal rearrangement, confluent differentiated podocytes were exposed for 30 minutes, and 1, 2, 6, 24, and 48 hours to medium alone or in the presence of 10 mg/ml of HSA or IgG (6 and 24 hours) (Sigma). Then cells were fixed and processed for immunofluorescence studies. Synaptopodin expression was evaluated by immunofluorescence experiments in podocytes challenged for 6 and 24 hours with HSA or IgG. The concentration of HSA and IgG was selected on the basis of previous experiments of ours and other investigators on podocytes[16] and tubular cells.[31–33] Because phenotypic changes induced by protein load have been found duration-dependent,[34] the relatively high concentration of plasma proteins in our short-term culture system would simulate the actual total amount of proteins handled by the cells in a chronic pathological condition.

The expression of ET-1 gene was evaluated in differentiated podocytes exposed to 10 mg/ml of albumin for different time intervals by Northern blot analysis and real-time polymerase chain reaction (PCR). Podocytes challenged with IgG (10 mg/ml) for 24 hours were also studied (real-time PCR). The time course of ET-1 protein synthesis was assessed by radioimmunoassay (RIA) in supernatants of podocytes exposed to HSA.

To study the possible role of cytoskeleton in the regulation of ET-1 gene in podocytes laden with proteins, cells were treated with Y27632 (10 μmol/L; Calbiochem, La Jolla, CA), a specific inhibitor of Rho kinase pathway involved in stress fiber formation,[35] or jasplakinolide (200 nmol/L; Molecular Probes, Cambridge, UK), an F-actin stabilizer,[36] 30 minutes prior and during 3, 6, 15, and 24 hours of incubation with albumin, taken as representative protein. Then ET-1 mRNA transcript and protein levels were measured.

The activation of the transcription factors NF-κB and Ap-1 was investigated in podocytes exposed to medium alone, HSA, or IgG (10 mg/ml, 30 minutes). The effect of the cytoskeleton inhibitors, Y27632 and jasplakinolide, on DNA-binding activity of these transcription factors was also assessed. To elucidate the role of focal adhesion kinase (FAK), an integrin-associated nonreceptor tyrosine kinase, in HSA-induced ET-1 expression, we first investigated the phosphorylation of FAK by Western blot in podocytes treated for 5 minutes, 30 minutes, and 1, 2,

3, and 6 hours with HSA (10 mg/ml). We then assessed the impact of cytoskeleton rearrangement on FAK activation by studying the effect of Y27632 or jasplakinolide in podocytes exposed for 30 minutes to HSA. Next, functional blockade of FAK with genistein (25 μmol/L, Calbiochem)[37] on NF-κB and AP-1 activation was investigated. Finally, the effect of FAK inhibition on ET-1 expression was evaluated by studying the effect of genistein, an inhibitor of tyrosine kinases, or the transfection with a recombinant adenovirus encoding FAK-related nonkinase (Ad-FRNK)[38] in podocytes challenged with HSA for 3 hours. To understand the functional significance of increased ET-1 production we evaluated the effect of exogenous ET-1 (100 nmol/L, Sigma),[39] added to podocytes for 2, 6, and 15 hours, on F-actin distribution.

Albumin Labeling

Ten mg of human albumin (Sigma) were dissolved in 1 ml of buffer carbonate, pH 8.5, added to a solution of 1 mg of FLUOS in dimethylsulfoxide (Sigma). Labeled HSA was separated from unbound material by gel chromatography using Sephadex G50 column (Pharmacia Fine Chemicals, Uppsala, Sweden) pre-equilibrated and eluted with carbonate buffer. The eluted fraction was analyzed with a spectrometer, UV/Vis at the wavelengths of 280 and 486 nm, and final concentration of albumin was determined by Coomassie blue G dye-binding method.

Binding and Uptake Studies

HSA Binding and Uptake

For binding experiments, podocytes were grown on collagen-coated plastic Petri dishes and used 14 days after seeding. The cells were maintained for 24 hours in serum-free condition and then washed with Ringer's solution, pH 6.0, at 4°C to remove proteins or amino acids. Binding inhibition studies were performed incubating podocytes with Ringer's solution, pH 6.0, containing 50 μg/ml of FLUOS-HSA on ice for 15 minutes in the absence or presence of increasing concentrations of cold HSA (0 to 10 mg/ml). Unbound FLUOS-HSA was removed by washing with Ringer's solution, pH 7.4. Cells were lysed in 10 mmol/L MOPS solution (morpholinopropanesulfonic acid, Sigma) containing 0.1% Triton X-100 and the cell-associated fluorescence was measured by spectrofluorometer. Protein content was determined using the BCA Protein Assay Reagent kit (Pierce, Rockford, IL) with bovine serum albumin as standard. Binding was expressed as mg/g protein.

For uptake studies, podocytes were grown on collagen-coated glass coverslips for 14 days. The monolayers were maintained for 24 hours in serum-free condition and then washed with Ringer's solution at pH 6.0. Podocytes were incubated in Ringer's solution, pH 6.0, containing 50 μg/ml of FLUOS-HSA with or without 5 mg/ml of unlabeled HSA at 37°C for 3 hours. At the end of incubation the cells were washed with Ringer's solution, pH 7.4, and fixed with 2% paraformaldehyde and 4% sucrose for 10 minutes at 37°C. The fixed monolayers were mounted in 1% *N*-propyl-gallate in 50% glycerol and 0.1 mol/L Tris-HCl, pH 8, and photographs were taken using immunofluorescence microscopy.

IgG Binding and Uptake

Podocytes were grown on collagen-coated coverslips for 14 days and maintained for 24 hours in serum-free conditions. For binding studies the cells were washed with Ringer's solution at pH 6.0 and incubated with human FITC-IgG (Sigma), 50 μg/ml, with or without 5 mg/ml of unlabeled human IgG (Sigma) at 4°C for 1 hour. Uptake was performed by incubating the monolayers for 3 hours at 37°C with the concentration of FITC-human IgG and unlabeled IgG used for binding. At the end of the incubation the cells were washed and processed as described for HSA uptake.

Fluorescence Confocal Microscopy

Podocytes plated on collagen type I-coated glass coverslips were maintained in nonpermissive conditions for 14 days and incubated with medium alone, HSA, IgG, or ET-1 for different time intervals. At the end of incubation, cells were fixed in 2% paraformaldehyde plus 4% sucrose in phosphate-buffered saline (PBS), pH 7.4, for 10 minutes at 37°C, and then permeabilized with 0.3% Triton X-100 (Sigma) in PBS for 4 minutes at room temperature. After three washings with PBS, nonspecific binding sites were saturated in blocking solution (2% fetal bovine serum, 2% bovine serum albumin, 0.2% bovine gelatin in PBS) for 30 minutes at room temperature. Podocytes were incubated with mouse monoclonal antibody anti-synaptopodin (undiluted; Progen Immunodiagnostica, Heidelberg, Germany) for 1 hour at room temperature, washed, and then incubated with FITC-conjugated goat anti-mouse antibody (30 μg/ml; Jackson ImmunoResearch Laboratories, West Grove, PA). Negative control experiments with secondary antibody alone were performed. For F-actin staining, fixed and permeabilized cells were incubated with rhodamine-phalloidin, 20 U/ml, for 45 minutes (Molecular Probes Inc., Eugene, OR); negative control experiments without rhodamine-phalloidin were performed. For double labeling of F-actin and ZO-1, cells were preincubated overnight with polyclonal rabbit anti-ZO-1 antibody (10 μg/ml; Zymed Laboratories, San Francisco, CA) followed by rhodamine phalloidin. Coverslips were washed and mounted in 1% *N*-propyl-gallate in 50% glycerol, 0.1 mol/L Tris-HCl, pH 8, and examined using inverted confocal laser microscopy (LSM 510 meta; Zeiss, Jena, Germany). Representative fields were digitalized with millions of colors and printed.

Northern Blot Analysis

Total RNA was isolated from podocytes by the guanidium isothiocyanate/cesium chloride procedure. Fifteen μg of total RNA was then fractionated on 1.2% agarose gel and

blotted onto synthetic membranes (Zeta-probe; Bio-Rad, Richmond, CA). ET-1 mRNA was detected by using a 319-bp fragment of rat ET-1 cDNA. The probes were labeled with α-^{32}P dCTP by random-primed method. Hybridization was performed overnight at 60°C in 0.25 mol/L Na_2HPO_4, pH 7.2, and 7% sodium dodecyl sulfate. Filters were washed twice for 30 minutes with 20 mmol/L Na_2HPO_4, pH 7.2, and 5% sodium dodecyl sulfate and twice for 10 minutes with 20 mmol/L Na_2HPO_4, pH 7.2, and 1% sodium dodecyl sulfate at 60°C. Membranes were subsequently probed with β-actin cDNA, taken as internal standard of equal loading of the samples on the membrane. Expression of ET-1 mRNA was corrected for β-actin expression and quantified densitometrically.

Quantitative Real-Time PCR

Total RNA was extracted from podocytes by the guanidium isothiocyanate/cesium chloride procedure. Contaminating genomic DNA was removed by RNase-free DNase (Promega, Ingelheim, Germany) for 1 hour at 37°C. The purified RNA (1 μg) was reverse-transcribed using random hexamers (50 ng) and 200 U of SuperScript II RT (Life Technologies, San Giuliano Milanese, Italy) for 1 hour at 42°C. No enzyme was added for reverse transcriptase-negative controls.

Real-time PCR was performed with the ABI Prism 5700 sequence detection system (PE Biosystems, Warrington, UK) using heat-activated *Taq*DNA polymerase (Amplitaq Gold, PE Biosystems). The TaqMan PCR reagents kit was used according to the manufacturer's protocol. After an initial hold of 2 minutes at 50°C and 10 minutes at 95°C, the samples were cycled 40 times at 95°C for 15 seconds and 60°C for 60 seconds. Ct, or threshold cycle, is used for relative quantification of the input target number. The comparative Ct method normalizes the number of target gene copies to a housekeeping gene such as glyceraldehyde-3-phosphate dehydrogenase (GAPDH) (ΔCt). Gene expression was then evaluated by the quantification of cDNA corresponding with the target gene relative to a calibrator sample serving as a physiological reference (eg, untreated cells, $\Delta\Delta$Ct). On the basis of exponential amplification of target gene as well as calibrator, the amount of amplified molecules at the threshold cycle is given by: $2^{-}\Delta\Delta$Ct. The following specific primers (300 nmol/L) were used: mouse ET-1: sense, 5′-AACTACGAAGGTTGGAGGCCA; anti-sense, 5′-CACGAAAAGATGCCTTGATGC; GAPDH sense, 5′-TCATCCCTGCATCCACTGGT; anti-sense, 5′-CTGGGATGACCTTGCCCAC. All primers were obtained from Sigma Genosys (Cambridgeshire, UK).

Radioimmunoassay

ET-1 production was assayed in podocyte supernatants by radioimmunoassay (RIA). Either standard compounds or unknown samples (100 μl) were mixed with 100 μl of antiserum (Peninsula Laboratories Inc., Belmont, CA) diluted in phosphate buffer, pH 7.2 (RIA buffer), at a final dilution of 1:72,000. The reaction mixture was incubated for 24 hours at 4°C, then 15,000 cpm of (^{125}I) ET-1 in 100 μl was added and the incubation prolonged for 24 hours at 4°C. Separation of free from antibody-bound (^{125}I) ET-1 was achieved by addition of a second antibody (500 μl of immunoprecipitating mixture consisting of a sheep anti-rabbit IgG and polyethylene glycol) for 30 minutes at room temperature. Finally, 500 μl of RIA buffer was added to stop the reaction, and the immunoprecipitates were centrifuged at 5000 × *g* for 30 minutes. Supernatants were discarded and pellet radioactivity detected by gamma counter (Beckman, Irvine, CA). Results were expressed as pg/10^6 cells. The minimum detectable concentration was 0.4 pg/tube. Nonspecific binding did not exceed 2% of total radioactivity. The cross-reactivity of the antibody with other endothelins is as follows: endothelin-2, 46.9%; endothelin-3, 17%; and big endothelin-1, 9.4%. Intra-assay and interassay variability averaged 10% and 12%, respectively, throughout a range between 0.4 and 100 pg/tube.

Preparation of Nuclear Extracts and Electrophoretic Mobility Shift Assay (EMSA)

Nuclear extracts were prepared from podocytes with the NE-PER nuclear and cytoplasmic extraction reagents kit (Pierce/Celbio, Pero, Italy) according to the manufacturer's instructions. To minimize proteolysis, all buffers contained protease inhibitor cocktail (Boehringer Mannheim, Mannheim, Germany). The protein concentration was determined by the Bradford assay using the Bio-Rad protein assay reagent.

EMSAs were performed as previously described[40] with the kb DNA sequence of the immunoglobulin gene (5′-CCGGTCAGAGGGGACTTTCCGAGACT) and consensus binding site for Ap-1 (5′-CGCTTGATGACTCAGCCGGAA). Nuclear extracts (3 μg) were incubated with 50 kcpm of ^{32}P-labeled oligonucleotide in a binding reaction mixture [10 mmol/L Tris-HCl, pH 7.5, 80 mmol/L NaCl, 1 mmol/L ethylenediamine tetraacetic acid, 1 mmol/L dithiothreitol, 5% glycerol, 1.5 μg of poly (dI-dC)] for 30 minutes on ice. In competition studies, a 100-fold molar excess of unlabeled oligonucleotide was added to the binding reaction mixture before the addition of the labeled NF-κB or Ap-1 probes. For densitometric analysis the volume density for each band was determined in arbitrary units. The sum of the volume density of bands for a single sample was used as an indirect measure of NF-κB or Ap-1 activation and expressed as a fold increase of the mean densitometry of respective control (represented as 1).

Western Blot Analysis

Podocytes were lysed in the lysis buffer: 20 mmol/L Tris-HCl , pH 7.5, 150 mmol/L NaCl, 2 mmol/L ethylenediamine tetraacetic acid, 1% Triton X-100, 2.5 mmol/L sodium pyrophosphate, 1 mmol/L β-glycerophosphate, plus phosphatase inhibitors 1 mmol/L Na_3VO_4, 50 mmol/L NaF, and protease inhibitors 1 mmol/L phenylmethyl sulfonyl fluoride and 1 μg/ml leupeptin. Protein

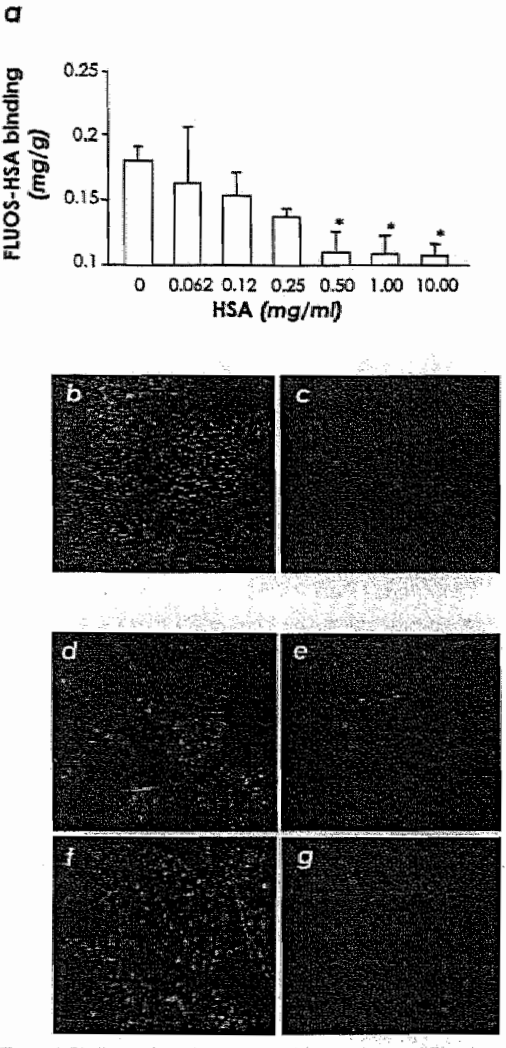

Figure 1. Binding and uptake of HSA and human IgG on differentiated podocytes. Top: Binding studies. a: Confluent differentiated podocytes were incubated with 50 μg/ml of FLUOS-HSA with or without increasing concentrations of cold HSA. Complete inhibition of FLUOS-HSA binding by unlabeled HSA showed that binding was specific and not due to an interaction of FLUOS-HSA with plasma membrane (n = 5 experiments). Data are expressed as mean ± SE. *, $P < 0.05$ versus 0 mg/ml HSA. Representative images of binding of 50 μg/ml of FITC-IgG on podocytes in the absence (b) or presence of 5 mg/ml of cold IgG (c). Bottom: Uptake studies. Cellular staining of 50 μg/ml of FLUOS-HSA incubated without (d) or with (e) 5 mg/ml of unlabeled HSA. Endocytosis of 50 μg/ml of FITC-IgG in podocytes in the absence (f) or presence (g) of 5 mg/ml of unlabeled IgG. Original magnifications, ×600.

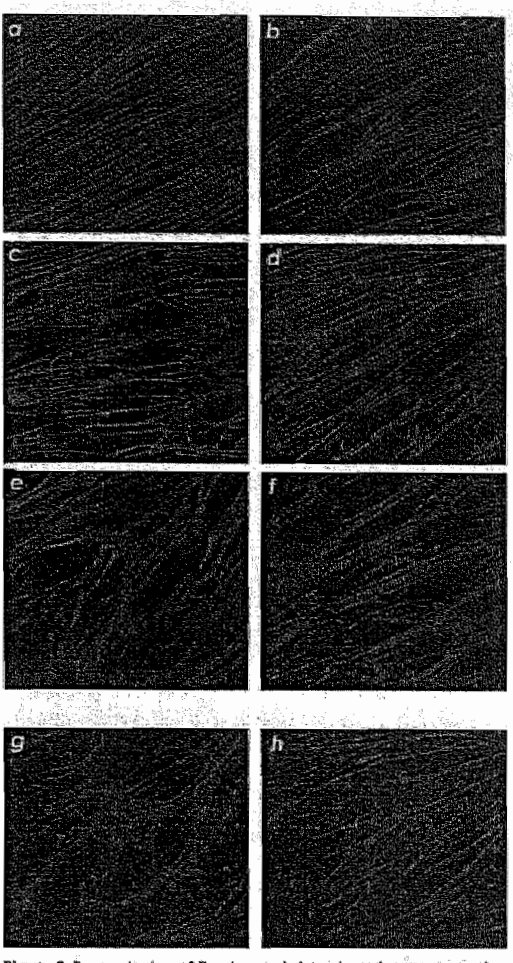

Figure 2. Reorganization of F-actin cytoskeleton in podocytes exposed to protein overload. Confluent differentiated podocytes exhibited a pattern of F-actin filaments distributed as stress fiber-like bundles along the axis of the cells after 6 hours (a) incubation with medium alone. Redistribution of F-actin fibers to the periphery of the cells was observed in podocytes exposed to HSA already at 30 minutes (b) that was maintained at 1 (c), 2 (d), 6 (e), and 24 hours (f). A similar effect was observed after podocyte exposure to IgG for 6 and 24 hours (g, h). Original magnifications, ×600.

concentration was determined by protein assay based on bicinchoninic acid color formation (Pierce, Milan, Italy). Proteins (30 μg) were separated on 7.5% polyacrylamide gels by sodium dodecyl sulfate-polyacrylamide gel electrophoresis and transferred to nitrocellulose membranes. Membranes were blocked for 1 hour at room temperature with PBS containing 5% bovine serum albumin (for p-FAK detection) or 5% nonfat dry milk (for FAK detection) and 0.1% Tween 20, and then incubated overnight at 4°C with the following primary antibodies (Biosource Europe, Nivelles, Belgium): rabbit polyclonal anti-FAK (pY397) (1:1000); rabbit polyclonal anti-FAK (1:1000). After incubation with the secondary antibodies, horseradish peroxidase-conjugated goat anti-IgG rabbit (Sigma) diluted 1:10,000, for 1 hour at room temperature in PBS with 1% bovine serum albumin or 1% nonfat dry milk and 0.1% Tween 20, proteins bands were detected by Supersignal chemiluminescent substrate (Pierce).

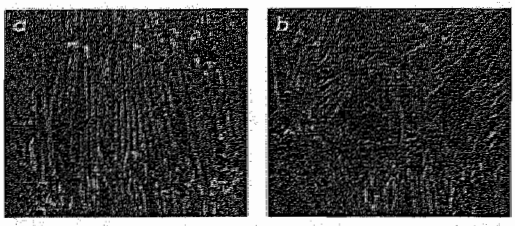

Figure 3. Double immunolabeling for F-actin and ZO-1 in podocytes challenged with HSA. Immunofluorescence images of F-actin and ZO-1 in podocytes exposed to medium alone (a) or HSA for 6 hours (b) indicate that protein overload rearranged F-actin fibers at the periphery of the cells as outlined by ZO-1 staining (b). Original magnifications, ×1000.

Adenoviral Constructs and Transfection Experiments

A replication-defective adenovirus encoding FAK-related nonkinase (Ad-FRNK) was constructed using a 1.2-kb wild-type chick FRNK cDNA (the gift of Dr. J.T. Parsons, Department of Microbiology, Health Sciences Center, University of Virginia, Charlottesville, VA).[38] For adenoviral infection, podocytes were incubated with Ad-FRNK or Ad-null at a multiplicity of infection of 50 in RPMI 1640 without serum for 3 hours at 37°C. The adenoviruses were washed off and cells maintained in serum-free medium for 24 hours. Then, podocytes were exposed to HSA (10 mg/ml) for 3 hours and processed for ET-1 mRNA expression. Transfection did not affect cell viability.

Statistical Analysis

Results are expressed as mean ± SE. Statistical analysis was performed using Student's *t*-test, one-way analysis of variance, followed by Tukey test for multiple comparisons, and Kruskal Wallis test, as appropriate. Statistical significance was defined as $P < 0.05$.

Results

Binding and Uptake of Albumin and IgG in Differentiated Mouse Podocytes

We investigated binding and uptake of HSA and IgG in differentiated mouse podocytes. FLUOS-HSA was displaced by cold HSA in a concentration-dependent manner at 4°C, indicating the presence of saturable binding sites for albumin on the podocyte surface (Figure 1a). Similarly, podocytes exposed to FITC-IgG showed (Figure 1b) a specific binding of the protein, with a granular pattern on the apical surface of podocytes that was completely displaced by cold IgG (Figure 1c). HSA and IgG endocytosis into podocytes was detected after 3 hours of exposure at 37°C to FLUOS-HSA or FITC-IgG (Figure 1, d and f, respectively). Uptake was markedly inhibited by an excess of both unlabeled proteins (Figure 1, e and g), suggesting a receptor-mediated endocytosis of HSA and IgG in podocytes.

Effect of Protein Overload on F-Actin Cytoskeleton and Synaptopodin Distribution in Differentiated Podocytes

Differentiated podocytes maintained for 14 days in nonpermissive culture conditions exhibited, when confluent, a pattern of F-actin filaments distributed as stress fiber-like bundles along the axis of the cells or into the process of arborized cells, as visualized by confocal microscopy (Figure 2a). Albumin induced a marked redistribution of F-actin fibers toward the periphery of the cells already after 30 minutes (Figure 2b), which was maintained thereafter (Figure 2; c to f) until 48 hours (data not shown). A similar effect was observed after podocyte challenge with IgG (Figure 2, g and h). To demonstrate the peripheral distribution of F-actin fibers induced by excess proteins, double immunostaining of actin and ZO-1, a cell membrane marker that defines podocyte outline, was performed. Figure 3 shows that HSA induces actin rearrangement at the cell periphery in the vicinity of ZO-1 at

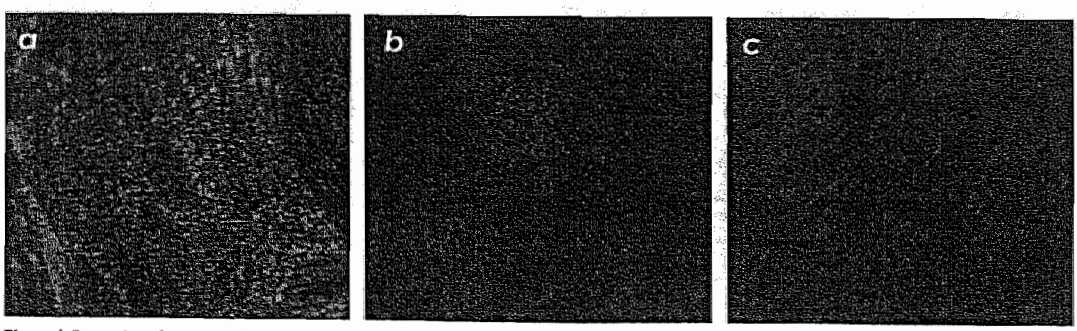

Figure 4. Expression of synaptopodin in podocytes exposed to HSA or IgG. a: High level of synaptopodin in a punctate pattern was observed along actin filament in unstimulated cells. After 6 hours of exposure of podocytes with HSA (b) or IgG (c) at the concentration of 10 mg/ml, synaptopodin was markedly reduced in respect to control cells. Original magnifications, ×600.

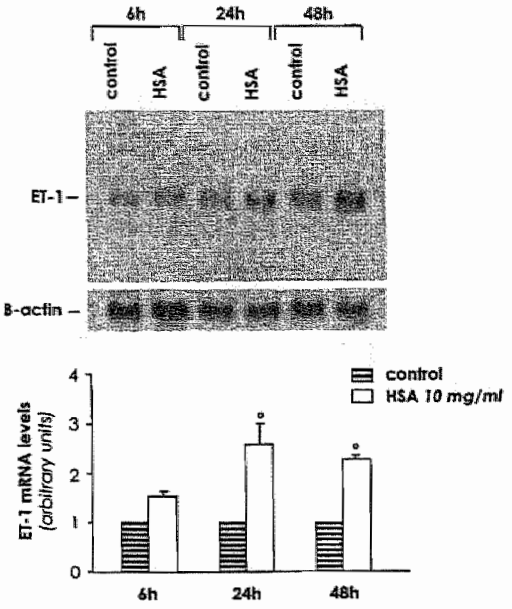

Figure 5. ET-1 mRNA expression in podocytes exposed to protein overload. Top: Northern blot experiments were performed using total RNA isolated from podocytes exposed to medium alone (control) or albumin (10 mg/ml) for 6, 24, and 48 hours. The results are representative of four independent experiments. Bottom: Densitometric analysis of autoradiograph signals for ET-1. The optical density of the autoradiographic signals was quantified and calculated as the ratio of ET-1 to β-actin mRNA. Results (mean ± SE) are expressed as fold increase greater than control (considered as 1) in densitometric arbitrary units. °, $P < 0.01$ versus control.

the expense of transcytoplasmic filaments (Figure 3b). Cytoskeletal changes were accompanied by loss of staining for synaptopodin, an F-actin-associated protein, considered a specific marker of podocyte differentiation.[41] As shown in Figure 4, unstimulated cells revealed high levels of synaptopodin in a punctate pattern along the actin filaments and at focal contact. Exposure of podocytes to HSA or IgG for 6 or 24 hours resulted in a similar marked reduction of synaptopodin staining.

Protein Overload Induces ET-1 Gene Expression and Protein via Cytoskeleton Rearrangement

Because reorganization of cytoskeletal network is functionally linked to modification of transcriptional events that regulate inflammatory and vasoactive genes, including ET-1,[42–44] we studied the ability of a high concentration of plasma proteins to modulate the expression of ET-1 gene and protein in differentiated podocytes, and the potential role of cytoskeleton in such induction. By Northern blot, a 1.3-kb mRNA transcript specific for ET-1 was observed in unstimulated control podocytes (Figure 5). Albumin promoted after 6 hours of incubation a 1.5-fold increase in ET-1 transcript level as compared to control cells, which was further enhanced at 24 and 48

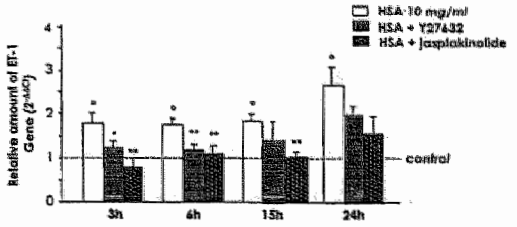

Figure 6. Effect of the cytoskeleton inhibitors Y27632 and jasplakinolide on albumin-induced ET-1 gene expression. Cells were treated with medium alone or with HSA (10 mg/ml) for 3, 6, 15, and 24 hours in the presence or absence of Y27632 (10 μmol/L), an inhibitor of Rho kinase pathway, or jasplakinolide (200 nmol/L), an F-actin stabilizer. ET-1 mRNA was assessed by real-time PCR. The results shown are mean ± SE of five independent experiments. °, $P < 0.01$ versus control; *, $P < 0.05$; **, $P < 0.01$ versus HSA.

hours (2.5- and 2.2-fold, respectively) (Figure 5). The effect of albumin on ET-1 gene expression was consistent with data of real-time PCR experiments (Figure 6). Actually, ET-1 message levels increased within 3 hours of albumin exposure and was elevated at 6 and 15 hours with a peak at 24 hours ($P < 0.01$ versus unstimulated cells at all of the times considered). ET-1 mRNA overexpression was also observed when podocytes were challenged with IgG for 24 hours (1.5-fold increase greater than control, $P < 0.05$). As shown in Figure 6, exposure of podocytes to Y27632, a specific Rho kinase inhibitor involved in stress fiber formation, resulted in a significant inhibition of ET-1 gene expression at 3 and 6 hours. The effect was no more significant at 24 hours. Treatment with jasplakinolide, an F-actin stabilizer, normalized ET-1 mRNA expression until 15 hours. Thereafter, a less inhibitory effect was observed. The up-regulation of ET-1 mRNA was associated with a time-dependent increase of the native peptide secreted into cell supernatants (Figure 7). Unstimulated cells synthesized constitutively low levels of ET-1 protein. After HSA exposure, a significant increase in peptide secretion was found at 3 hours, which was more pronounced at 15 and 24 hours. Y27632 had an early inhibitory effect, resulting in the normalization of ET-1 secretion at 3 hours. This effect was less pro-

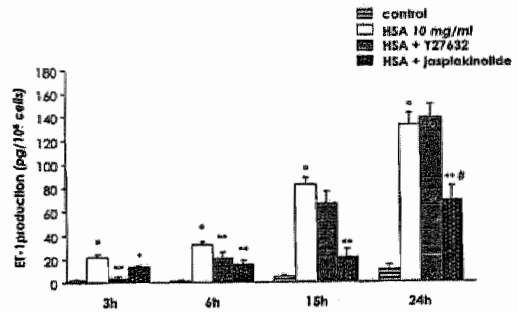

Figure 7. ET-1 production in podocytes exposed to albumin and effect of Y27632 and jasplakinolide. Podocytes were incubated with medium alone or with HSA (10 mg/ml) for 3, 6, 15, and 24 hours in the presence or absence of Y27632 (10 μmol/L) and jasplakinolide (200 nmol/L). ET-1 production was measured in cell supernatants by RIA. Data are expressed as mean ± SE. °, $P < 0.01$ versus control; *, $P < 0.05$; **, $P < 0.01$ versus HSA; #, $P < 0.01$ versus HSA + Y27632.

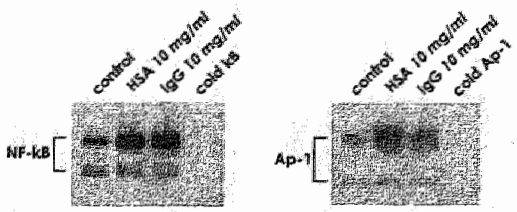

Figure 8. Activation of NF-κB and Ap-1 in protein-laden podocytes. NF-κB and AP-1 activity was evaluated by EMSA in nuclear extracts from podocytes exposed for 30 minutes to medium alone, HSA, or IgG (10 mg/ml). To demonstrate the specificity of binding of the NF-κB and Ap-1 oligonucleotides, a 100-fold molar excess unlabeled (cold) nucleotides were used to compete with the labeled NF-κB or AP-1 probes for binding to nuclear proteins. Results are representative of three experiments.

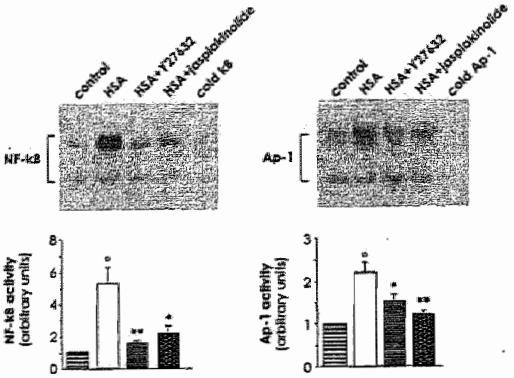

Figure 9. Effect of Y27632 and jasplakinolide on NF-κB and Ap-1 activation induced by protein overload. **Top:** EMSA for NF-κB and Ap-1 was performed in nuclear extracts from podocytes exposed for 30 minutes to medium alone or HSA (10 mg/ml), in the presence or absence of Y27632 (10 μmol/L) and jasplakinolide (200 nmol/L). The results are representative of five independent experiments using different nuclear extracts. **Bottom:** Densitometric analysis of autoradiographic signals of NF-κB and AP-1. Results are mean ± SE. °, $P < 0.01$ versus control; *, $P < 0.05$; and **, $P < 0.01$ versus HSA.

nounced, although still significant until 6 hours. Podocytes exposed to jasplakinolide showed instead a long lasting inhibitory effect on ET-1 production, to the extent that a significant reduction over HSA still persisted at 24 hours (Figure 7).

Albumin and IgG Activate NF-κB and Ap-1 in Podocytes via Cytoskeleton

The effect of HSA and IgG on NF-κB and Ap-1 activation in podocytes is depicted in Figure 8. Nuclear extracts were assayed for NF-κB and Ap-1 DNA binding activity using radiolabeled specific oligonucleotide probes. Unstimulated cells displayed two constitutive bands of NF-κB: an upper complex and a faster migrating lower complex. Thirty minutes of incubation of podocytes either with albumin or IgG led to a substantial rise in NF-κB-binding activity of the two complexes. A remarkable increase of the Ap-1-binding activity greater than control was detected after podocyte challenge with either protein. The specificity of binding reactions was confirmed in competition experiments by the ability of excess unlabeled (cold) NF-κB or Ap-1 oligonucleotides to inhibit binding.

Next, we investigated whether the activation of NF-κB and Ap-1 induced by protein overload could be regulated by intracellular signals evoked by cytoskeleton rearrangement. To this purpose, experiments were performed in podocytes exposed to albumin, taken as representative protein. As shown in Figure 9, densitometric analysis of five independent experiments revealed a 5.3-fold increase of NF-κB activity greater than control. Treatment with Y27632 reduced by nearly 70% NF-κB activation induced by albumin. A 58% inhibition was observed after jasplakinolide. Ap-1 DNA binding activity was significantly enhanced by albumin (2.2-fold greater than control) (Figure 9). In the presence of Y27632 and jasplakinolide, AP-1 activation was reduced by 30% and 44%, respectively.

Role of FAK in Protein Overload-Induced ET-1

Integrin-mediated activation of the nonreceptor tyrosine kinase FAK results in the propagation of intracellular signals that turn on transcriptional events. First, we studied the contribution of FAK in the regulation of ET-1 gene expression induced by HSA overload. By Western blot experiments, albumin-loaded podocytes exhibited a marked FAK phosphorylation at 5 minutes, that remained sustained until 6 hours (Figure 10a, left).

Next, to assess a possible involvement of cytoskeleton changes in FAK activation, we evaluated the effect of Y27632 or jasplakinolide in albumin-treated podocytes. As shown in Figure 10a (right), both compounds reduced FAK phosphorylation after 30 minutes of exposure with HSA, suggesting a downstream regulation of FAK by Rho kinase-triggered actin redistribution. We also observed that the tyrosine kinase inhibitor genistein markedly reduced NF-κB- and Ap-1-binding activity (Figure 10b) in HSA-laden podocytes. As a consequence, ET-1 mRNA levels were significantly decreased by genistein in respect to HSA alone, as documented by real-time PCR assessment (Figure 10c). Transient overexpression of FAK-related nonkinase, an endogenous inhibitor of FAK activity, by adenoviral gene transfer interfered with ET-1 gene expression to the extent that ET-1 mRNA transcript levels were reduced by 50% compared to cells transfected with null gene.

Effect of Exogenous ET-1 on Podocyte Cytoskeleton

We then evaluated the functional effect of ET-1 on the distribution of F-actin. Figure 11 shows that in control cells actin stress fibers were arranged in parallel, whereas on exposure to ET-1 (100 nmol/L) for 2 and 6 hours, this pattern changed, leading to F-actin redistribution at the cell periphery, at the expense of transcytoplasmic microfilaments. The effect was transient and partially recovered at 15 hours. These data provide the first evidence that ET-1 may alter podocyte F-actin contractile

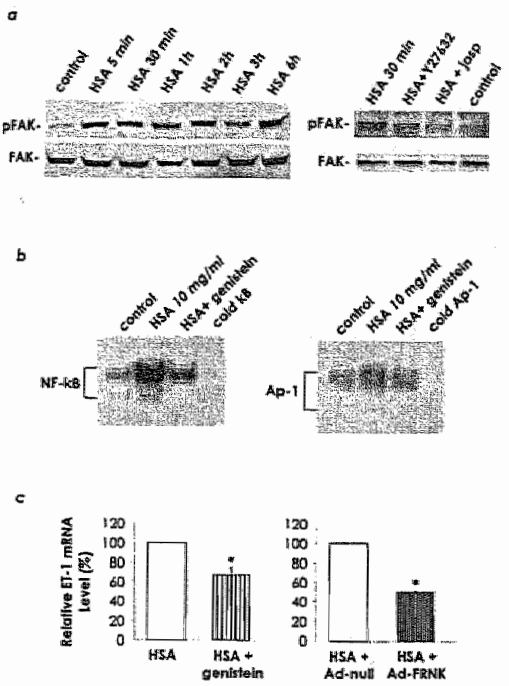

Figure 10. Role of FAK on ET-1 gene activation/expression in HSA-treated podocytes. a: Left: Activation of FAK in podocytes exposed to HSA (10 mg/ml) for 5 minutes, 30 minutes, and 1, 2, 3, and 6 hours. a: Right: Effect of Y27632 (10 μmol/L) and jasplakinolide (jasp, 200 nmol/L) on FAK phosphorylation in podocytes treated for 30 minutes with HSA. Cell lysates were analyzed by Western blot using antibody against the phosphorylated form. The blots were stripped and reprobed with an antibody anti-nonphosphorylated FAK to confirm equal loading of the proteins on the gel. The blot is representative of three independent experiments. b: Effect of genistein on NF-κB and Ap-1 activation induced by protein overload. EMSA for NF-κB and Ap-1 was performed in nuclear extracts from podocytes exposed for 30 minutes to medium alone or HSA in the presence or absence of genistein (25 μmol/L). The autoradiographs are representative of three independent experiments using different nuclear extracts. c: Effect of inhibition of FAK phosphorylation on ET-1 expression. Left: Cells were treated with medium alone or with HSA for 3 hours in the presence or absence of genistein. Right: Cells were transfected with a replication-defective adenovirus encoding FAK-related nonkinase (Ad-FRNK), an endogenous inhibitor of FAK activity or Ad-null, before HSA exposure. ET-1 mRNA was assessed by real-time PCR. *, $P < 0.01$ versus HSA + Ad-null.

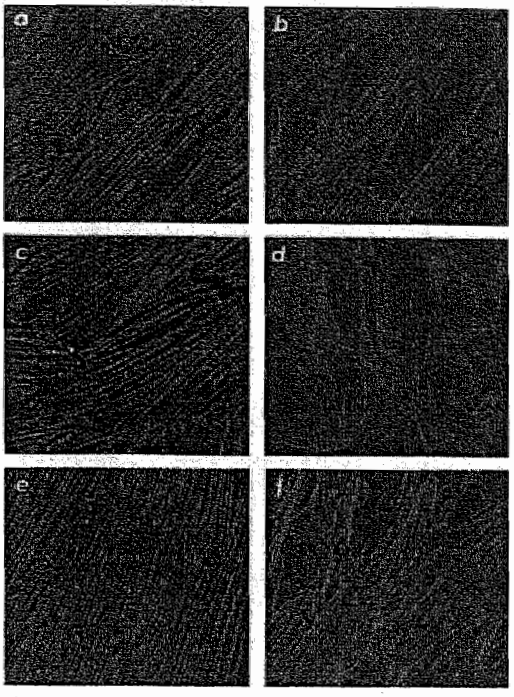

Figure 11. Effect of ET-1 on cytoskeletal F-actin distribution in podocytes. Immunofluorescence staining of F-actin fibers in podocytes exposed for 2, 6, and 15 hours to control medium (a, c, e) or ET-1 (b, d, f). In unstimulated cells F-actin microfilaments were arranged in parallel, whereas on exposure to ET-1 (100 nmol/L) for 2 and 6 hours, this pattern changed leading to F-actin redistribution at the cell periphery. This effect partially recovered at 15 hours. Original magnifications, ×600.

apparatus relevant for the maintenance of glomerular permselectivity.

Discussion

Far from being a simple prognostic clinical parameter, proteinuria has been considered a pivotal causative factor for progressive tubular injury that precedes the relentless deterioration of renal function in progressive nephropathies.[6] Proteins filtered in exuberant amounts as a consequence of the alteration of the size-selective function of the glomerular barrier in proteinuric conditions, have an intrinsic renal toxicity because of over-reabsorption by proximal tubular cells, which causes activation of tubular-dependent pathways of interstitial inflammation and fibrosis.[6,45] Ultrafiltered plasma proteins also induce morphological changes in podocytes,[5] which include reversible retraction and flattening of the epithelial foot processes, suggesting podocyte-GBM adhesion of critical relevance for a functional filter.[14,46] Mechanisms and mediators underlying phenotypic changes in glomerular epithelium induced by protein overload are poorly defined.

In the present study, we found that albumin and IgG bind to cultured murine podocytes in a receptor-specific manner. Because of the recent demonstration of the presence of megalin,[47] which acts as a receptor for albumin and Ig light chain, on this very cell line, it is possible that in our setting albumin and IgG binding to the murine podocyte is mediated by megalin. The fact that megalin possesses endocytotic function in differentiated podocytes[47] would also suggest that albumin and IgG uptake, here documented, may occur through their binding to this receptor. Downstream pathway-transducing signals after protein binding to the receptors are currently poorly understood. It has been recently shown that the cytoplasmic carboxy-terminal NPXZ domain of megalin interacts with Disable protein (Dab) 2, an intracellular adaptor protein that is potentially involved in transmembrane signal transduction and regulates cellu-

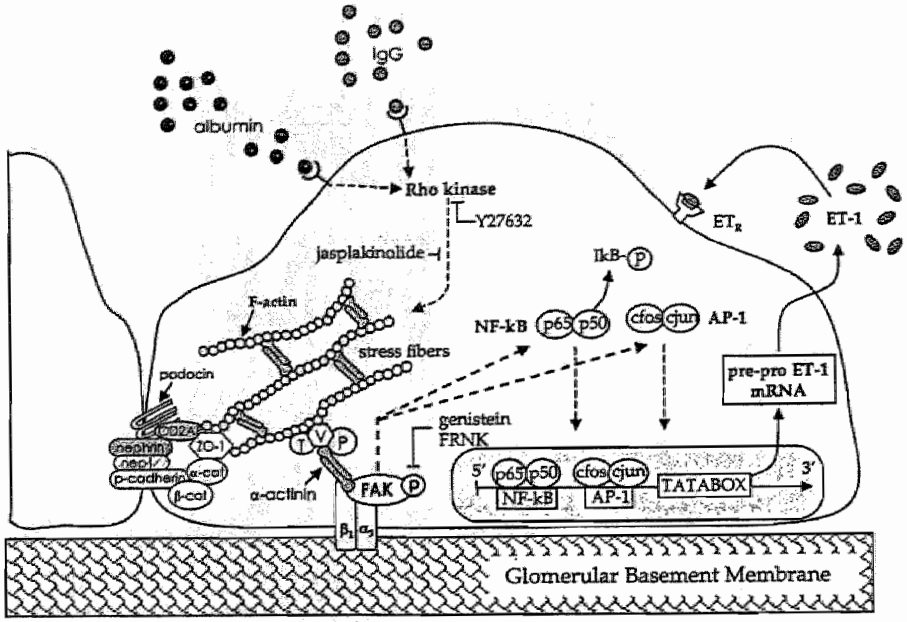

Figure 12. Proposed pathway mediating protein overload-induced ET-1 expression. Ultrafiltered plasma proteins, by binding to specific receptors on podocyte surface, cause cytoskeleton rearrangement and new F-actin stress fiber formation via Rho kinase pathway. Rho kinase-triggered actin reorganization leads to FAK phosphorylation. FAK activation integrates signals from cytoskeleton to the downstream activation of NF-κB and Ap-1 which in turn translocate to the nucleus and promote pre-pro ET-1 gene transcription.

lar growth and differentiation.[48] Whether Dab 2 could transduce the signal after protein binding to megalin on podocytes is worth investigating.

Exposure of podocytes to albumin and IgG induces early phenotypic changes consisting of cytoskeleton F-actin rearrangement with marked decrease of synaptopodin staining. The ultimate effect of proteins on actin-associated synaptopodin would be taken as to indicate protein accumulation as a trigger of podocyte dedifferentiation, a phenomenon already described *in vivo* in areas of segmental sclerosis.[49,50] Podocytes are highly differentiated cells that possess a complex contractile structure composed of F-actin microfilaments, most abundant in the foot process, exhibiting a high degree of organization.[7,35,51,52] F-actin is connected with adaptor molecules that anchor the slit diaphragm proteins and α3β1 integrins, transmembrane proteins that form focal adhesion complexes and mediate podocyte-GBM matrix interaction.[7,46,52] Cytoskeleton F-actin rearrangement is closely associated with podocyte shape changes and dysfunction in disease.[7,14,46] *In vitro*, actin filament disorganization affects cell adhesion to the extracellular matrix through α3β1 integrin that functions as receptor-transducing signals. The consequent outside-in signals trigger specific cellular responses that lead to activation of gene expression of adhesive molecules, cytokines, and vasoactive mediators.[42,53,54] Based on this evidence, we asked whether rearrangement of the cytoskeleton induced by protein overload was associated with up-regulation of the ET-1 gene. Our results indicate that ET-1 gene expression is efficiently enhanced by albumin and IgG load, in parallel with the generation of the protein, in a time-dependent manner, suggesting that glomerular epithelial cells in the proteinuric setting are an important source of ET-1. These data are in line with *in vivo* evidence in a murine model of protein overload that renal ET-1 transcript levels increased together with the renal synthesis of the peptide in concomitance with the development of podocyte structural damage.[55]

Endothelin-1 secreted by podocytes may function in a paracrine manner on glomerular cells affecting the tone of the glomerular capillary, enhancing the vascular permeability, and stimulating mesangial cell contraction by virtue of its vasoconstrictor effects. Finding that the cytoskeleton stabilizer jasplakinolide significantly reduced expression and production of ET-1 would support the notion that protein-induced rearrangement of the actin cytoskeleton contributes to regulate ET-1. Furthermore, the addition of Y27632, an inhibitor of Rho kinases crucial for the formation of stress fibers and focal adhesions,[26,27] also markedly decreased ET-1 expression indicating that ET-1 gene transcription is regulated by Rho-dependent pathway. In agreement with our findings are data that the Rho GTPase family modulates basal expression of pre-proET-1 transcript levels in vascular endothelial cells in culture.[28] Regulation of the preproET-1 gene is complex and has been attributed to multiple regulatory elements. It is well-known that human preproET-1 gene possesses in the promoter region consensus sequences for transcription factors including NF-κB and Ap-1.[23,24] In the

present study, electrophoretic analysis of the nuclear extracts of podocytes loaded with albumin or IgG revealed a rapid increase in NF-κB- and Ap-1 DNA-binding activities. Of interest, inhibition of cytoskeleton rearrangement by jasplakinolide and by Rho kinase inhibitor prevented NF-κB and Ap-1 activation, indicating the presence of cytoskeleton-regulated signal transduction pathway of gene activation. These data are in line with previous observations of the involvement of Rho GTPase family in regulating NF-κB and Ap-1 in genetically modified cultured fibroblasts.[25,26,56]

We finally investigated the role of FAK, a cytoplasmic nonreceptor tyrosine kinase that localizes in integrin-extracellular matrix complexes,[46] as the effector molecule linking actin reorganization with transcriptional events. Evidence is available as to indicate that FAK activation is dependent on actin cytoskeleton.[57] Phosphorylation of FAK on Tyr397 is a docking site for activation of other tyrosine kinases such as the Src-family protein kinases[58] that transduce the signals from focal adhesions to intracellular targets resulting in gene activation. The present experiments showed that exposure of murine podocytes to albumin induced a rapid and sustained FAK phosphorylation that was substantially affected by the Rho kinase inhibitor and jasplakinolide. Inhibition of FAK activation with genistein, a tyrosine kinase inhibitor, markedly reduced NF-κB and Ap-1 DNA-binding activity, and consequently inhibited ET-1 mRNA expression. Transfection experiments with an adenoviral construct encoding a replication-defective FAK-related nonkinase (FRNK),[36] further confirmed that FAK signaling contributes to ET-1 gene regulation to the extent that overexpression of FRNK resulted in a partial but significant inhibition of ET-1 mRNA expression in albumin-laden podocytes.

We finally addressed a possible effect of ET-1 on cultured podocytes that express on their surface-specific receptors for the peptide.[59,60] Podocytes exposed to exogenous ET-1 exhibited rapid and consistent cytoskeletal changes, as revealed by the redistribution of F-actin fibers to the cell periphery. This result unravels a novel clue of the effect of ET-1 on kidney cells. So far data are available to indicate the pivotal role of ET-1 in the biology of mesangial cells, in that the peptide can elicit proliferation, hypertrophy, and contraction of the mesangium.[19] In view of the fact that ET-1 acts as a local hormone whose effects are exerted in a paracrine as well as autocrine manner, it is possible that overproduction of ET-1 by podocytes may regulate the contractile status of either mesangial or glomerular epithelial cells.

In conclusion, we have demonstrated that in podocytes the abnormal uptake of plasma proteins induces Rho kinase-dependent F-actin cytoskeletal rearrangement leading to possible cell dedifferentiation. Such structural changes translate into the activation of FAK in turn responsible for NF-κB- and Ap-1-dependent ET-1 gene up-regulation (Figure 12). Endothelin-1 overproduction may act on the podocyte contractile apparatus altering the glomerular capillary surface area thus leading to protein permeability dysfunction. These results indicate podocytes as a novel cellular target for the toxic effect of excess plasma ultrafiltered proteins.

Acknowledgments

We thank Dr. J.T. Parsons (Department of Microbiology, Health Sciences Center, University of Virginia, Charlottesville, VA) for providing adenovirus encoding FAK-related nonkinase; Dr. Federica Valsecchi and Fabio Sangalli for their precious contribution; and Manuela Passera for help in preparing the manuscript. Dr. Buelli is a recipient of a fellowship of "Helsinn Healthcare SA" through the courtesy of "Fondazione ainti per la Ricerca sulle malatti rare".

References

1. Olson JL, Hostetter TH, Rennke HG, Brenner BM, Venkatachalam MA: Altered glomerular permselectivity and progressive sclerosis following extreme ablation of renal mass. Kidney Int 1982, 22:112–126
2. Brenner BM, Meyer TW, Hostetter TH: Dietary protein intake and progressive nature of kidney disease: the role of hemodynamically mediated glomerular injury in the pathogenesis of progressive glomerular sclerosis in aging, renal ablation, and intrinsic renal disease. N Engl J Med 1982, 307:652–659
3. Anderson SMT, Rennke HG, Brenner BM: Control of glomerular hypertension limits glomerular injury in rats with reduced renal mass. J Clin Invest 1985, 76:612–619
4. Fries JW, Sandstrom DJ, Meyer TW, Rennke HG: Glomerular hypertrophy and epithelial cell injury modulate progressive glomerulosclerosis in the rat. Lab Invest 1989, 60:205–218
5. Remuzzi G, Bertani T: Is glomerulosclerosis a consequence of altered glomerular permeability to macromolecules? Kidney Int 1990, 38:384–394
6. Remuzzi G, Bertani T: Pathophysiology of progressive nephropathies. N Engl J Med 1998, 339:1448–1456
7. Barisoni L, Kopp JB: Update in podocyte biology: putting one's best foot forward. Curr Opin Nephrol Hypertens 2003, 12:251–258
8. Pavenstadt H: Roles of the podocyte in glomerular function. Am J Physiol 2000, 278:F173–F179
9. Kriz W, Gretz N, Lemley KV: Progression of glomerular diseases: is the podocyte the culprit? Kidney Int 1998, 54:687–697
10. Shih NY, Li J, Karpitskii V, Nguyen A, Dustin ML, Kanagawa O, Miner JH, Shaw AS: Congenital nephrotic syndrome in mice lacking CD2-associated protein. Science 1999, 286:312–315
11. Kestila M, Lenkkeri U, Mannikko M, Lamerdin J, McCready P, Putaala H, Ruotsalainen V, Morita T, Nissinen M, Herva R, Kashtan CE, Peltonen L, Holmberg C, Olsen A, Tryggvason K: Positionally cloned gene for a novel glomerular protein—nephrin—is mutated in congenital nephrotic syndrome. Mol Cell 1998, 1:575–582
12. Somlo S, Mundel P: Getting a foothold in nephrotic syndrome. Nat Genet 2000, 24:333–335
13. Rennke HG: How does glomerular epithelial cell injury contribute to progressive glomerular damage? Kidney Int Suppl 1994, 45:S58–S63
14. Shirato I: Podocyte process effacement in vivo. Microsc Res Tech 2002, 57:241–246
15. Davies DJ, Brewer DB, Hardwicke J: Urinary proteins and glomerular morphometry in protein overload proteinuria. Lab Invest 1978, 38:232–243
16. Abbate M, Zoja C, Morigi M, Rottoli D, Angioletti S, Tomasoni S, Zanchi C, Longaretti L, Donadelli R, Remuzzi G: Transforming growth factor-beta1 is up-regulated by podocytes in response to excess intraglomerular passage of proteins: a central pathway in progressive glomerulosclerosis. Am J Pathol 2002, 161:2179–2193
17. Yanagisawa M, Kurihara H, Kimura S, Tomobe Y, Kobayashi M, Mitsui Y, Yazaki Y, Goto K, Masaki T: A novel potent vasoconstrictor peptide produced by vascular endothelial cells. Nature 1988, 332:411–415
18. Benigni A, Zoja C, Corna D, Orisio S, Longaretti L, Bertani T, Remuzzi G: A specific endothelin subtype A receptor antagonist protects against injury in renal disease progression. Kidney Int 1993, 44:440–444
19. Sorokin A, Kohan DE: Physiology and pathology of endothelin-1 in renal mesangium. Am J Physiol 2003, 285:F579–F589

20. Cybulsky AV, Stewart DJ, Cybulsky MI: Glomerular epithelial cells produce endothelin-1. J Am Soc Nephrol 1993, 3:1398–1404
21. Kasinath BS, Fried TA, Davalath S, Marsden PA: Glomerular epithelial cells synthesize endothelin peptides. Am J Pathol 1992, 141:279–283
22. Inoue A, Yanagisawa M, Takuwa Y, Mitsui Y, Kobayashi M, Masaki T: The human preproendothelin-1 gene. Complete nucleotide sequence and regulation of expression. J Biol Chem 1989, 264:14954–14959
23. Kawana M, Lee ME, Quertermous EE, Quertermous T: Cooperative interaction of GATA-2 and AP1 regulates transcription of the endothelin-1 gene. Mol Cell Biol 1995, 15:4225–4231
24. Quehenberger P, Bierhaus A, Fasching P, Muellner C, Klevesath M, Hong M, Stier G, Sattler M, Schleicher E, Speiser W, Nawroth PP: Endothelin 1 transcription is controlled by nuclear factor-kappaB in AGE-stimulated cultured endothelial cells. Diabetes 2000, 49: 1561–1570
25. Marinissen MJ, Chiariello M, Tanos T, Bernard O, Narumiya S, Gutkind JS: The small GTP-binding protein RhoA regulates c-jun by a ROCK-JNK signaling axis. Mol Cell 2004, 14:29–41
26. Van Aelst L, D'Souza-Schorey C: Rho GTPases and signaling networks. Genes Dev 1997, 11:2295–2322
27. Ridley AJ, Hall A: The small GTP-binding protein Rho regulates the assembly of focal adhesions and actin stress fibers in response to growth factors. Cell 1992, 70:389–399
28. Hernandez-Perera O, Perez-Sala D, Soria E, Lamas S: Involvement of Rho GTPases in the transcriptional inhibition of preproendothelin-1 gene expression by simvastatin in vascular endothelial cells. Circ Res 2000, 87:616–622
29. Mundel P, Reiser J, Zuniga Mejia Borja A, Pavenstadt H, Davidson GR, Kriz W, Zeller R: Rearrangements of the cytoskeleton and cell contacts induce process formation during differentiation of conditionally immortalized mouse podocyte cell lines. Exp Cell Res 1997, 236:248–258
30. Gekle M, Mildenberger S, Freudinger R, Silbernagl S: Long-term protein exposure reduces albumin binding and uptake in proximal tubule-derived opossum kidney cells. J Am Soc Nephrol 1998, 9:960–968
31. Donadelli R, Zanchi C, Morigi M, Buelli S, Batani C, Tomasoni S, Corna D, Rottoli D, Benigni A, Abbate M, Remuzzi G, Zoja C: Protein overload induces fractalkine upregulation in proximal tubular cells through nuclear factor kappaB- and p38 mitogen-activated protein kinase-dependent pathways. J Am Soc Nephrol 2003, 14:2436–2446
32. Tang S, Leung JC, Abe K, Chan KW, Chan LY, Chan TM, Lai KN: Albumin stimulates interleukin-8 expression in proximal tubular epithelial cells in vitro and in vivo. J Clin Invest 2003, 111:515–527
33. Wang Y, Chen J, Chen L, Tay YC, Rangan GK, Harris DC: Induction of monocyte chemoattractant protein-1 in proximal tubule cells by urinary protein. J Am Soc Nephrol 1997, 8:1537–1545
34. Erkan E, De Leon M, Devarajan P: Albumin overload induces apoptosis in LLC-PK(1) cells. Am J Physiol 2001, 280:F1107–F1114
35. Endlich N, Kress KR, Reiser J, Uttenweiler D, Kriz W, Mundel P, Endlich K: Podocytes respond to mechanical stress in vitro. J Am Soc Nephrol 2001, 12:413–422
36. Bubb MR, Spector I, Beyer BB, Fosen KM: Effects of jasplakinolide on the kinetics of actin polymerization. An explanation for certain in vivo observations. J Biol Chem 2000, 275:5163–5170
37. Moreno-Manzano V, Lucio-Cazana J, Konta T, Nakayama K, Kitamura M: Enhancement of TNF-alpha-induced apoptosis by immobilized arginine-glycine-aspartate: involvement of a tyrosine kinase-dependent, MAP kinase-independent mechanism. Biochem Biophys Res Commun 2000, 277:293–298
38. Richardson A, Parsons T: A mechanism for regulation of the adhesion-associated protein tyrosine kinase pp125FAK. Nature 1996, 380:538–540
39. Simonson MS, Dunn MJ: Endothelin-1 stimulates contraction of rat glomerular mesangial cells and potentiates beta-adrenergic-mediated cyclic adenosine monophosphate accumulation. J Clin Invest 1990, 85:790–797
40. Zoja C, Donadelli R, Colleoni S, Figliuzzi M, Bonazzola S, Morigi M, Remuzzi G: Protein overload stimulates RANTES production by proximal tubular cells depending on NF-kappa B activation. Kidney Int 1998, 53:1608–1615
41. Mundel P, Heid HW, Mundel TM, Kruger M, Reiser J, Kriz W: Synaptopodin: an actin-associated protein in telencephalic dendrites and renal podocytes. J Cell Biol 1997, 139:193–204
42. Imberti B, Morigi M, Zoja C, Angioletti S, Abbate M, Remuzzi A, Remuzzi G: Shear stress-induced cytoskeleton rearrangement mediates NF-kappaB-dependent endothelial expression of ICAM-1. Microvasc Res 2000, 60:182–188
43. Witteck A, Yao Y, Fechir M, Forstermann U, Kleinert H: Rho protein-mediated changes in the structure of the actin cytoskeleton regulate human inducible NO synthase gene expression. Exp Cell Res 2003, 287:106–115
44. Morita T, Kurihara H, Maemura K, Yoshizumi M, Nagai R, Yazaki Y: Role of Ca2+ and protein kinase C in shear stress-induced actin depolymerization and endothelin 1 gene expression. Circ Res 1994, 75:630–636
45. Zoja C, Benigni A, Remuzzi G: Cellular responses to protein overload: key event in renal disease progression. Curr Opin Nephrol Hypertens 2004, 13:31–37
46. Kretzler M: Regulation of adhesive interaction between podocytes and glomerular basement membrane. Microsc Res Tech 2002, 57:247–253
47. Yamazaki H, Saito A, Ooi H, Kobayashi N, Mundel P, Gejyo F: Differentiation-induced cultured podocytes express endocytically active megalin, a Heymann nephritis antigen. Nephron Exp Nephrol 2004, 96:e52–e58
48. Gallagher H, Oleinikov AV, Fenske C, Newman DJ: The adaptor disabled-2 binds to the third Psi xNPxY sequence on the cytoplasmic tail of megalin. Biochimie 2004, 86:179–182
49. Barisoni L, Kriz W, Mundel P, D'Agati V: The dysregulated podocyte phenotype: a novel concept in the pathogenesis of collapsing idiopathic focal segmental glomerulosclerosis and HIV-associated nephropathy. J Am Soc Nephrol 1999, 10:51–61
50. Srivastava T, Garola RE, Whiting JM, Alon US: Synaptopodin expression in idiopathic nephrotic syndrome of childhood. Kidney Int 2001, 59:118–125
51. Drenckhahn D, Franke RP: Ultrastructural organization of contractile and cytoskeletal proteins in glomerular podocytes of chicken, rat, and man. Lab Invest 1988, 59:673–682
52. Ichimura K, Kurihara H, Sakai T: Actin filament organization of foot processes in rat podocytes. J Histochem Cytochem 2003, 51: 1589–1600
53. Ortega-Velazquez R, Diez-Marques ML, Ruiz-Torres MP, Gonzalez-Rubio M, Rodriguez-Puyol M, Rodriguez Puyol D: Arg-Gly-Asp-Ser (RGDS) peptide stimulates transforming growth factor beta1 transcription and secretion through integrin activation. FASEB J 2003, 17:1529–1531
54. Gonzalez-Santiago L, Lopez-Ongil S, Griera M, Rodriguez-Puyol M, Rodriguez-Puyol D: Regulation of endothelin synthesis by extracellular matrix in human endothelial cells. Kidney Int 2002, 62:537–543
55. Benigni A, Corna D, Zoja C, Longaretti L, Gagliardini E, Perico N, Coffman TM, Remuzzi G: Targeted deletion of angiotensin II type 1A receptor does not protect mice from progressive nephropathy of overload proteinuria. J Am Soc Nephrol 2004, 15:2666–2674
56. Perona R, Montaner S, Saniger L, Sanchez-Perez I, Bravo R, Lacal JC: Activation of the nuclear factor-kappaB by Rho, CDC42, and Rac-1 proteins. Genes Dev 1997, 11:463–475
57. Chen HC, Appeddu PA, Parsons JT, Hildebrand JD, Schaller MD, Guan JL: Interaction of focal adhesion kinase with cytoskeletal protein talin. J Biol Chem 1995, 270:16995–16999
58. Schlaepfer DD, Hanks SK, Hunter T, van der Geer P: Integrin-mediated signal transduction linked to Ras pathway by GRB2 binding to focal adhesion kinase. Nature 1994, 372:786–791
59. Spath M, Pavenstadt H, Muller C, Petersen J, Wanner C, Scholmeyer P: Regulation of phosphoinositide hydrolysis and cytosolic-free calcium induced by endothelin in human glomerular epithelial cells. Nephrol Dial Transplant 1995, 10:1299–1304
60. Yamamoto T, Hirohama T, Uemura H: Endothelin B receptor-like immunoreactivity in podocytes of the rat kidney. Arch Histol Cytol 2002, 65:245–250

CHAPTER 7

SHIGA TOXIN-2 UP-REGULATES ENDOTHELIN-1 GENE IN GLOMERULAR PODOCYTES AND PROMOTES CYTOSKELETAL DYSFUNCTION: IMPLICATIONS FOR GLOMERULAR ISCHEMIA AND HEMODYNAMIC CHANGES OF HUS

M. Morigi, S. Buelli, C. Zanchi, L. Longaretti, D. Macconi, A. Benigni, G. Remuzzi and C. Zoja

Am J Pathol 2006; manuscript in submission

Podocyte derived endothelin-1 induces actin remodeling and mediates Shigatoxin renal toxicity

Marina Morigi*, Simona Buelli*, Cristina Zanchi*, Lorena Longaretti*, Daniela Macconi*, Ariela Benigni*, Giuseppe Remuzzi*# and Carla Zoja*

* *Mario Negri Institute for Pharmacological Research,*

Via Gavazzeni 11, 24125 Bergamo, Italy;

 # Unit of Nephrology and Dialysis,

Azienda Ospedaliera, Ospedali Riuniti di Bergamo,

Largo Barozzi 1, 24128 Bergamo, Italy;

Running Title: Stx-2 induces podocyte dysfunction via ET-1

Correspondence to:

Marina Morigi, Biol.Sci.D.
'Mario Negri' Institute for Pharmacological Research
Via Gavazzeni 11, 24125 Bergamo, Italy
Phone: +39-035-319 888;
Fax: +39-035-319 331
E-mail: morigi@marionegri.it

ABSTRACT

Shigatoxin (Stx) is the offending agent of post-diarrheal HUS, characterized by glomerular ischemic changes preceeding microvascular thrombosis. Since podocytes are highly sensitive to Stx cytotoxicity and represent a source of vasoactive molecules, we studied whether Stx-2 modulated the production of endothelin (ET)-1, taken as candidate mediator of podocyte dysfunction. Stx-2 enhanced ET-1 mRNA and protein via activation of NF-kB and Ap-1, to the extent that transfection with dominant negative mutant of IkB kinase2 or with Ap-1 decoy oligodeoxynucleotides reduced ET-1 mRNA. A role for p38 and p42/44 MAPK in mediating NF-kB-dependent gene transcription induced by Stx-2 has been proposed based on data that Stx-2 phosphorylated p38 and p42/44 MAPK and that inhibitors of both MAPK reduced transcription of NF-kB promoter/luciferase reporter gene construct induced by Stx-2. Stx-2 caused F-actin redistribution and intercellular gaps via ET-1 induction since cytoskeleton changes were prevented by ET_A receptor blockade. As Stx-2, exogenous ET-1 induced cytoskeleton rearrangement and gaps, and increased protein permeability. These data suggest that podocyte is a target of Stx, novel stimulus for the synthesis of ET-1 that may control in autocrine and paracrine fashion glomerular remodeling and hemodynamic derangement in HUS.

INTRODUCTION

Shigatoxin (Stx)-producing *E. coli* has been strongly indicated as the offending agent of typical post-diarrheal hemolytic uremic syndrome (D+HUS), a disorder of thrombocytopenia, microangiopathic hemolytic anemia and acute renal failure that mainly affects infants and small children (1-3). The kidney is the privileged organ of Stx toxicity, because it expresses high levels of the specific receptor glycosphingolipid globotriaosyl ceramide (Gb3) (4, 5). The characteristic lesion consists of swelling and detachment of glomerular endothelial cells that have been extensively recognized as the main target of Stx (6). Retraction and collapse of the capillary tuft in the glomerulus are prominent and tipically occur in association with fusion of foot processes and swelling of podocytes (6, 7). While ischemic lesion in the glomerular microcirculation can significantly contribute to renal dysfunction, the precise role of podocyte injury in the toxic response to Stx and the underlying cellular and molecular mechanisms have not been established yet.

Recent studies have indicated that glomerular visceral epithelial cells (podocytes) are sensitive to the toxic effects of Stx-1 and 2 isoforms because they express high levels of Gb3 and bind Stx, as documented either in cultured cells (8) or in human renal biopsies (9). In vitro, Stx-1 activated podocytes to release inflammatory cytokines like IL-1 and TNF, which remarkably increased the cellular content of Gb3 receptor, thereby enhancing renal toxin responsiveness (8, 10). In an experimental model of HUS in baboons, swelling of podocytes with osmophilic inclusions was found in

association with the typical glomerular endothelial lesions after intravenous infusion of Stx-1 (11).

Podocytes represent a crucial component of the glomerular filter barrier. They are highly specialized cells endowed with foot processes that through a contractile structure, composed of actin and associated proteins connected to the glomerular basement membrane, stabilize glomerular architecture by counteracting the distension of the basement membrane (12, 13). The contractile apparatus of the foot processes responds to vasoactive hormones, thus controlling the glomerular capillary surface area and the ultrafiltration coefficient. Podocytes are an important source of the vasoconstrictor peptide endothelin-1 (ET-1), recognized to play a key role in the control of glomerular hemodynamics (14, 15). They constitutively express preproET-1 mRNA and synthesize the mature peptide, whose generation is markedly upregulated by TGFβ, MAC and thrombin (14). Studies have shown that podocytes are target of ET-1 because they express ET_A and ET_B receptors (16, 17).

With the attempt to identify possible mechanisms evoked by Stx that could contribute to podocyte dysfunction and renal function impairment in HUS, we tested whether Stx-2 induced in cultured podocytes the expression and synthesis of ET-1, instrumental for cytoskeletal remodeling and cellular retraction. Intracellular signals involved in ET-1 gene regulation were also investigated.

METHODS

Cell culture and incubation

Immortalized mouse podocytes were grown according to the method described by Mundel et al (18). Briefly, cells were cultured under growth-permissive conditions on rat tail collagene type I coated plastic dishes (BD Bioscience Bedfird, MA), at 33°C in RPMI 1640 medium (Invitrogen, Gaithesburg, MA) supplemented with 10% fetal bovine serum (FBS, Invitrogen), 10 U/ml mouse recombinant γ -interferon (Sigma Chemical Co, Saint Louis, MI, USA) and 100 U/ml penicillin plus 0.1 mg/ml streptomycin (Sigma). To induce differentiation, podocytes were maintained in nonpermissive conditions at 37°C without γ -interferon for 14 days and used for the experiments. In this culture conditions, cells stopped proliferating and were identified as differentiated podocytes by their arborized morphology and the presence of high levels of synaptopodin, using indirect immunofluorescence microscopy. Cells were routinely maintained for 24 h in serum free medium before all the experiments.

To investigate the effect of Stx-2 on the expression of ET-1 gene, differentiated podocytes were exposed for 3, 6 and 24 h to medium alone or to Stx-2, 50pM and 1nM (Toxin Technology Inc., Sarasota, FL, USA); preliminary experiments showed that these concentrations did not affect podocyte viability as evaluated by viable cell count by Trypan blue dye exclusion (Sigma). ET-1 mRNA transcript levels were measured by Northern blot analysis and real time PCR. To exclude any possible effect of lipopolysaccharide (LPS) contamination of Stx-2 preparation on ET-1 mRNA

expression, in some cases podocytes were incubated with Stx-2 in the presence of the LPS inhibitor polymyxin B (10μg/ml, Sigma) (19).

The time-course of ET-1 protein synthesis was assessed by radioimmunoassay (RIA) in supernatants of podocytes exposed to both concentrations of Stx-2.

To study intracellular signaling pathways that regulate ET-1 gene transcription in Stx-2 loaded podocytes, we first assessed the potential role of NF-kB and Ap-1 by determining the activity of both transcription factors in nuclear extracts from podocytes exposed for 30 min to Stx-2 (50pM and 1nM) and by evaluating the effect of NF-kB and Ap-1 inhibition on ET-1 gene expression. Podocytes were transfected for 3h with a dominant negative mutant of the IkB kinase2 (IKK2) (20), a kinase that acts as an upstream activator of NF-kB, and then exposed to Stx-2 (50pM) for 24 h. In other experiments, podocytes were transfected for 2 h with double-stranded oligodeoxynucleotides (ODN) (21) that scavenge Ap-1 activity by competitive reaction, or mutated control ODN, and then exposed to the toxin for 6h. Then, we studied whether Stx-2 induced activation/phosphorylation of p38 MAPK and p42/44 MAPK -known activators of NF-kB and Ap-1- in podocytes treated with 50pM Stx-2 for 15, 30, 60, 180 min. To elucidate whether MAPK were involved in NF-kB regulation, podocytes were transfected with NF-kB luciferase reporter gene and incubated with Stx-2 (50 pM, 6h) in the presence or absence of the p38 inhibitor SB-202190 (20 μM) (22) or the p42-44 inhibitor PD-98059 (10 μM) (23) .

The effect of Stx-2 on F-actin cytoskeletal rearrangement and gap formation was assessed in differentiated podocytes exposed for 15 h to Stx-2 (50 pM). The involvement of ET-1 in the process of F-actin changes and gap formation was

investigated by using a specific ET_A/ET_B receptor antagonist J-104132 (1nM, Banyu Pharmaceutical co., Ibaraki, Japan) (24) or an ETA receptor antagonist, LU-302146 (1μM, Knoll AG, Ludwighafen, Germany) (25), added 1 h prior and during 15 h of Stx-2 incubation.

Northern blot analysis

Total RNA was isolated from podocytes by the guanidium isothyocianate/cesium chloride procedure. Fifteen μg of total RNA was then fractionated on 1.2% agarose gel and blotted onto synthetic membranes (Zeta-probe; Bio-Rad, Richmond, CA, USA). ET-1 mRNA was detected by using a 319 bp fragment of rat ET-1 cDNA. The probe was labeled with α–^{32}P dCTP by random-primed method. Hybridization was performed overnight at 60° in 0.25 M Na_2HPO_4, pH 7.2, 7% SDS. Filters were washed twice for 30 min with 20 mM Na_2HPO_4, pH 7.2, 5% SDS and twice for 10 min with 20 mM Na_2HPO_4, pH 7.2, 1% SDS at 60°. Membranes were subsequently probed with β-actin cDNA, taken as internal standard of equal loading of the samples on the membrane. Expression of ET-1 mRNA was corrected for β-actin expression and quantited densitometrically.

Quantitative Real Time PCR

Total RNA was extracted from podocytes by the guanidium isothiocyanate/cesium chloride procedure. Contaminating genomic DNA was removed by RNase-free DNase (Promega, Ingelheim, Germany) for 1 h at 37°C. The purified RNA (1 μg) was reverse transcribed using random examers (50 ng) and 200 U of SuperScript II RT

(Life Technologies, San Giuliano Milanese, Italy) for 1 h at 42°C. No enzyme was added for reverse transcriptase-negative controls (RT^-).

Real-time PCR was performed with ABI PRISM 5700 Sequence Detection System (PE Biosystems , Warrington, UK) using heat-activated TaqDNA polymerase (Amplitaq Gold, PE Biosystems) (26). The SYBR Green I PCR Reagents kit was used according to the manufacturer's protocol. After an initial hold of 2 min at 50°C and 10 min at 95°C, the samples were cycled 40 times at 95°C for 15 s and 60°C for 60 s. Fluorescence detection, defined as threshold cycle (Ct), is picked in the exponential phase of the PCR and used for relative quantification of the target gene. The comparative Ct method normalizes the number of target gene copies to an house-keeping gene as Glyceraldehyde-3-phosphate dehydrogenase (GAPDH) (ΔCt). Gene expression was then evaluated by the quantification of cDNA corresponding with the target gene relative to a calibrator sample serving as a physiologic reference (e.g., untreated cells, ΔΔCt). On the basis of exponential amplification of target gene as well as calibrator, the amount of amplified molecules at the Ct is given by: $2^{-\Delta\Delta Ct}$. The following specific primers (300 nM) were used:

mouse ET-1: sense 5'-AACTACGAAGGTTGGAGGCCA, antisense 5'-CACGAAAAGATGCCTTGATGC; GAPDH sense 5'-TCATCCCTGCATCCACTGGT, antisense 5'-CTGGGATGACCTTGCCCAC. All primers were obtained from Sigma Genosys (Cambridgeshire, UK). True identity of the amplification products was ensured by primer specificity for ET-1 mouse

sequence, the presence of a single dissociation curve at a constant T melting, and the lack of genomic DNA contamination or primer dimers in RT⁻ sample.

Radioimmunoassay

ET-1 production was assayed in podocyte supernatants by radioimmunoassay (RIA). Either standard compounds or unknown sample (100µl) were mixed with 100 µl of antiserum (Peninsula Laboratories Inc. Belmont, CA) diluted in phosphate buffer pH 7,2 (RIA buffer) at final dilution 1:72000. The reaction mixture was incubated for 24 h at 4°C; then 15000 cpm of (^{125}I) ET-1 in 100 µl was added and the incubation prolonged for 24 h at 4°C. Separation of free from antibody-bound (^{125}I) ET-1 was achieved by addition of a second antibody (500 µl of immunoprecipitating mixture consisting of a sheep anti-rabbit IgG and polyethylene glycol) for 30 minutes at room temperature. Finally, 500 µl RIA buffer was added to stop the reaction, and the immunoprecipitates were centrifuged at 5000g for 30 min. Supernatants were discarded and pellet radioactivity detected by gamma counter (Beckman, Irvine, CA). Results were expressed as pg/10^6 cells. The minimum detectable concentration was 0.4 pg/tube. Nonspecific binding did not exceed 2% of total radioactivity.

The cross-reactivity of the antibody with other endothelins is as follows: endothelin-2, 46.9%; endothelin-3, 17%; and big endothelin-1, 9.4%. Intra-assay and inter-assay variability averaged 10% and 12% respectively, over a range between 0.4 and 100 pg/tube.

Preparation of nuclear extracts and electrophoretic mobility shift assay

Nuclear extracts were prepared from podocytes with the NE-PER™ Nuclear and Cytoplasmic Extraction Reagents Kit (Pierce/Celbio, Pero, Italy) according to the manufacturer's instructions. To minimize proteolysis, all buffers contained protease inhibitor cocktail (Boehringer Manneheim, Germany). The protein concentration was determined by the Bradford assay using the Bio-Rad protein assay reagent.

Electrophoretic mobility shift assays (EMSAs) were performed as previously described (22) with the kB DNA sequence of the immunoglobulin gene (5'-CCGGTCAGAGGGGACTTTCCGAGACT) and consensus binding site for Ap-1 (5'-CGCTTGATGACTCAGCCGGAA). Nuclear extracts (3 μg) were incubated with 50 kcpm of ^{32}P labeled oligonucleotide in a binding reaction mixture [10 mM Tris-HCl pH 7.5, 80 mM NaCl, 1 mM EDTA, 1mM dithiothreitol, 5% glycerol, 1.5 μg of poly (dI-dC)] for 30 min on ice. In competition studies, a 100-fold molar excess of unlabeled oligonucleotide was added to the binding reaction mixture before the addition of the labeled kB or Ap-1 probes. For densitometric analysis the volume density for each band was determined in arbitrary units. The sum of the volume density of bands for a single sample was used as an indirect measure of NF-kB or Ap-1 activation and expressed as a fold increase of the mean densitometry of respective control (represented as 1).

Adenoviral vector-mediated gene transfer in podocytes

Replication-deficient adenovirus encoding for kinase-defective dominant negative form of human IKK2 (AdV-dnIKK2) was a kind gift of Dr.R. de Martin (University of

Vienna, Austria) (20). Replication-deficient adenoviral vector having no insert (AdV-0) was from Novartis Pharma (Basel, Swiss). All viruses used belong to Ad5 serotype. For transfection experiments, podocytes were incubated with adenoviruses at a multiplicity of infection of 50 in RPMI 1640 without serum for 3 h at 37°C. The adenovirus was washed off and cells were maintained in serum-free medium for 24 h. Then cells were exposed to 50 pM Stx-2 for additional 24 h and processed for endothelin-1 mRNA expression (real time PCR analysis). Transfection did not affect cell viability.

Ap-1 decoy oligodeoxynucleotide (ODN) technique

The sequences of the phosphorothioate double stranded ODN against the Ap-1 binding site and the mutated control ODN were as follows:

Ap-1 decoy ODN (consensus sequences are underlined), 5'-CGCTTGATGACTCAGCCGGAA-3', 3'-GCGAACTACTGAGTCGGCCTT-5',

mutated control ODN, 5'-CGCTTGATGACTTGGCCGGAA-3', 3'-TTCCGGCCAAGTCATCAAGCG-5'.

Double stranded ODN (21) were prepared from complementary single stranded phosphorotioate oligonucleotides, by melting at 80°C for 5 minutes followed by 3-4 h reconstitution period at room temperature. To study the effect of Ap-1 decoy, podocytes were transfected with 200 nM Ap-1 decoy ODN or mutated control ODN in serum free medium, using Oligofectamine™ Reagent according to the manufacturer's instructions (Invitrogen, San Giuliano Milanese, Italy). Two hours after transfection, Stx-2 at the final concentration of 50 pM was added to the cells for

6 h without removing transfection mixture. Then, cells were processed for ET-1 mRNA expression (real time PCR analysis).

Western blot analyses

Podocytes were lysed with lysis buffer (Tris-HCl 20 mM pH 7.5, NaCl 150 mM, EDTA 2 mM, Triton-X100 1%, sodium pyrophosphate 2.5 mM, β-glycerophosphate 1 mM) plus phosphatase inhibitors (Na_3VO_4 1 mM, NaF 50 mM) and protease inhibitors (PMSF 1 mM, leupeptin 1μg/ml). Protein concentration was determined by protein assay based on bicinchoninic acid color formation (Pierce, Milan, Italy). Proteins (30 μg) were separated on 10% polyacrylamide gels by SDS-PAGE and transferred to nitrocellulose membranes. Membranes were blocked for 1 h at room temperature with PBS containing 0.1% Tween-20 and 5% BSA (for phosphorylated protein detection) or 5% non-fat dry milk (for un-phosphorylated protein detection), and then incubated overnight at 4°C with the following primary antibodies: mouse monoclonal IgM anti phospho-p38 (1:300) or mouse monoclonal IgG phospho-p42/44 [Thr202/Tyr204] (1:1000) in PBS plus 1% BSA; mouse monoclonal IgG anti-p38 (Santa Cruz Biotechnology, Santa Cruz, CA) 1:200 or mouse monoclonal IgG anti-p42/44 (Cell Signaling Technology Inc., Beverly, MA) 1:2000 in PBS plus 1% non-fat dry milk. After incubation with the secondary antibodies, horseradish peroxidase-conjugated rabbit anti-IgG mouse or goat anti-IgM mouse (Sigma), for 1 h at room temperature in PBS with 0.1% Tween-20 and 1% BSA or 1% non-fat dry milk, proteins bands were detected by Supersignal chemiluminescent substrate (Pierce).

Reporter luciferase gene assay

Podocytes were transfected with 1 μg NF-kB luciferase reporter gene (Stratagene; M-Medical, Florence, Italy) by the Superfect transfection reagent following manufacturer's protocol (Qiagen, Milan, Italy). Three hours after transfection, the reporter gene was washed off and cells were maintained overnight in fresh medium without serum (22). Then cells were exposed to Stx-2 (50 pM) for additional 6 h. The p38 inhibitor SB-202190 (20 μM) or the p42/44 inhibitor PD-98059 (10 μM) were added 1 h before and during stimulation with Stx-2. Podocytes were subsequently lysed in 1X reporter lysis buffer for 15 min at room temperature. The lysates were cleaned by centrifugation. The luciferase activity was measured according to standard protocols (Stratagene; M-Medical), with a Lumat LB9507 luminometer (EG&G Berthold, Bad Wildbad, Germany). Induced luciferase activities were normalized on the basis of protein contents and expressed as fold stimulation compared with unstimulated controls.

Immunofluorescence staining for F-actin

Podocytes plated on type I collagen-coated glass coverslips were maintained in non-permissive conditions for 14 days and incubated with medium alone, Stx-2 at 50pM 15 h and in additional experiments with ET-1 (100 nM) for 6 h. At the end of incubation, cells were fixed in 2% paraformaldehyde plus 4% sucrose in PBS pH 7.4 for 10 min at 37°C. After three washings with PBS, non-specific binding sites were saturated in blocking solution (2% FBS, 2% bovine serum albumin, 0.2% bovine gelatin in PBS) for 30 min at room temperature. Then podocytes were incubated with

rhodamine-phalloidin 20 U/ml for 45 min (Molecular Probes Inc., Eugene, OR, USA); negative control experiments without rhodamine-phalloidin were performed. Coverslips were washed and mounted in 1% N-propyl-gallate in 50% glycerol, 0.1 M Tris-HCl, pH 8 and examined using fluorescence microscopy Olympus IX70 (Olympus Italia srl, Segrate-Milano, Italy) at the original magnification X600. To evaluate gap formation, we counted the number of gaps of 15 fields taken randomly for each sample.

Permeability studies

Permeability was determined by measuring the transepithelial passage of FITC-BSA from apical to basolateral compartment of transwell bicameral chambers (0.4 μm pore Corning Costar Corporation, Cambridge, MA) as previously described with slight modifications (27). Podocytes were exposed to test medium or ET-1 (100 nM, Sigma) for 6 h, then FITC-BSA 100 μg/ml (Sigma) was loaded into the apical compartment for 1 h at 37°C. Fluorescence in the basolateral compartment was measured using fluorescence spectroscopy (ex=490; em=525). Permeability index (PI) was calculated as follows:

$$\text{Permeability index } \% = \frac{\text{(experimental clearance-spontaneous clearance)}}{\text{(clearance of filter alone-spontaneous clearance)}} \times 100$$

where experimental clearance was fluorescence from the basolateral compartment upon ET-1, spontaneous clearance was average fluorescence in unstimulated control, and clearance of filter alone fluorescence without cells.

Statistical analysis

Results are expressed as mean ± SE. Statistical analysis was performed using Student's t test, ANOVA followed by Tukey test for multiple comparisons, and Kruskall Wallis test, as appropriate. Statistical significance was defined as $P<0.05$.

RESULTS

Stx-2 increases ET-1 expression and protein in cultured podocytes

We assessed the capability of Stx-2 to modulate ET-1 mRNA expression and protein synthesis in differentiated mouse podocytes maintained for 14 days in non permissive culture condition. By Northern blot, a 1.3 kb mRNA transcript specific for ET-1 was observed in unstimulated control podocytes (Figure 1A). Stx-2 at the subtoxic concentrations of 50 pM and 1nM induced a significant increase of ET-1 transcript levels over control at 3 and 6 h, which further enhanced after 24 h incubation (2.9- and 3.2 -fold increase). The upregulation of ET-1 gene was also confirmed by real time PCR studies (Figure 3). The stimulatory effect of Stx-2 on ET-1 mRNA expression (24 h) was not due to LPS contamination as indicated by experiments using LPS inhibitor polymyxin B (Stx-2: 3.1, Stx-2+polymyxin B: 3.6-fold increase of ET-1 mRNA over control).

Overexpression of ET-1 gene was paralleled by a significant time-dependent increase of the native peptide released into the supernatants of Stx-treated podocytes. ET-1 production, already detected at 6 hours, was more pronounced starting from 15 hour exposure to both Stx-2 concentrations (Figure 1B).

Upregulation of ET-1 mRNA in response to Stx-2 is dependent on NF-kB and Ap-1

Since the promoter region of ET-1 has consensus sequences for NF-kB and Ap-1 (28, 29), we studied the DNA binding activity of these transcription factors in podocytes challenged with Stx-2. As shown in Figure 2A, nuclear extracts from unstimulated

cells displayed two constitutive bands of NF-kB: an upper complex and a faster migrating lower complex. Thirty min incubation of podocytes with Stx-2 (50 pM and 1 nM) elicited a substantial rise in NF-kB binding activity of the two complexes. Densitometric analysis of three independent experiments revealed a 6- and 10-fold increase of NF-kB activity induced by Stx-2 over control ($P<0.05$). Similarly, Ap-1 activation was detected in podocytes exposed to both concentrations of Stx-2 ($P<0.05$ vs control) (Figure 2B). The specificity of binding reaction was confirmed by the ability of excess cold NF-kB and Ap-1 oligonucleotides to inhibit binding.

To establish whether upregulation of ET-1 mRNA in response to Stx-2 was dependent on NF-kB, podocytes were infected with a recombinant adenovirus encoding the dominant negative mutant of the IkB kinase 2 (AdV-dnIKK2), which fails in promoting the dissociation of IkBα from NF-kB, and then treated for 24 hours with Stx-2 (50 pM). Real time PCR experiments indicated that overexpression of dnIKK2 resulted in a significant ($P<0.01$) reduction of ET-1 mRNA in respect to Stx-treated cells infected with the control adenovirus (AdV-0) (Figure 3A). Notably, dnIKK2 almost completely normalized ET-1 mRNA levels. No difference in ET-1 mRNA levels was observed between Stx-treated podocytes infected or not infected with AdV-0.

The role of Ap-1 was assessed by transfection of podocytes with double stranded (decoy) ODN that scavenge active Ap-1, thereby blocking its binding to the promoter regions of target genes. A partial, although significant reduction (26 %) of ET-1 expression was found in cells transfected with decoy ODN against Ap-1 in respect to mutated control ODN podocytes treated with Stx-2 (Figure 3B).

Stx-2 activates p38 and p42/44 MAPK, instrumental for NF-kB transcriptional activity

Given that in other cellular systems p38 and p42/44 MAPK modulate the transcriptional activity of NF-kB and Ap-1 (22, 30-34), we investigated whether Stx-2 induced activation/phosphorylation of both MAPK. By Western blot analysis, podocytes challenged with Stx-2 (50 pM) exhibited a rapid p38 MAPK phosphorylation within 15 min that further increased at 30 and 60 min in respect to control (Figure 4A). As shown in Figure 4B, Stx-2 induced a marked increase in the level of p42/44 MAPK phosphorylation starting at 30 min, then declining to the basal level by 180 min.

Next, we assessed whether p38 and p42/44 MAPK activated by Stx-2 were involved in NF-kB transcriptional activity, responsible for ET-1 gene regulation. The effect of p38 and p42/44 MAPK inhibitors, SB-202190 and PD-98059, was assessed in Stx-2 treated podocytes transfected with a vector encoding the luciferase reporter gene driven by a promoter containing consensus sequence for NF-kB. Results showed that Stx-2 increased luciferase activity by 2.7-fold in respect to control, which was reduced by 37% by the p38 MAPK inhibitor and almost completely abrogated after p42/44 MAPK functional blockade (Figure 4C).

Stx-2 promotes cytoskeleton rearrangement and gap formation via ET-1

Differentiated podocytes possess a contractile structure composed of F-actin fibers extended across the entire cell body (Figure 5A) that after Stx-2 (50 pM) were greatly

redistributed to the cell periphery (Figure 5B-C). Alterations in actin-based cytoskeleton were associated with the formation of intercellular gaps (Figure 5B-C). Quantitation of gaps revealed a higher frequency in podocytes exposed to Stx-2 compared to unstimulated cells (Figure 5F). To document that ET-1 is a major mediator of Stx-induced podocyte structural changes, we tested the effect of the ET_A/ET_B and ET_A receptor antagonists J-104132 and LU-302146. Both agents, similarly prevented F-actin redistribution induced by Stx-2 (Figure 5D,E), and reduced gap formation (Figure 5F), thus suggesting a role of ET-1 via ET_A receptor.

ET-1 induces F-actin redistribution and alters protein permeability in podocytes

That ET-1 modifies podocyte cytoskeleton was further confirmed by another series of experiments where the peptide was exogenously added to cultured podocytes (Figure 6A,B). Following exposure to ET-1 (100 nM, 6 h), podocytes underwent cytoskeleton alterations, as visualized by the redistribution of F-actin fibers to the cell periphery, and intercellular gap formation (Figure 6B). This effect was remarkably comparable to that seen after Stx-2 treatment.

Evaluation of transepithelial passage of fluorescent albumin to the basolateral compartment of bicameral chambers showed unequivocal increase in albumin permeability across podocyte monolayer upon ET-1 challenge (Figure 6C).

DISCUSSION

The kidney is the privileged target of Shigatoxin, the causative agent of D+HUS. The role of podocyte in the toxic response to Stx, and the underlying cellular and molecular mechanisms have been explored in the present study. We focused on the vasoconstrictor peptide ET-1 found to be elevated in plasma and urine of children during the acute phase of HUS (35, 36). In the kidney ET-1 is produced by all glomerular cell types and by tubules (37), and when bound to ET_A receptor it elicits different biological activities including contraction, proliferation, and inflammatory cell recruitment (38). The present results indicate that Stx-2, at subtoxic concentrations, enhanced gene expression of ET-1 in cultured murine podocytes, which was followed by increased synthesis of the mature peptide. *In vivo*, the increased production of vasoactive ET-1 by podocytes might have an impact on glomerular microcirculation, and possibly account for renal dysfunction in HUS, considering the podocyte location in the glomerulus at close proximity with the endothelium.

A pivotal aspect of this study was the identification of the intracellular signals involved in Stx-induced ET-1 overexpression in podocytes. Regulation of the pre-pro ET-1 gene is complex and has been attributed to multiple regulatory elements. Evidence is available showing that pre-proET-1 gene possesses in the promoter region specific consensus sequences for the transcription factors NF-kB and Ap-1 (28, 29). Podocytes exposed to Stx-2 exhibited a rapid and massive activation of NF-kB. Ap-1 was also significantly activated by the toxin, although to a lesser extent. In

other cellular systems, as monocytes (39) and endothelial cells (40), previous reports showed that Stx increased either NF-kB or AP-1 binding activity, responsible for cytokine and chemokine gene expression. The direct demonstration that NF-kB modulates ET-1 mRNA expression derives from experiments where transfected podocytes that overexpressed a dominant negative mutant of the IKK2 (20, 22) -a specific kinase that acts as upstream activator of NF-kB (41)- failed to increase ET-1 gene expression in response to Stx-2. In addition, finding that Stx -treated podocytes transfected with the Ap-1 decoy ODN showed a significant decrease of ET-1 mRNA indicates that ET-1 gene expression is at least in part dependent on Ap-1 activation.

It has been consistently documented that p38 and p42/44 MAPK pathways are fundamental for initiating the transcriptional activity of NF-kB and Ap-1 (22, 30-34). The involvement of p38 and p42/44 MAPK in mediating NF-kB-dependent gene transcription rests on data that Stx-2 phosphorylated p38 and p42/44 MAPK and that inhibitors of both MAPK decreased the transcription of NF-kB promoter/luciferase reporter gene construct induced by the toxin. Consistently with our results, other studies have implicated MAPK activation in Stx-induced gene transcription in various target cells. In human adenocarcinoma-derived renal tubular cell line (ACHN), Stx-2 induced p38 and p42/44 MAPK activation instrumental for NF-kB-induced TNFα transcription (30). In addition, Stx-1-induced TNFα gene expression in a mononuclear cell line was decreased by blockade of p38 pathway (42).

Another major finding that arises from this study is that Stx-2 caused a marked rearrangement of the contractile F-actin apparatus of podocytes, associated with the formation of intercellular gaps reflecting effective podocyte process retraction.

In vivo, podocyte cytoskeletal derangement, consisting of marked disaggregation and redistribution of actin filaments, results in foot process effacement and cell retraction, structural alterations common to both human and experimental glomerulopathies associated with proteinuria and renal function impairment (43-45). Foot process effacement, which possibly develops in association with increased mechanical stress, can be considered as an adaptive change in the podocyte phenotype to counteract glomerular capillary expansion, at the price of reducing the actual filtration area (43).

As for possible mechanisms by which Stx may influence cytoskeleton remodeling, a study (46) performed in ACHN cells derived from renal tubular epithelial carcinoma showed that binding of Stx-1 B subunit to Gb3 receptor caused the phosphorylation of ezrin, a linker protein that connects the plasma membrane with actin filaments. Ezrin phosphorylation occurred via activation of Src PTK, crucial determinant of cell contraction and cytoskeleton remodeling (47), and was followed by redistribution of cytoskeletal organizing proteins including actin, vimentin, cytokeratin, paxillin and FAK (46). In our experimental setting we tested the hypothesis that cytoskeletal changes induced by Stx-2 in podocytes could be related to the production of ET-1, on account of its ability to induce stress-fiber formation (48) and to activate Src PTK family (49). Finding that treatment of podocytes with ET_A/ET_B or ET_A receptor antagonists prevented F-actin redistribution and decreased gap formation induced by Stx-2, does suggest a role for ET-1 in the dysfunction of the contractile apparatus

eventuating into cell retraction. Moreover, the observation that both agents protected podocytes against Stx-2 toxicity to a similar extent would indicate that the effects of ET-1 are transduced by ET_A receptor. Notably, morphological alterations similar to those caused by Stx-2 were observed when exogenous ET-1 was added to cultured podocytes, causing F-actin redistribution and gap formation. In addition, ET-1 significantly increased transepithelial passage of fluorescent albumin to the basolateral compartment of podocytes grown on a bicameral chamber, which probably reflected an alteration of podocyte-podocyte contact. Altogether these data point to ET-1 as a key mediator of toxin-induced podocyte alterations.

In conclusion, our results document that the podocyte is a functionally relevant target of Stx-2 that via upregulation of ET-1 gene induces podocyte activation and cytoskeletal derangement. These changes might contribute to glomerular dysfunction in D+HUS.

ACKNOWLEDGMENTS

Part of this work was presented at the annual meeting of the American Society of Nephrology (San Diego, CA, November 12-17, 2003). The Authors thank Dr. Peter Mundel (Department of Medicine, Albert Einstein College of Medicine, New York, USA) for providing the conditionally immortalized murine cell line and Dr. Rainer de Martin (Department of Vascular Biology and Thrombosis Research, University of Vienna, Vienna, Austria) for providing recombinant adenovirus expressing dnIKK2. The Authors are indebted to Dr. Mauro Abbate and Dr. Susanna Tomasoni for their precious contribution. Dr. Simona Buelli is a recipient of a fellowship "Helsinn Healthcare SA" through the courtesy of "Fondazione Aiuti per la Ricerca sulle Malattie Rare". Manuela Passera helped preparing the manuscript.

REFERENCES

1. Ruggenenti P, Noris M, Remuzzi G: Thrombotic microangiopathy, hemolytic uremic syndrome, and thrombotic thrombocytopenic purpura. Kidney International 60:831-846, 2001
2. Andreoli SP: The pathophysiology of the hemolytic uremic syndrome. Curr Opin Nephrol Hypertens 8:459-464, 1999
3. Karmali MA: Infection by Shiga toxin-producing Escherichia coli: an overview. Mol Biotechnol 26:117-122, 2004
4. Lingwood CA: Role of verotoxin receptors in pathogenesis. Trends Microbiol 4:147-153, 1996
5. Lingwood CA: Verotoxin-binding in human renal sections. Nephron 66:21-28, 1994
6. Habib R: Pathology of the Hemolytic Uremic Syndrome. In Hemolytic Uremic Syndrome and Thrombotyc Thrombocytopenic Purpura. B.S. Kaplan, R.S. Trompeter, and J.L. Moake, editors, New York, Dekker, M. Inc., 1992, 315-353.
7. Striker GE, Striker LJ, D'Agati V: Renal Lesions in Hypertension. In The Renal Biopsy Major Problems in Pathology. V.A. Livolsi, editor, Philadelphia, Saunders, W.B. Company, 1997, 258-268.
8. Hughes AK, Stricklett PK, Schmid D, Kohan DE: Cytotoxic effect of Shiga toxin-1 on human glomerular epithelial cells. Kidney International 57:2350-2359, 2000

9. Ergonul Z, Clayton F, Fogo AB, Kohan DE: Shigatoxin-1 binding and receptor expression in human kidneys do not change with age. Pediatr Nephrol 18:246-253, 2003

10. Hughes AK, Stricklett PK, Kohan DE: Shiga toxin-1 regulation of cytokine production by human glomerular epithelial cells. Nephron 88:14-23, 2001

11. Taylor FB, Jr., Tesh VL, DeBault L, Li A, Chang AC, Kosanke SD, Pysher TJ, Siegler RL: Characterization of the baboon responses to Shiga-like toxin: descriptive study of a new primate model of toxic responses to Stx-1. Am J Pathol 154:1285-1299, 1999

12. Barisoni L, Kopp JB: Update in podocyte biology: putting one's best foot forward. Curr Opin Nephrol Hypertens 12:251-258, 2003

13. Pavenstadt H: Roles of the podocyte in glomerular function. Am J Physiol Renal Physiol 278:F173-179, 2000

14. Cybulsky AV, Stewart DJ, Cybulsky MI: Glomerular epithelial cells produce endothelin-1. Journal of American Society Nephrology 3:1398-1404, 1993

15. Kasinath BS, Fried TA, Davalath S, Marsden PA: Glomerular epithelial cells synthesize endothelin peptides. Am J Pathol 141:279-283, 1992

16. Yamamoto T, Hirohama T, Uemura H: Endothelin B receptor-like immunoreactivity in podocytes of the rat kidney. Arch Histol Cytol 65:245-250, 2002

17. Ortmann J, Amann K, Brandes RP, Kretzler M, Munter K, Parekh N, Traupe T, Lange M, Lattmann T, Barton M: Role of podocytes for reversal of

glomerulosclerosis and proteinuria in the aging kidney after endothelin inhibition. Hypertension 44:974-981, 2004

18. Mundel P, Reiser J, Zuniga Mejia Borja A, Pavenstadt H, Davidson GR, Kriz W, Zeller R: Rearrangements of the cytoskeleton and cell contacts induce process formation during differentiation of conditionally immortalized mouse podocyte cell lines. Exp Cell Res 236:248-258, 1997

19. Giambartolomei GH, Zwerdling A, Cassataro J, Bruno L, Fossati CA, Philipp MT: Lipoproteins, not lipopolysaccharide, are the key mediators of the proinflammatory response elicited by heat-killed Brucella abortus. Journal Immunology 173:4635-4642, 2004

20. Oitzinger W, Hofer-Warbinek R, Schmid JA, Koshelnick Y, Binder BR, de Martin R: Adenovirus-mediated expression of a mutant IkappaB kinase 2 inhibits the response of endothelial cells to inflammatory stimuli. Blood 97:1611-1617, 2001

21. Viedt C, Dechend R, Fei J, Hansch GM, Kreuzer J, Orth SR: MCP-1 induces inflammatory activation of human tubular epithelial cells: involvement of the transcription factors, nuclear factor-kappaB and activating protein-1. Journal of American Society Nephrology 13:1534-1547, 2002

22. Donadelli R, Zanchi C, Morigi M, Buelli S, Batani C, Tomasoni S, Corna D, Rottoli D, Benigni A, Abbate M, Remuzzi G, Zoja C: Protein overload induces fractalkine upregulation in proximal tubular cells through nuclear factor kappaB- and p38 mitogen-activated protein kinase-dependent pathways. Journal of American Society Nephrology 14:2436-2446, 2003

23. Hannken T, Schroeder R, Zahner G, Stahl RA, Wolf G: Reactive oxygen species stimulate p44/42 mitogen-activated protein kinase and induce p27(Kip1): role in angiotensin II-mediated hypertrophy of proximal tubular cells. Journal of American Society Nephrology 11:1387-1397, 2000

24. Nishikibe M, Ohta H, Okada M, Ishikawa K, Hayama T, Fukuroda T, Noguchi K, Saito M, Kanoh T, Ozaki S, Kamei T, Hara K, William D, Kivlighn S, Krause S, Gabel R, Zingaro G, Nolan N, O'Brien J, Clayton F, Lynch J, Pettibone D, Siegl P: Pharmacological properties of J-104132 (L-753,037), a potent, orally active, mixed ETA/ETB endothelin receptor antagonist. J Pharmacol Exp Ther 289:1262-1270, 1999

25. Brehm BR, Klaussner M, Wolf SC: Chronic elevated endothelin-1 concentrations regulate mitogen-activated protein kinases ERK 1 and ERK 2 in vascular smooth muscle cells. Clin Sci (Lond) 103 Suppl 48:137S-140S, 2002

26. Morigi M, Buelli S, Angioletti S, Zanchi C, Longaretti L, Zoja C, Galbusera M, Gastoldi S, Mundel P, Remuzzi G, Benigni A: In response to protein load podocytes reorganize cytoskeleton and modulate ET-1 gene: implication for permselective dysfunction of chronic nephropathies. Am J Pathol:In press, 2005

27. Oshima T, Laroux FS, Coe LL, Morise Z, Kawachi S, Bauer P, Grisham MB, Specian RD, Carter P, Jennings S, Granger DN, Joh T, Alexander JS: Interferon-gamma and interleukin-10 reciprocally regulate endothelial junction integrity and barrier function. Microvasc Res 61:130-143, 2001

28. Quehenberger P, Bierhaus A, Fasching P, Muellner C, Klevesath M, Hong M, Stier G, Sattler M, Schleicher E, Speiser W, Nawroth PP: Endothelin 1 transcription is controlled by nuclear factor-kappaB in AGE-stimulated cultured endothelial cells. Diabetes 49:1561-1570, 2000

29. Kawana M, Lee ME, Quertermous EE, Quertermous T: Cooperative interaction of GATA-2 and AP1 regulates transcription of the endothelin-1 gene. Mol Cell Biol 15:4225-4231, 1995

30. Nakamura A, Johns EJ, Imaizumi A, Yanagawa Y, Kohsaka T: Activation of beta(2)-adrenoceptor prevents shiga toxin 2-induced TNF-alpha gene transcription. Journal of American Society Nephrology 12:2288-2299, 2001

31. Ryoo SW, Kim DU, Won M, Chung KS, Jang YJ, Oh GT, Park SK, Maeng PJ, Yoo HS, Hoe KL: Native LDL induces interleukin-8 expression via H2O2, p38 Kinase, and activator protein-1 in human aortic smooth muscle cells. Cardiovasc Res 62:185-193, 2004

32. Wang T, Hu YC, Dong S, Fan M, Tamae D, Ozeki M, Gao Q, Gius D, Li JJ: Co-activation of ERK, NF-kappa B and GADD45beta in response to ionizing radiation. Journal Biological Chemistry, 2005

33. Carter AB, Knudtson KL, Monick MM, Hunninghake GW: The p38 mitogen-activated protein kinase is required for NF-kappaB-dependent gene expression. The role of TATA-binding protein (TBP). Journal Biological Chemistry 274:30858-30863, 1999

34. Goebeler M, Gillitzer R, Kilian K, Utzel K, Brocker EB, Rapp UR, Ludwig S: Multiple signaling pathways regulate NF-kappaB-dependent transcription of

the monocyte chemoattractant protein-1 gene in primary endothelial cells. Blood 97:46-55, 2001

35. Yamamoto T, Nagayama K, Satomura K, Honda T, Okada S: Increased serum IL-10 and endothelin levels in hemolytic uremic syndrome caused by Escherichia coli O157. Nephron 84:326-332, 2000

36. Siegler RL, Edwin SS, Christofferson RD, Mitchell MD: Endothelin in the urine of children with the hemolytic uremic syndrome. Pediatrics 88:1063-1066, 1991

37. Wilkes BM, Susin M, Mento PF, Macica CM, Girardi EP, Boss E, Nord EP: Localization of endothelin-like immunoreactivity in rat kidneys. Am J Physiol 260:F913-920, 1991

38. Sorokin A, Kohan DE: Physiology and pathology of endothelin-1 in renal mesangium. Am J Physiol Renal Physiol 285:F579-589, 2003

39. Sakiri R, Ramegowda B, Tesh VL: Shiga toxin type 1 activates tumor necrosis factor-alpha gene transcription and nuclear translocation of the transcriptional activators nuclear factor-kappaB and activator protein-1. Blood 92:558-566, 1998

40. Zoja C, Angioletti S, Donadelli R, Zanchi C, Tomasoni S, Binda E, Imberti B, te Loo M, Monnens L, Remuzzi G, Morigi M: Shiga toxin-2 triggers endothelial leukocyte adhesion and transmigration via NF-kappaB dependent up-regulation of IL-8 and MCP-1. Kidney International 62:846-856, 2002

41. Mercurio F, Zhu H, Murray BW, Shevchenko A, Bennett BL, Li J, Young DB, Barbosa M, Mann M, Manning A, Rao A: IKK-1 and IKK-2: cytokine-activated IkappaB kinases essential for NF-kappaB activation. Science 278:860-866, 1997

42. Foster GH, Armstrong CS, Sakiri R, Tesh VL: Shiga toxin-induced tumor necrosis factor alpha expression: requirement for toxin enzymatic activity and monocyte protein kinase C and protein tyrosine kinases. Infection and Immunity 68:5183-5189, 2000

43. Shirato I: Podocyte process effacement in vivo. Microsc Res Tech 57:241-246, 2002

44. Ito K, Ger YC, Kawamura S: Actin filament alterations in glomerular epithelial cells of adriamycin-induced nephrotic rats. Acta Pathol Jpn 36:253-260, 1986

45. Lachapelle M, Bendayan M: Contractile proteins in podocytes: immunocytochemical localization of actin and alpha-actinin in normal and nephrotic rat kidneys. Virchows Arch B Cell Pathol Incl Mol Pathol 60:105-111, 1991

46. Takenouchi H, Kiyokawa N, Taguchi T, Matsui J, Katagiri YU, Okita H, Okuda K, Fujimoto J: Shiga toxin binding to globotriaosyl ceramide induces intracellular signals that mediate cytoskeleton remodeling in human renal carcinoma-derived cells. J Cell Sci 117:3911-3922, 2004

47. Platek A, Mettlen M, Camby I, Kiss R, Amyere M, Courtoy PJ: v-Src accelerates spontaneous motility via phosphoinositide 3-kinase, phospholipase C and phospholipase D, but abrogates chemotaxis in Rat-1 and MDCK cells. J Cell Sci 117:4849-4861, 2004

48. Kawanabe Y, Okamoto Y, Nozaki K, Hashimoto N, Miwa S, Masaki T: Molecular mechanism for endothelin-1-induced stress-fiber formation:

analysis of G proteins using a mutant endothelin(A) receptor. Mol Pharmacol 61:277-284, 2002

49. Imamura T, Huang J, Dalle S, Ugi S, Usui I, Luttrell LM, Miller WE, Lefkowitz RJ, Olefsky JM: beta -Arrestin-mediated recruitment of the Src family kinase Yes mediates endothelin-1-stimulated glucose transport. Journal Biological Chemistry 276:43663-43667, 2001

LEGEND TO FIGURES

Figure 1. *ET-1 mRNA expression and protein synthesis in podocytes exposed to Stx-2.*

(A) Northern blot experiments were performed using total RNA isolated from podocytes exposed to medium alone (control), Stx-2 (50 pM, 1 nM) for 3, 6 and 24 h. The results are representative of 5 independent experiments. The optical density of the autoradiographic signals was quantified and calculated as the ratio of ET-1 to β-actin mRNA. Results (mean±SE) are expressed as fold increase over control (considered as 1) in densitometric arbitrary units. *$p<0.05$, **$p<0.01$ vs control.

(B) Stx-2 stimulates ET-1 production by podocytes. Podocytes were incubated with medium alone, Stx-2 (50 pM, 1 nM) for 6, 15, 24 and 48 h. ET-1 production was measured in cell supernatants by RIA. The results are representative of 3 independent experiments. Data are expressed as mean ± SE. *$p<0.01$ vs control.

Figure 2. *Activation of NF-kB and Ap-1 in podocytes exposed to Stx-2.*

(Top) Electrophoretic mobility shift assay (EMSA) for NF-kB (A) and Ap-1 (B) was performed in nuclear extracts of podocytes exposed for 30 min to medium alone, Stx-2 (50 pM, 1 nM). To confirm the specificity of the binding reaction, a 100-fold molar excess unlabeled (cold) nucleotide was used to compete with the labeled NF-kB or AP-1 probes for binding to nuclear proteins. The results are representative of 3 independent experiments employing different nuclear extracts. (Bottom) Densitometric analysis of

autoradiographic signals of NF-kB (A) and AP-1 (B). Results are mean ± SE. *p<0.05 vs control.

Figure 3. *ET-1 mRNA upregulation induced by Stx-2 is inhibited by adenovirus-mediated dominant negative mutant of IKK2 or by Ap-1 decoy ODN.*

(A) Cells were left untreated or infected for 3 h with a recombinant adenovirus coding for a dominant kinase-negative mutant of IKK2 (AdV-dnIKK2) or with a control adenovirus (AdV-0) and then were maintained in serum free medium for 24 h before incubation with medium alone or Stx-2 (50 pM) for 24 h. Cells were processed for ET-1 mRNA expression by real time PCR. The results shown are mean ± SE of 3 independent experiments. *p<0.05, **p<0.01 vs control; °°p<0.01 vs AdV-0+ Stx-2.

(B) Ap-1 decoy ODN or mutated control ODN were added to podocytes 2 h before incubation with medium alone or Stx-2 (50 pM) for 6 h. ET-1 mRNA was assessed by real time PCR. The results shown are mean ± SE of 3 independent experiments. **p<0.01 vs control; °p<0.05 vs control ODN+Stx-2.

Figure 4. *Stx-2 activates p38 and p42/44 MAPK instrumental for NF-kB activation.*

Activation of p38 (A) and p42/44 (B) in podocytes exposed to Stx-2 (50 pM) for 15, 30, 60 and 180 min. Cell lysates were analyzed by Western blot using antibodies against the phosphorylated form of each MAPK. The blots were

stripped and reprobed with anti-nonphosphorylated p38 or p42/44 antibodies to confirm equal loading of the proteins on the gel.

(C) Effect of pharmacological inhibition of p38 and p42/44 MAPK on Stx-2-induced NF-kB-dependent promoter activity. Podocytes were transfected for 3 h with NF-kB luciferase reporter gene. Then cells were maintained in serum free medium for 15 h before exposure to Stx-2 (50 pM) for additional 6 h. The p38 inhibitor SB-202190 (20 μM) and the p42/44 inhibitor PD-98059 (10 μM) were added 1 h before and during stimulation with Stx-2. Relative luciferase activity is expressed as fold stimulation by assuming control as 1. Data are mean ± SE (three experiments). *$p<0.01$ vs control; ° $p<0.01$ vs Stx-2.

Figure 5. *Stx-2 induces cytoskeletal F-actin redistribution and gap formation via* ET_A *receptor.*

Immunofluorescence staining of F-actin fibers in podocytes stimulated for 15 h with medium alone (A), Stx-2 (50 pM) (B-C), Stx-2 in the presence of J-104132 (1 nM), an ET_A/ET_B receptor antagonist (D), or LU-302146 (1 μM), an ET_A receptor antagonist (E). Each ET-1 receptor antagonist was added 1 h before and during the incubation with Stx-2. In unstimulated cells F-actin microfilaments are arranged in parallel, whereas Stx-2 leads to F-actin redistribution at the cell periphery in association with gap formation. Both agents prevent cytoskeletal redistribution and gaps. Magnification 600X.

The number of gaps was counted in fifteen random fields for each sample and the results are expressed as mean ± SE (seven experiments) (F). *$p<0.01$ vs control; °$p<0.01$ vs Stx-2.

Figure 6. *Effect of exogenous ET-1 on cytoskeletal F-actin distribution and albumin permeability in podocytes.*

Immunofluorescence staining of F-actin fibers in podocytes exposed for 6 h to control medium (A) or ET-1 (100 nM) (B). ET-1 promotes changes in cytoskeleton distribution leading to F-actin rearrangement at the cell periphery and intercellular gap formation. Magnification X600.

(C) The permeability index reflecting transepithelial passage of fluorescent albumin to the basolateral compartment of the bicameral chamber is increased in cells exposed to ET-1 (100 nM) for 6 h (n=3 experiments). *$p<0.01$ vs control.

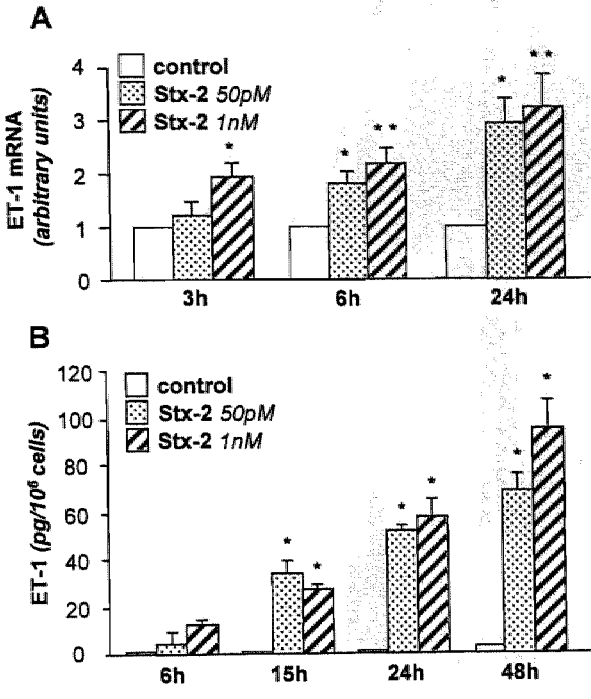
A
control
Stx-2 50pM
Stx-2 1nM
ET-1 mRNA
(arbitrary units)
4
3
2
1
0
3h
6h
24h
B
control
Stx-2 50pM
Stx-2 1nM
ET-1 (pg/10^6 cells)
120
100
80
60
40
20
0
6h
15h
24h
48h

Figure 1

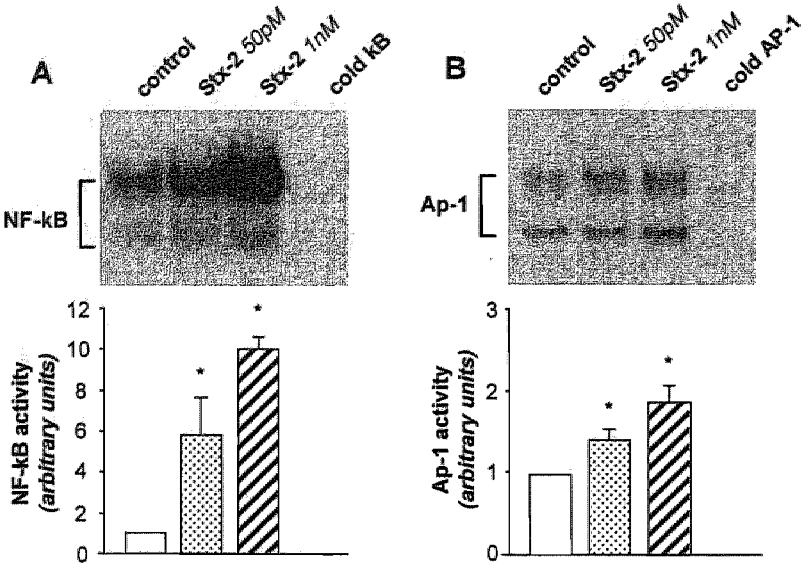
A
control
Stx-2 50pM
Stx-2 1nM
cold kB
NF-kB
NF-kB activity (arbitrary units)
12
10
8
6
4
2
0
*
*
B
control
Stx-2 50pM
Stx-2 1nM
cold AP-1
Ap-1
Ap-1 activity (arbitrary units)
3
2
1
0
*
*

Figure 2

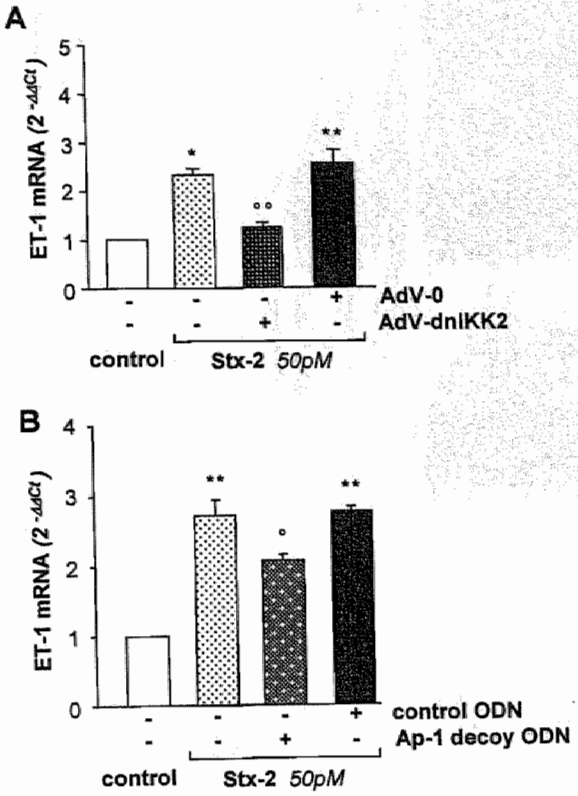
A
ET-1 mRNA (2 -ΔΔCt)
5
4
3
2
1
0
*
°°
**
-
-
-
+
AdV-0
-
-
+
-
AdV-dnIKK2
control
Stx-2 50pM
B
ET-1 mRNA (2 -ΔΔCt)
4
3
2
1
0
**
°
**
-
-
-
+
control ODN
-
-
+
-
Ap-1 decoy ODN
control
Stx-2 50pM

Figure 3

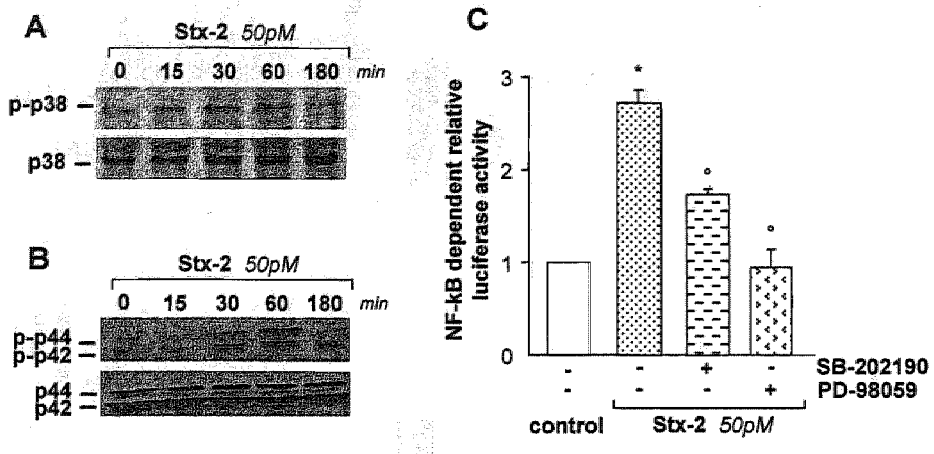
A
Stx-2 50pM
0 15 30 60 180 min
p-p38
p38
B
Stx-2 50pM
0 15 30 60 180 min
p-p44
p-p42
p44
p42
C
NF-kB dependent relative luciferase activity
3
2
1
0
SB-202190
PD-98059
control
Stx-2 50pM

Figure 4

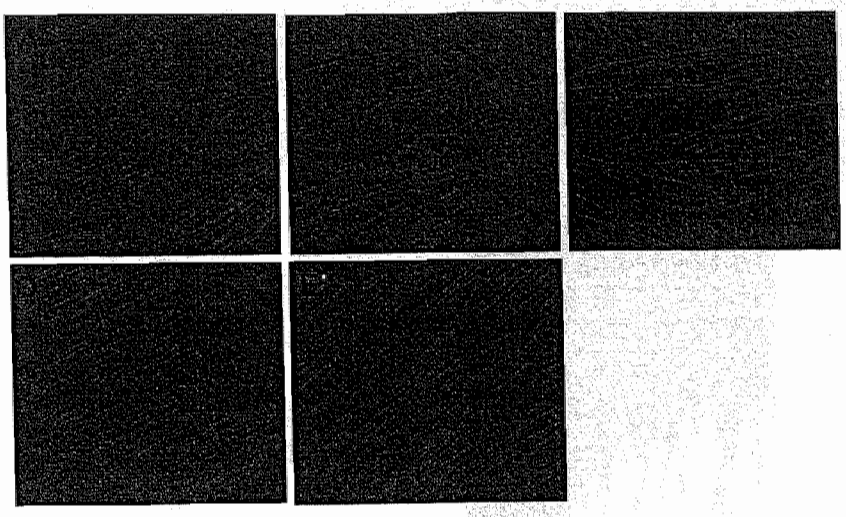

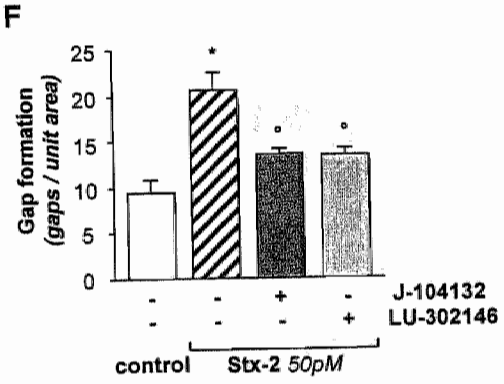
F
Gap formation
(gaps / unit area)
25
20
15
10
5
0
*
°
°
J-104132
LU-302146
control
Stx-2 50pM

Figure 5

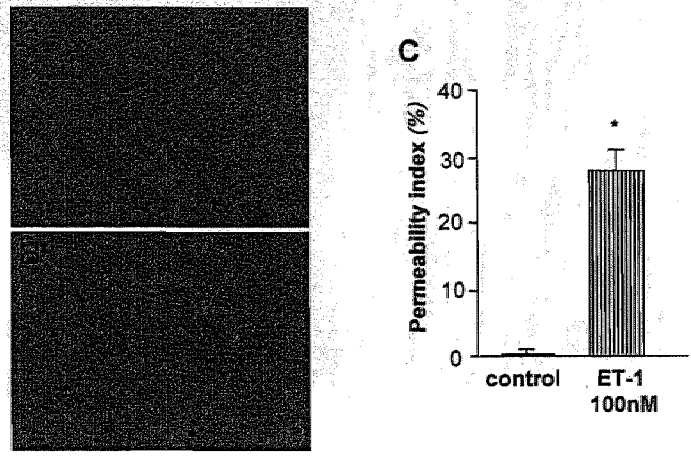

Figure 6

CHAPTER 8

GENERAL DISCUSSION

GENERAL DISCUSSION

In D+HUS, the pathological hallmark of Stx-mediated tissue injury is the development of vascular lesions in renal and other target organs in which endothelial cells are swollen and detached from the underlying basement membranes. Several evidence indicate that leukocyte as well as platelet activation participate in endothelial damage (**Chapter 2**).

In **Chapter 3** of the present thesis it has been documented that exposure of human umbilical vein endothelial cells (HUVEC) to VT-1 induced a dose-dependent increase in the number of leukocytes that stable adhered to endothelium under flow conditions that mimic post-capillary venule circulation. The adhesion response by VT-1 was quite comparable to that of IL-1 β, one of the most potent inducers of leukocyte/endothelium interaction. The events that modulate the adhesion and infiltration of leukocytes into the endothelium are critically dependent on the adhesive molecules and chemokines possibly expressed on the surface of the endothelium/leukocytes, or induced by circulating cytokines and flow condition [1]. Early molecules involved in the process of leukocyte rolling belong to the selectin family [2, 3]. Firm leukocyte adhesion and consequent transmigration implies the involvement of leukocyte β2 and β1 integrin receptors with specific endothelial ligand, i.e., Intercellular adhesion molecule-1 (ICAM-1) and vascular adhesion molecule-1 (VCAM-1), belonging to the Immunoglobulin G (IgG) gene superfamily [4]. Experiments with functional blocking antibody have demonstrated that the adhesive response elicited by VT-1 was dependent on the upregulation on endothelial surface of the adhesive molecules E-selectin, ICAM-1 and VCAM-1. The concept that leukocytes have a key role in the pathogenesis of microvascular lesions of D+HUS rests on the evidence that the degree of leukocytosis may be predictive for the outcome of the disease [5]. Neutrophils isolated from patients during the acute phase of the disease, are

activated [6], adhere to endothelium more avidly than neutrophils from healthy subjects, and damage the endothelium by producing elastase [7] and superoxide [8]. In addition, ultrastructural examination of renal biopsies from HUS patients with evidence of VT-producing E.coli infection, revealed the presence of polymorphonuclear and mononuclear cell infiltration at glomerular level [9], along with microvascular injury.

In the present study, giving TNFα before challenge with VT-1 significantly increased the number of adherent leukocytes under flow in respect to cells challenged with the toxin alone. These data may be explained by the observation that TNFα –a cytokine mainly produced by VT-activated monocytes/macrophages- upregulated the endothelial expression of Gb3, the specific endothelial receptor of VT-1, and increased VT-1 binding [10]. An important role of TNF in toxin–mediated microvascular injury derives from the finding that mice genetically defective in TNFα production were less sensitive to the lethal effect of VT-1 [11] and have a longer time to death in respect to control mice. Thus damage to blood vessels in VT-producing *E.coli* infections might be caused in part by the action of leukocytes secondary to the role of VT in upregulating vascular adhesion proteins.

Relevant to better understanding the nature of the adhesive phenomena triggered by Stx-2, may be the data presented in **Chapter 4** that described the effect of the toxin on endothelial expression of the chemoattractant proteins IL-8 and MCP-1, and their functional role on leukocyte adhesion and transmigration across the endothelium. We observed that subtoxic concentrations of Stx significantly increase the number of leukocytes, mainly polymorphonuclear cells, that adhered and then transmigrated through HUVEC monolayer under flow. Challenge of glomerular endothelial cells with Stx-2 induced massive adhesion and transmigration to a similar extent than that observed on

HUVEC, thus suggesting that both cell types exhibited a similar sensitivity to the toxin, which possibly stimulated identical intracellular signals involved in the adhesive phenomena.

Evidence is available that in HUS patients, urinary levels of IL-8 and MCP-1 were significantly increased during the acute phase of the disease and decreased until recovery, implying a role of these chemokines in the recruitment of inflammatory cells at glomerular levels [12, 13]. In this respect, we focused our attention on these chemokines and we found a strong expression of IL-8 and MCP-1 mRNA after a short exposure of HUVEC to Stx-2. The functional role of both chemokines in the adhesive process evoked by Stx-2 rests on data that blocking antibodies against IL-8 and MCP-1 -that drive recruitment and activation of neutrophils and monocytes, respectively- significantly reduced the adhesion and subendothelial transmigration of distinct leukocyte subsets in HUVEC, as well as in glomerular endothelial cells treated with the toxin. It is known that these chemokines may trigger leukocyte adhesive process either as soluble proteins or as immobilized molecules bound to heparan sulfate proteoglycans of the endothelial surface of post- capillary venules and small veins [14, 15]. Reports have clearly demonstrated that in a model of monocytes rolling on adenovirally mediated E-selectin transduced endothelial cells under flow condition, IL-8 and MCP-1 caused stable adhesion of monocytes to the endothelium through the activation of leukocyte integrins [16].

Since molecular studies have identified NF-kB binding sites within the promoter region of both IL-8 and MCP-1 [17, 18] we investigated whether Stx-2 induced chemokine expression through a transcriptional activation mechanism mediated by NF-kB. This transcription factor belongs to Rel family and exists in an inactive form in the cell cytoplasm bound to the inhibitory protein IkB. Upon activation by different stimuli, NF-kB translocates into the nucleus for binding to DNA motifs in gene promoters [19]. We found that challenge

of endothelial cells with Stx-2 elicited a substantial rise in NF-kB binding activity and that the subunits involved were p65/p50 heterodimer and p50/p50 homodimer. These findings are consistent with a previous study showing that Stx-1 treatment of human monocytes resulted in activation and subsequent nuclear translocation of NF-kB, an event that preceded cytokine gene induction [20]. That upregulation of IL-8 and MCP-1 in Stx-treated endothelium is dependent on NF-kB activation was proven by our data that overexpression of IKBα, the specific inhibitor of NF-kB, produced by transfecting endothelial cells with adhenovirus encoding IKBα, fully suppressed the property of the toxin of inducing the expression of both chemokines by endothelial cells. As expected, delivery of IkBα also inhibited the adhesion and transmigration of leukocytes in Stx-treated HUVEC. Altogether these data might be relevant to understand the role of adhesive molecules and chemokines in promoting leukocyte–endothelium interaction which favors microvascular lesions in D+HUS and could help to identify novel molecular targets for therapeutic intervention.

Thrombocytopenia and formation of renal thrombi in the microcirculation are characteristic lesions of D+HUS. The mechanism by which these thrombi are formed is unclear, and several conflicting reports have investigated the potential interactions of VT with platelets [21, 22]. In **Chapter 5** we addressed the possibility that VT-1 could directly modulate anti-thrombogenic properties of the endothelium under high shear stress typically present in the microcirculation. We have demonstrated that VT-1 was a potent promoter of platelet adhesion and thrombus formation on cultured endothelial cells perfused with whole blood in a flow chamber system under high shear stress levels. The effect of VT-1 was higher than that of thrombogenic agonists such as thrombin and cytokines. Microvascular endothelial cells -of dermal origin- demonstrated a remarkably greater sensitivity to the

thrombogenic effect of VT-1 than endothelium derived from large vessels (HUVEC), possibly because they expressed higher levels of Stx receptors (20-fold more). Similar expression of Gb3 receptor was described on renal microvascular endothelial cells [23], which may account for the different sensitivity of different vascular districts to VT-induced injury.

In order to identify the adhesive proteins involved in thrombus formation elicited by Stx on microvascular endothelial cells, we first focused on von Willebrand factor (vWF) an indispensable adhesive substrate to promote thrombus formation in high shear stress environments [24]. We observed that polymeric aurin tricarboxylic acid, an inhibitor of vWF-platelet GPIb interaction, and chimeric 7E3 Fab which blocks α_{IIb}-β_3 on activated platelets, completely prevented platelet deposition and thrombus formation, suggesting the involvement of vWF-platelet interaction at high shear stress in this phenomenon. These findings are consistent with the evidence, in a different experimental setting, that the mechanism supporting platelet adhesion and thrombus formation requires binding of GPIb to vWF at high shear stress [24]. The engagement of this receptor determines activation of the α_{IIb}-β_3 receptor that in turn promotes irreversible platelet adhesion by interacting with the RGD sequence of vWF. We also provided the observation that upon endothelial exposure to VT-1, vWF-mediated platelet deposition occurred mainly on endothelial surface rather than in the subendothelium. Based on the evidence that vWF can interact with endothelial β_3 integrin subunit, the vitronectin receptor [25], via RGD sequence, we have documented that VT-1 induced on the luminal endothelial surface upregulation and/or redistribution of the vitronectin receptor. Functional blocking of this endothelial ligand almost completely prevented platelet deposition, thus suggesting that the toxin possibly alters endothelial thromboresistance by inducing changes in the surface expression of

vitronectin receptor that in turn leads to platelet adhesion via a vWF-dependent bridging mechanism. On the other hand, functional blockade of endothelial P-selectin and PECAM-1 with specific antibodies was associated with a marked reduction of the endothelial area covered by thrombi under flow condition. As for the prothrombotic role of both adhesive proteins, previous studies documented their involvement in the process of platelet adhesion on activated or damaged endothelium by their direct binding to platelets [26, 27]. Thus, in a model of ischemia/reperfusion injury endothelial overexpression of P-selectin was instrumental for the process of platelet rolling and deposition [28]. The proof of a direct contribution of endothelial PECAM-1 to platelet adhesion derives from data that in a model of laser-induced endothelial injury in brain arterioles, anti-PECAM-1 antibody reduced microvascular thrombosis over damaged but not denuded endothelium [27]. In our experimental condition, the thrombogenic effect of P-selectin and PECAM-1 was associated with an increased expression of P-selectin, and redistributed PECAM-1 away from cell-cell border of VT-1-treated endothelial cells, thus indicating that alteration of endothelial adhesion molecule expression induced by VT-1 is a critical step in enhancing platelet adhesion and thrombus formation in microvascular endothelium. In conclusion, our results might be relevant to understand why thrombi in HUS localize in microvessels rather than in larger ones and could help to formulate therapeutic strategies to prevent endothelial injury without the need to suppress platelet function.

In D+HUS renal susceptibility has been ascribed to the relatively high levels of Gb3 receptor expressed by this tissue. Ischemic lesions in the glomerular microcirculation typically occur in association with fusion of foot process and swelling of podocytes [29]. Studies directed at understanding the role of podocytes in the toxic response of Stx-2 are discussed **in Chapter 7.** We reasoned that podocytes in virtue of their susceptibility to the toxic effect of the toxin and the capability to produce vasoactive mediators could have an

impact in glomerular microcirculation and account for renal functional derangement in Stx-associated HUS.

Propedeutic to this study was a previous paper - described in **Chapter 6** - focused on the mechanisms underlying podocyte phenotypic changes induced by protein overload, and ultimately leading to cell dysfunction. In many proteinuric nephropathies, proteins filtered in exuberant amounts through the glomerular capillary barrier may have an intrinsic renal toxicity and serve as an early trigger of tubular interstitial inflammation [30]. Ultrafiltered plasma proteins also induced morphological changes in podocytes, which include reversible retraction and flattening of the epithelial foot processes suggesting podocyte/glomerular basement membrane (GBM) interaction to be of critical relevance to functional filter. We documented that in murine podocytes in culture, the abnormal uptake of plasma proteins, albumin and Immunoglobulin G (IgG), induced a marked redistribution of F-actin fibers accompanied by loss of synaptopodin, an F-actin-associated protein considered a specific marker of podocyte differentiation [31]. This effect would be taken to suggest that protein accumulation at glomerular level triggers podocyte dedifferentiation, a phenomenon already described in vivo in areas of segmental sclerosis [32]. F-actin is connected with adaptor molecules that anchor the slit diaphragm proteins and $\alpha 3\beta 1$ integrins, transmembrane proteins that form focal adhesion complexes and mediate podocyte/GBM matrix interaction [33]. Cytoskeletal rearrangement affects cell adhesion to matrix with consequent activation of out-side in signals that trigger specific cellular responses and lead to activation of gene expression of inflammatory and vasoactive mediators [34]. Consistently, we found that the F-actin redistribution induced by protein load was instrumental to the upregulation of the vasoactive peptide Endothelin –1 (ET-1) in parallel with the generation of the protein. Increased DNA-binding activity of the transcription factors NF-kB and Ap-1, known to regulate ET-1 gene expression, were also

measured in nuclear extracts of podocytes exposed to excess proteins. Furthermore, treatment of podocytes with an inhibitor of Rho kinases - crucial in the formation of stress fibers and focal adhesion complex [35] - markedly decreased NF-kB and Ap-1-dependent ET-1 gene upregulation, thus suggesting that podocytes in proteinuric setting are an important source of ET-1 regulated via Rho dependent-cytoskeleton signal transduction pathway of gene activation. These data are in line with previous reports *in vitro* of the involvement of Rho-GTPase family in modulating basal expression of ET-1 transcript levels in vascular endothelial cells and also in regulating NF-kB and Ap-1 in genetically modified cultured fibroblasts [36, 37]. Finally, we assessed the role of focal adhesion kinase (FAK) - a cytoplasmic non receptor tyrosine kinase localized in integrin-extracellular matrix complexes [33] - that acts as an effector molecule linking actin reorganization with transcriptional events. Results showed that FAK is phosphorylated by protein treatment and that FAK signaling contributes to ET-1 gene regulation to the extent that transient overexpression by adenoviral gene transfer of FAK-related non kinase, an endogenous inhibitor of FAK activity, resulted in a partial but significant inhibition of ET-1. These data suggest that reorganization of cytoskeletal network in response to protein load plays a central role in the cascade of intracellular events that lead to podocyte dysfunction and ET-1 gene regulation.

On the basis of this study, and once verified that murine podocytes effectively represent an important source of ET-1, as also described by other groups for rat podocytes [38], we moved to investigate (**Chapter 7**) possible mechanisms evoked by Stx that could contribute to podocyte phenotipic alteration and ET-1 gene expression. We focused on the vasoconstrictor peptide ET-1 found to be elevated in plasma and urine of children during the acute phase of D+HUS [39]. Our results indicate that Stx-2 at subtoxic concentrations, increased mRNA transcript levels of ET-1 which was followed by the enhanced synthesis

of the mature peptide. The relevance of this finding rests on the evidence that ET-1, if produced at glomerular level, may induce cell proliferation, chemotaxis, extracellular matrix accumulation and may stimulate the contraction of mesangial cells, regulating glomerular capillary surface area and filtration rate [40] .

An important aspect of this study has been the identification of intracellular pathways activated by Stx-2 and involved in ET-1 overexpression in podocytes. Our data showed that Stx-2 induced a rapid and massive activation of the transcription factor NF-kB and to lesser extent of Ap-1. The direct demonstration that NF-kB and Ap-1 modulates ET-1 gene expression derives from experiments where transfection of podocytes with dominant negative mutant of IKB kinase2 or with Ap-1 decoy oligodeoxynucleotide failed to increase ET-1 mRNA transcript levels in response to the toxin. The present results indicate that the Stx-2, besides the capability to activate NF-kB-dependent inflammatory genes in glomerular endothelial cells, responsible of leukocyte recruitment and endothelial injury, is also able to activate glomerular podocytes to express NF-kB dependent vasoactive genes that might contribute to renal function impairment in HUS patients.

Furthermore, the involvement of p38 and p42/44 MAPK in mediating NF-kB dependent gene transcription rests on data that Stx-2 phosphorylated/activated p38 and p42/44 MAPK and that inhibitors of both kinases decreased the transcription of NF-kB promoter/luciferase reporter gene construct induced by Stx-2. In line with our results, other studies have implicated p38 and p42/44 MAPK activation in Stx-induced NFkB-dependent gene expression of TNF in human adenocarcinoma-derived renal tubular cell line [41].

Another important finding that arises from this study is that the toxin caused a marked redistribution of the contractile F-actin apparatus accompanied by intercellular gap formation, reflecting podocyte process retraction. *In vivo*, podocyte cytoskeletal derangement results in foot process effacement and cell retraction, characteristic adaptive

changes in a wide variety of human and experimental glomerulopathies with heavy proteinuria and renal function impairment [42]. Data that an ET_A receptor antagonist prevented Stx-2 induced structural changes does suggest a role of ET-1 in the dysfunction of podocyte contractile apparatus. Of interest, ET-1 added exogenously to cultured podocytes determined morphological alterations similar to those of Stx-2 and increased protein permeability, thus implicating a modification of podocyte-podocyte contact.

In conclusion, our finding point to podocytes as critical targets of Stx-2, a novel stimulus for the synthesis of ET-1 that besides its autocrine action might exerts toxic effects in paracrine fashion by stimulating mesangial cell contraction and affecting the glomerular capillary surface area and filtration rate, thus contributing to glomerular ischemic changes and hemodynamic derangement in HUS.

REFERENCES

1. Morigi M, Zoja C, Figliuzzi M, Foppolo M, Micheletti G, Bontempelli M, Saronni M, Remuzzi G, Remuzzi A: Fluid shear stress modulates surface expression of adhesion molecules by endothelial cells. *Blood* 85:1696-1703, 1995
2. Lawrence MB, Springer TA: Neutrophils roll on E-selectin *J Immunol* 151:6338-6346, 1993
3. Alon R, Rossiter H, Wang X, Springer TA, Kupper TS: Distinct cell surface ligands mediate T lymphocyte attachment and rolling on P and E selectin under physiological flow. *J Cell Biol* 127:1485-1495, 1994
4. Wuthrich RP: Intercellular adhesion molecules and vascular cell adhesion molecule-1 and the kidney. *J Am Soc Nephrol* 3:1201-1211, 1992
5. Milford DV, Staten J, MacGreggor I, Dawes J, Taylor CM, Hill FG: Prognostic markers in diarrhoea-associated haemolytic-uraemic syndrome: initial neutrophil count, human neutrophil elastase and von Willebrand factor antigen. *Nephrol Dial Transplant* 6:232-237, 1991
6. Fitzpatrick MM, Shah V, Trompeter RS, Dillon MJ, Barratt TM: Interleukin-8 and polymorphoneutrophil leucocyte activation in hemolytic uremic syndrome of childhood. *Kidney Int* 42:951-956, 1992
7. Forsyth KD, Simpson AC, Fitzpatrick MM, Barratt TM, Levinsky RJ: Neutrophil-mediated endothelial injury in haemolytic uraemic syndrome. *Lancet* II:411-414, 1989
8. King AJ, Sundaram S, Cendoroglo M, Acheson DW, Keusch GT: Shiga toxin induces superoxide production in polymorphonuclear cells with subsequent impairment of phagocytosis and responsiveness to phorbol esters. *J Infect Dis* 179:503-507, 1999

9. Inward CD, Howie AJ, Fitzpatrick MM, Rafaat F, Milford DV, Taylor CM: Renal histopathology in fatal cases of diarrhoea-associated haemolytic uraemic syndrome. British Association for Paediatric Nephrology. *Pediatr Nephrol* 11:556-559, 1997

10. van de Kar NCAJ, Monnens LAH, Karmali MA, van Hinsbergh VWM: Tumor necrosis factor and interleukin-1 induce expression of the verocytotoxin receptor globotriaosylceramide on human endothelial cells: implications for the pathogenesis of the hemolytic uremic syndrome. *Blood* 80:2755-2764, 1992

11. Barrett TJ, Potter ME, Strockbine NA: Evidence for participation of the macrophage in Shiga like toxin-II induced lethality in mice. *Microbial Pathogenesis* 9:95-103, 1990

12. van Setten PA, van Hinsbergh VW, van den Heuvel LP, Preyers F, Dijkman HB, Assmann KJ, van der Velden TJ, Monnens LA: Monocyte chemoattractant protein-1 and interleukin-8 levels in urine and serum of patents with hemolytic uremic syndrome. *Pediatr Res* 43:759-767, 1998

13. Inward CD, Varagunam M, Adu D, Milford DV, Taylor CM: Cytokines in haemolytic uraemic syndrome associated with verocytotoxin-producing Escherichia coli infection. *Arch Dis Child* 77:145-147, 1997

14. Luster AD: Chemokines--chemotactic cytokines that mediate inflammation. *N Engl J Med* 338:436-445, 1998

15. Webb LM, Ehrengruber MU, Clark-Lewis I, Baggiolini M, Rot A: Binding to heparan sulfate or heparin enhances neutrophil responses to interleukin 8. *Proc Natl Acad Sci U S A* 90:7158-7162, 1993

16. Gerszten RE, Garcia-Zepeda EA, Lim YC, Yoshida M, Ding HA, Gimbrone MA, Jr., Luster AD, Luscinskas FW, Rosenzweig A: MCP-1 and IL-8 trigger firm adhesion of monocytes to vascular endothelium under flow conditions. *Nature* 398:718-723, 1999

17. Kunsch C, Rosen CA: NF-kB subunit-specific regulation of the interleukin-8 promoter. *Mol Cell Biol* 13:6137-6146, 1993

18. Ueda A, Okuda K, Ohno S, Shirai A, Igarashi T, Matsunaga K, Fukushima J, Kawamoto S, Ishigatsubo Y, Okubo T: NF-kappa B and Sp1 regulate transcription of the human monocyte chemoattractant protein-1 gene. *J Immunol* 153:2052-2063, 1994

19. Tak PP, Firestein GS: NF-kappaB: a key role in inflammatory diseases. *J Clin Invest* 107:7-11, 2001

20. Sakiri R, Ramegowda B, Tesh VL: Shiga toxin type 1 activates tumor necrosis factor-alpha gene transcription and nuclear translocation of the transcriptional activators nuclear factor-kappaB and activator protein-1. *Blood* 92:558-566, 1998

21. Karpman D, Papadopoulou D, Nilsson K, Sjogren AC, Mikaelsson C, Lethagen S: Platelet activation by Shiga toxin and circulatory factors as a pathogenetic mechanism in the hemolytic uremic syndrome. *Blood* 97:3100-3108, 2001

22. Thorpe CM, Flaumenhaft R, Hurley B, Jacewicz M, Acheson DW, Keusch GT: Shiga toxins do not directly stimulate alpha-granule secretion or enhance aggregation of human platelets. *Acta Haematol* 102:51-55, 1999

23. Obrig TG, Moran TP, Brown JE: The mode of action of Shiga toxin on peptide elongation of eukaryotic protein synthesis. *Biochemical Journal* 244:287-294, 1987

24. Ruggeri ZM: von Willebrand factor. *J Clin Invest* 99:559-564, 1997

25. Cheresh DA: Human endothelial cells synthesize and express an Arg-Gly-Asp-directed adhesion receptor involved in attachment to fibrinogen and von Willebrand factor. *Proc Natl Acad Sci U S A* 84:6471-6475, 1987

26. Frenette PS, Johnson RC, Hynes RO, Wagner DD: Platelets roll on stimulated endothelium in vivo: an interaction mediated by endothelial P-selectin. *Proc Natl Acad Sci U S A* 92:7450-7454, 1995

27. Rosenblum WI, Nelson GH, Wormley B, Werner P, Wang J, Shih CC: Role of platelet-endothelial cell adhesion molecule (PECAM) in platelet adhesion/aggregation over injured but not denuded endothelium in vivo and ex vivo. *Stroke* 27:709-711, 1996

28. Massberg S, Enders G, Leiderer R, Eisenmenger S, Vestweber D, Krombach F, Messmer K: Platelet-endothelial cell interactions during ischemia/reperfusion: the role of P-selectin. *Blood* 92:507-515, 1998

29. Striker GE, Striker LJ, D'Agati V: Renal Lesions in Hypertension, in *The Renal Biopsy Major Problems in Pathology*, edited by Livolsi VA, Third ed, Philadelphia, Saunders, W.B. Company, 1997, pp 258-268

30. Remuzzi G, Bertani T: Pathophysiology of progressive nephropathies. *N Engl J Med* 339:1448-1456, 1998

31. Mundel P, Reiser J, Zuniga Mejia Borja A, Pavenstadt H, Davidson GR, Kriz W, Zeller R: Rearrangements of the cytoskeleton and cell contacts induce process formation during differentiation of conditionally immortalized mouse podocyte cell lines. *Exp Cell Res* 236:248-258, 1997

32. Srivastava T, Garola RE, Whiting JM, Alon US: Synaptopodin expression in idiopathic nephrotic syndrome of childhood. *Kidney Int* 59:118-125, 2001

33. Kretzler M: Regulation of adhesive interaction between podocytes and glomerular basement membrane. *Microsc Res Tech* 57:247-253, 2002

34. Gonzalez-Santiago L, Lopez-Ongil S, Griera M, Rodriguez-Puyol M, Rodriguez-Puyol D: Regulation of endothelin synthesis by extracellular matrix in human endothelial cells. *Kidney Int* 62:537-543, 2002

35. Ridley AJ, Hall A: The small GTP-binding protein rho regulates the assembly of focal adhesions and actin stress fibers in response to growth factors. *Cell* 70:389-399, 1992

36. Hernandez-Perera O, Perez-Sala D, Soria E, Lamas S: Involvement of Rho GTPases in the transcriptional inhibition of preproendothelin-1 gene expression by simvastatin in vascular endothelial cells. *Circ Res* 87:616-622, 2000

37. Van Aelst L, D'Souza-Schorey C: Rho GTPases and signaling networks. *Genes Dev* 11:2295-2322, 1997

38. Cybulsky AV, Stewart DJ, Cybulsky MI: Glomerular epithelial cells produce endothelin-1. *J Am Soc Nephrol* 3:1398-1404, 1993

39. Siegler RL, Edwin SS, Christofferson RD, Mitchell MD: Endothelin in the urine of children with the hemolytic uremic syndrome. *Pediatrics* 88:1063-1066, 1991

40. Sorokin A, Kohan DE: Physiology and pathology of endothelin-1 in renal mesangium. *Am J Physiol Renal Physiol* 285:F579-589, 2003

41. Nakamura A, Johns EJ, Imaizumi A, Yanagawa Y, Kohsaka T: Activation of beta(2)-adrenoceptor prevents shiga toxin 2-induced TNF-alpha gene transcription. *J Am Soc Nephrol* 12:2288-2299, 2001

42. Shirato I: Podocyte process effacement in vivo. *Microsc Res Tech* 57:241-246, 2002

CHAPTER 9

SUMMARY

SUMMARY

Shiga toxins (Stx) has been strongly indicated as the causative agent for typical childhood D+HUS.The kidney is the privileged target of the toxin, with glomerular ischemic changes including tuft retraction and capillary wall thickening, both preceding microvascular thrombosis. Endothelial dysfunction is crucial to the development of microvascular lesions and increasing evidence suggests that Stx/VT by favoring interaction of endothelial cells with leukocytes and platelets, serve to amplify and extend the injury at renal level. Local thrombosis amplifies the inflammatory injury by promoting complement activation -in particular the alternative pathway- and deposition within capillary vessels (**Chapter 2).**

In this thesis further investigations where performed to address the renal toxicity of Stx with the aims of providing insights on the molecular events involved in microvascular lesions in HUS.

In **Chapter 3** we investigated *in vitro* the effect of VT-1 on leukocyte adhesion to vascular endothelium under physiologic flow condition using a parallell plate flow chamber. Incubation of human umbilical vein endothelial cells (HUVEC) with increasing concentrations of VT-1 resulted in a dose-dependent increase in the number of adhering leukocytes to HUVEC. The adhesive response induced by the toxin was quite comparable to the effect of IL-1β, one of the most potent inducer of endothelial cell adhesiveness. Rolling phenomenon was not affected by VT-1. We then explored the role of adhesive molecules in VT-induced leukocyte adhesion. Functional blocking of E-selectin, ICAM-1 and VCAM-1 on endothelial cells with respective antibodies, significantly reduced VT-induced increase in leukocyte adhesion. Pre-exposure of endothelium with TNFα before challenge with VT-1, significantly increased the number of adherent leukocytes under flow.

This observation is consistent with the finding that this cytokine does promote upregulation of endothelial Gb3 receptor and supports toxin-binding. These data identify a novel mechanism by which VT directly modulates leukocyte-endothelium interaction, thus increasing leukocyte adhesion and upregulating adhesive proteins on endothelial surface membrane.

Kidney specimens from HUS children with evidence of Stx-producing *E coli* infection revealed a massive infiltration of polymorphonuclear and mononuclear cells within the glomeruli, along with microvascular injury. Urinary levels of IL-8 and monocyte chemoattractant protein–1 (MCP-1), potent attractants of neutrophils, monocytes/macrophages and T lymphocytes, were elevated during the acute phase of the disease in these patients, suggesting the involvement of these chemokines in the recruitment of inflammatory cells at glomerular level. In **Chapter 4**, we tested the hypothesis that Stx-2 could modulate the endothelial expression of MCP-1 and IL-8 and their functional role on leukocyte adhesion and transmigration. We found that subtoxic concentrations of Stx-2 induced a significant increase in the number of leukocytes adhering to HUVEC, followed by a massive transmigration through the endothelium. MCP-1 and IL-8 mRNA expression was increased after exposure to Stx-2. Blocking of endothelial MCP-1 and IL-8 with the corresponding antibodies significantly reduced Stx-induced leukocyte adhesion and migration either on HUVEC or glomerular endothelial cells. Adenovirus-mediated gene transfer of IkBα down-regulated chemokine expression and also inhibited the adhesion and transmigration of leukocytes in Stx-treated HUVEC. These data suggest that Stx-2 via a transcriptional activation mechanism mediated by NF-kB upregulates MCP-1 and IL-8, key mediators of leukocyte adhesion and transmigration.

In D+HUS, thrombotic microangiopathy, defines a lesion of vessel wall thickening and intraluminal platelet thrombosis that occlude the microcirculation of the kidney and other organs. The reason why thrombi form only on arterioles and capillaries is not known. **In Chapter 5** we studied whether Stx-1 directly affected endothelial antithrombogenic properties promoting thrombus formation on human microvascular endothelial cells (HMEC-1) under high shear stress. HUVEC were used for comparison, as large vessel endothelium. VT-1 directly induced platelet adhesion on cultured endothelial cells perfused with whole blood in a flow chamber system under shear stress levels high enough to mimic the ones encountered in the microcirculation. This effect was more pronounced on VT-treated endothelial cells of microvascular (HMEC-1) in respect to large vessel (HUVEC) origin, since basal expression of Gb3 receptor in HMEC-1 was 50-fold higher than in HUVEC. In the attempt to identify the adhesive proteins involved in platelet-endothelium interactions elicited by VT-1, we first focused on von Willebrand factor (vWf), which is indispensable substrate to promote thrombus formation. Blocking the binding of vWf to platelet glycoprotein 1b by aurintricarboxylic acid and the glycoprotein $\alpha_{IIb}\beta_3$ integrin by chimeric 7E3 Fab resulted in a significant reduction of VT-induced platelet deposition, indicating a role of vWf-platelet interaction at high shear stress in this phenomenon.

Inhibition of endothelial vitronectin receptor, P-selectin and PECAM-1 with specific antibodies markedly reduced the endothelial surface area covered by thrombi. These data along with the observation of a strong expression of these adhesive proteins due to upregulation/redistribution, on the endothelial surface of HMEC-1 after VT challenge, provide insights on the determinants possibly involved in the process of microvascular thrombosis associated with D+HUS.

Podocytes are sensitive to the toxic effects of Stx-1 and 2 isoforms, as documented either in cultured cells or in human renal biopsies. Podocytes, a crucial component of the glomerular filter, are highly specialized epithelial cells endowed with foot processes. They possess a contractile structure that respond to vasoactive hormones to control glomerular capillary surface area and in turn ultrafiltration coefficient. Effacement of foot processes occurs in many proteinuric nephropathies and is accompanied by rearrangement of the actin cytoskeleton. Instrumental in studying the effect of Stx on podocytes, in **Chapter 6** we first set up the technique to maintain in culture immortalized mouse podocytes and to induce differentiation of podocytes which in this conditions stop to proliferate and express high levels of synaptopodin. Then, we assessed whether protein overload -reproducing the condition of exaggerated plasma protein traffic through the glomerular capillary barrier- affects intracellular pathways, leading to cytoskeletal architecture changes and ultimately to podocyte dysfunction. We have found that in podocytes the abnormal uptake of plasma proteins induces Rho kinase-dependent F-actin cytoskeletal rearrangement leading to cell dedifferentiation. Such structural changes translate into the activation of FAK in turn responsible for NF-kB- and Ap-1 dependent ET-1 gene upregulation. ET-1 overproduction may act on the podocyte contractile apparatus altering the glomerular capillary surface area thus leading to protein permeability dysfunction. These results indicate podocyte as a novel cellular target for the toxic effect of excess plasma ultrafiltered protein.

Since podocytes express Stx specific receptor, are susceptible to Stx citotoxicity and represent an important source of vasoactive molecules, we investigated in **Chapter 7** whether Stx-2 modulates the expression and production of the vasoconstrictor peptide, Endothelin-1 (ET-1), taken as candidate mediator of podocyte dysfunction. Stx-2 enhanced ET-1 mRNA and protein through the activation of NF-kB and Ap-1 to the extent that

transfection with dominant negative mutant of IKB kinase2 or with Ap-1 decoy oligodeoxynucleotide reduced ET-1 mRNA. We further investigated the intracellular signals activated by Stx-2 possibly involved in the upregulation of ET-1 gene. A role for p38 and p42/44 MAPK in mediating NF-kB-dependent gene transcription induced by Stx-2 has been proposed based on data that Stx-2 phosphorylated p38 and p42/44 MAPK and that inhibitors of both MAPK reduced transcription of NF-kB promoter luciferase reporter gene construct induced by Stx-2. Additionally, Stx-2 induced F-actin redistribution and intercellular gap formation via ET-1 induction since cytoskeletal changes were prevented by ET_A receptor blockade. Findings that podocyte challenge with ET-1 induced podocyte F-actin redistribution and in parallel increased protein permeability, unravel ET-1 as a major mediator of the toxin-induced effect. In summary, our data are the first to document that podocyte is a functionally relevant target of Stx, a novel stimulus for the synthesis of ET-1 synthesis that controls in autocrine and paracrine fashion glomerular remodeling and hemodynamic derangement in HUS.

CURRICULUM VITAE

Marina Morigi was born in Ravenna, Italy, on August 30th 1961. She took the upper-school leaving the certificate at "Liceo Scientifico Collegio Vescovile S. Alessandro" of Bergamo on 1980. She graduated in Biological Sciences at the University of Milano on December 17th 1987. From January 1988 she had a fellowship from Mario Negri Institute of Pharmacological Research of Bergamo in the Laboratory of Kidney Disease coordinated by Dr. Giuseppe Remuzzi, obtaining a position as Scientist on October 1995. She had the opportunity to spend some month at Women's Hospital of Boston, working in the laboratory of Prof. Barry Brenner with his collaborator Dr. Philip Marsden, during 1991. On 1996 she became head of the Unit of Renal and Endothelial Cell Biology and since 2000 she is head of the Laboratory of Cell Biology and Xenotransplantation. In these years she has contributed to define the mechanisms underlying endothelial cell dysfunction in thrombotic microangiopathies and hyperacute vascular rejection of xenograft. Moreover, she put her research effort in the identification of inflammatory mediators and mechanisms triggered by exaggerated protein traffic, characteristic of proteinuric progressive nephropathy, using in vitro systems of proximal tubular cells and podocytes exposed to protein overload. Another major research topic has related to the regenerative potential of adult bone marrow-derived stem cells in renal damage by acute and chronic insult in experimental mouse models. She is also involved in stem cell therapy with embryonic stem cells to correct genetic defect characteristic of Fabry disease in experimental K/O mouse model.

Dr. Marina Morigi has authored and co-authored 49 scientific articles and reviews.

ACKNOWLEDGMENTS

I wish to express my deep gratitude to Prof. Giuseppe Remuzzi who always supported and encouraged me and my work during these years.

I am indebted to Prof. Karel Leunissen for the opportunity he gave me to discuss my PhD thesis in the prestigious Universiteit Maastricht.

I thank my colleagues and friends, Carla Zoja, Ariela Benigni, Simona Buelli, Manuela Passera, Antoinette van Engelen and Antonella Piccinelli for their continued and helpful collaboration.